

UNCLASSIFIED

AD 413924

DEFENSE DOCUMENTATION CENTER

FOR

SCIENTIFIC AND TECHNICAL INFORMATION

CAMERON STATION, ALEXANDRIA, VIRGINIA



UNCLASSIFIED

NOTICE: When government or other drawings, specifications or other data are used for any purpose other than in connection with a definitely related government procurement operation, the U. S. Government thereby incurs no responsibility, nor any obligation whatsoever; and the fact that the Government may have formulated, furnished, or in any way supplied the said drawings, specifications, or other data is not to be regarded by implication or otherwise as in any manner licensing the holder or any other person or corporation, or conveying any rights or permission to manufacture, use or sell any patented invention that may in any way be related thereto.

63-4-4

413924

**U. S. A R M Y
TRANSPORTATION RESEARCH COMMAND
FORT EUSTIS, VIRGINIA**

CATALOGED BY DDC

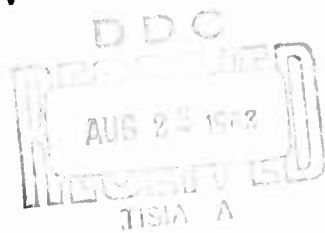
AS AD No.

TRECOM TECHNICAL REPORT 63-27

**RECIRCULATION PRINCIPLE FOR GROUND EFFECT MACHINES:
INVESTIGATION OF IMPROVEMENTS BY
MAJOR MODIFICATIONS TO MCTV**

Task 1D021701A04804
(Formerly Task 9R99-01-005-04)
Contract DA 44-177-AMC-9(T)

July 1963



• prepared by:

• MARTIN COMPANY
Orlando, Florida

413924



DISCLAIMER NOTICE

When Government drawings, specifications, or other data are used for any purpose other than in connection with a definitely related Government procurement operation, the United States Government thereby incurs no responsibility nor any obligation whatsoever; and the fact that the Government may have formulated, furnished, or in any way supplied the said drawings, specifications, or other data is not to be regarded by implication or otherwise as in any manner licensing the holder or any other person or corporation, or conveying any rights or permission, to manufacture, use, or sell any patented invention that may be related thereto.

DDC AVAILABILITY NOTICE

Qualified requestors may obtain copies of this report from

Defense Documentation Center
Arlington Hall Station
Arlington 12, Virginia

This report has been released to the Office of Technical Services, U. S. Department of Commerce, Washington 25, D. C., for sale to the general public.

The findings and recommendations contained in this report are those of the contractor and do not necessarily reflect the views of the U. S. Army Mobility Command, the U. S. Army Materiel Command, or the Department of the Army.

HEADQUARTERS
U. S. ARMY TRANSPORTATION RESEARCH COMMAND
Fort Eustis, Virginia

This report is one of a series of reports of investigations into the recirculation principle for ground effect machines. Previous reports have covered small-scale two- and three-dimensional model testing and construction and testing of a man-carrying test vehicle (MCTV) based on this principle.

The MCTV, as originally tested, did not meet the lift performance objectives and did not substantiate the results of the original model experiments. Therefore, a subsequent series of investigations was undertaken to re-evaluate the effects of various parameters such as area ratio, inlet and outlet ejector angle, and three-dimensional effects. The results of these experiments are presented herein.

Based on these results, the predicted performance of the existing experimental vehicle is computed assuming a completely redesigned duct system and compatible engine/compressor system. The hover height and gross weight which result from these modifications are estimated as 18 inches and 5,000 pounds, respectively. This level of performance is comparable to existing annular-jet GEMs of comparable size; however, the inherently lower air-mass flow of the recirculation GEM configuration would result in a drag advantage at forward speed and a reduction in signature.

KENNETH B. ABEL
Captain, TC
Adjutant

Approved:

W.D. Hinshaw
WILLIAM D. HINSHAW
USATRECOM Project Engineer

Task 1D021701A04804
(Formerly Task 9R99-01-005-04)
Contract DA 44-177-AMC-9(T)
TRECOM Technical Report 63-27
July 1963

RECIRCULATION PRINCIPLE FOR GROUND EFFECT
MACHINES: INVESTIGATION OF IMPROVEMENTS BY
MAJOR MODIFICATIONS TO MCTV

OR 3159 Final

Prepared by:
Martin Company
Orlando, Florida

for
U. S. ARMY TRANSPORTATION RESEARCH COMMAND
FORT EUSTIS, VIRGINIA

Task 1D021701AO4804
(Formerly Task 9R99-01-005-04)
Contract DA 44-177-AMC-9(T)
TRECOM Technical Report 63-27
July 1963

RECIRCULATION PRINCIPLE FOR GROUND EFFECT
MACHINES: INVESTIGATION OF IMPROVEMENTS BY
MAJOR MODIFICATIONS TO MCTV

OR 3159 Final

Prepared by:
Martin Company
Orlando, Florida

for
U. S. ARMY TRANSPORTATION RESEARCH COMMAND
FORT EUSTIS, VIRGINIA

FOREWORD

Martin-Orlando submits this report as a final report in full compliance with the requirements of Contract No. DA 44-177-AMC-9(T). It contains experimental data and analytical studies of its effort to determine the maximum performance obtainable in the man-carrying test vehicle (MCTV) with major modifications. The MCTV was constructed as a part of Contract No. DA 44-177-TC-710 and is described in TCREC Technical Reports 62-99, 62-100, and 63-1. The study was conducted from November 1962 through January 1963.

Mr. K. Cossairt, GEM Project Engineer, conducted this investigation and received significant contributions from Messrs. J. Butsko, C. Casteleiro and P. Vinson.

CONTENTS

	Page
FOREWORD	iii
ILLUSTRATIONS	vi
TABLES	ix
LIST OF SYMBOLS	x
SUMMARY	1
TWO-DIMENSIONAL PERFORMANCE	2
STABILITY AND CONTROL	7
SKIRTS AND TRUNKS	10
SURFACE ROUGHNESS	11
EVALUATION	12
BIBLIOGRAPHY	15
DISTRIBUTION	95

ILLUSTRATIONS

<u>Figure</u>	<u>Page</u>
1. Two-Dimensional Test Device	34
2. Original Model 1, Configurations 1, 2, 3 and 4	35
3. Original Model 1, Configurations 5 and 6	36
4. Modified Model 1, Configurations 7 and 8	37
5. Modified Model 1, Configuration 9	38
6. Typical Test Installation	39
7. Modified Model 1	40
8. Airfoil Header and Inlet Rake	41
9. Exit Flaps and Rakes	42
10. Airfoil Header, Sketch	43
11. Finger Header, Sketch	44
12. Primary Headers	45
13. Multiple Nozzle Headers	46
14. Finger Header, Installed	47
15. Rakes, Sketch	48
16. Original Model 1, Centerbody Location	49
17. Typical Tertiary Velocity and Total Head Profiles	50
18. Typical Tertiary Velocity - Cubed Profiles	51
19. Mass Flow as a function of Primary Pressure, Configurations 7, 8 and 9	52
20. Primary Horsepower as a function of Mass Flow, Configurations 7, 8 and 9	53
21. Primary Horsepower as a function of Mass Flow, Theory	54

<u>Figure</u>	<u>Page</u>
22. Primary Horsepower as a function of Primary Pressure, Configurations 7, 8 and 9	55
23. Base Pressure as a function of Height, Configuration 7	56
24. Base Pressure as a function of Height, Configuration 8	57
25. Cavity Pressure as a function of Primary Pressure, Configuration 7	58
26. Cavity Pressure as a function of Primary Pressure, Configuration 8	59
27. Cavity Pressure as a function of Height, Configuration 8	60
28. Optimum Exit Flap Angle, Configuration 8	61
29. Cavity Pressure as a function of Height, Theory, Configuration 7	62
30. Mass Augmentation as a function of Primary Pressure, Configuration 8, 9	63
31. Lift - Power Parameter as a function of Primary Pressure	64
32. Efficiency as a function of Primary Pressure, Configuration 8	65
33. Efficiency as a function of Primary Pressure, Configuration 9	66
34. Base Pressure as a function of Primary Pressure, Configuration 7	67
35. Base Pressure as a function of Primary Pressure, Configuration 8	68
36. Summary of Base Pressure as a function of Primary Pressure	69
37. Stability and Control Model	70
38. Lift Header, Stability and Control Model	71
39. Stability and Control Model	72
40. Manometer Board	73

<u>Figure</u>	<u>Page</u>
41. Base Pressure as a function of Height, Double Ejector	74
42. Lift and Moment as a function of Angle	75
43. Control Effectiveness, Ejector Tilt	76
44. Control Effectiveness, Differential Primary Pressure	77
45. Control With Inlet Flaps	78
46. Model 5, Reverse Flow	79
47. Model 5, Configuration 12	80
48. Model 5, Configurations 11 and 18	81
49. Model 5, Configurations 12 and 13	82
50. Model 5, Configurations 15, 16 and 17	83
51. Model 1, Configurations 18 through 21	84
52. Model 1, Configurations 22 through 25	85
53. Model 1, Centerbody and Inlets	86
54. Model 1, Centerbody Inner Exit Skirt	87
55. Base Pressure as a function of Height, Configurations 18, 24 and 25	88
56. Base Pressure as a function of Height, Configurations 9 and 26	89
57. Surface Roughness Models	90
58. Base Pressure as a function of Height, Surface Roughness	91
59. MCTV Base Modification, (Proposed)	92
60. MCTV Modification, (Proposed)	93
61. Two-Dimensional Performance, MCTV Modified	94

TABLES

	<u>Page</u>
I Configurations, Run Numbers, and Description	16
II Stability and Control	18
III 2-D Performance	21
IV Skirts and Trunks	29

LIST OF SYMBOLS

A''	Ejector Secondary Flow Area	in ²
A'	Ejector Primary Flow Area	in ²
R	Ejector Area Ratio, A''/A'	-
C	Ejector Length (Circumference)	ft
g	Acceleration Due to Gravity	32.17 ft/sec ²
h	Height Above Ground	in
j	Momentum per foot	lb/ft
J	Momentum of Total Ejector Flow	lb
J'	Momentum of Primary Ejector Flow	lb
L	Lift	lb
M	Pitching Moment	ft-lb
m	Total Ejector Mass Flow	lb/sec
m'	Primary Ejector Mass Flow	lb/sec
P_o	Ejector Primary Total Pressure	psig
P_B	Base Pressure	psfg
P_c	Cavity Pressure	psfg
P_t	Total Pressure	psf
q_j	Air Curtain Dynamic Pressure	psf
t	Ejector Exit Thickness	in
V	Velocity	ft/sec
W	Base Width for Double Ejector Model	ft
α	Base Pitch Angle	degrees
β	Ejector Tilt Angle from Horizontal	degrees
		psf

P_B	Pressure Jump Across Recirculating Curtain	psf
ϵ	Ejector Efficiency	per cent
δ_ϕ	Ejector Exit-Outer Flap Angle from Horizontal	degrees
δ_i	Ejector Exit-Inner Flap Angle from Horizontal	degrees
ρ	Density of Air	lb/ft ³
θ_1	Ejector Inlet Angle from Horizontal	degrees
θ_2	Ejector Exit Angle from Horizontal	degrees

SUMMARY

Analytical studies and experimental investigations were conducted to determine the best overall MCTV performance obtainable with essentially major modifications. Testing was done in the existing two-dimensional test facility with various configurations of old (existing) and new two-dimensional recirculating ejector models. Based on these experimental data, estimates are made as to the lifting capability, static stability and control of the proposed modified MCTV. In addition, experimental data is presented for the use of skirts and trunks for several configurations. The effect of ground surface roughness is also considered.

TWO-DIMENSIONAL PERFORMANCE

Recent investigations confirm that a decreased area ratio of the secondary inlet to the primary nozzle exit results in a performance increase of the ejectorjet recirculation concept. These tests further indicate that decreasing the area ratio in existing duct geometry, originally designed for a large area ratio, does not result in the maximum efficiency theoretically attributable to this system. Therefore, a new two-dimensional model was built and tested to determine the maximum MCTV performance obtainable with major modifications.

DESCRIPTION OF MODELS AND INSTRUMENTATION

The tests were conducted with a large scale two-dimensional device (Figure 1). The front side of the device is constructed of plexiglass to facilitate model adjustments and for observing flow patterns. The ground board is movable in a vertical direction to permit testing at heights up to 30 inches. Air is supplied to the ejector primary nozzles from the factory air source with pressures to 100 pounds per square inch and mass flows to 2 pounds per second. This primary air passes through a calibrated orifice at which point total head, temperature and mass flow are recorded. The original Model 1 (Figures 2 and 3) was tested with minor modifications as identified by the configuration numbers. For configurations 1 through 4 the only physical change made in the original model was relocating the centerbody, allowing various combinations of convergence and divergence in the mixing section and turn. The underside of the centerbody was modified and exit flaps were installed in Configurations 5 and 6.

A new modified Model 1 (Figures 4 and 5) was constructed incorporating the best features of the original Model 1 and with the addition of new primary headers.

Figure 6 shows a typical test installation with the manometer board in the foreground and the original Model 1 with modified centerbody in position on the two-dimensional test device. The original primary nozzles are installed at the inlet of the ejector and static pressure taps are located along the centerline at 2 inch intervals along the entire length of the board. Figure 7 shows the new modified Model 1 with the airfoil header installed. A detail view of the streamlined airfoil header is shown in Figure 8 along with the inlet rake assembly for measuring inlet pressure recovery. Inner and outer flaps and the permanently installed exit rake are located at the exit (Figure 9). Two basic header configurations were tested in the new Model 1, with header location and nozzle throat dimension variations. Detail views of these are shown in Figures 10 and 11 and an overall view is shown in Figure 12. The airfoil header (Figures 7 and 8) and the finger header was installed in Model 1 (Figure 14). In addition, the original

Model 1 header was modified to incorporate a multiple nozzle arrangement (Figure 13). The inlet and exit rakes (Figure 15) were used in all tests of the new Model 1.

EXPERIMENTAL RESULTS

Experimental results of the investigation are presented in two parts. The first part contains basic data such as mass flow, horsepower and base pressure for various configurations. The second part consists of summary cross plots of factors such as efficiency, base pressure per horsepower, and lift-power parameter.

Basic Data

The effect of relocating the centerbody of the original Model 1 to provide various combinations of dimensions in the mixing and turning sections is shown in Figure 16. The original Model 1, Configuration 1, provides the highest performance. However, it cannot be concluded at this time that a converging mixing section with a diffusing turn is necessarily optimum. From these data it can be concluded only that the original dimensions provide best results for this particular model over the range tested. The technique of moving the centerbody to obtain various combinations of convergence and diffusion simultaneously changes other factors, such as area ratio and mixing section pressure. These interactions compound the difficulty in analyzing data. Contrary to normal practice of minimizing turn losses by converging in the turn, best performance was obtained by Model 1 with either a constant area or diffusion turn. At lower primary pressures, improved results are obtained with a diffusing mixing section regardless of the condition of flow in the turn. This rapid rate of improvement in performance at the low primary pressure region of Configurations 2 and 3 seems to warrant further investigation.

Figures 17 and 18 show typical velocity and total head profiles of the tertiary flow measured at the ejector exit. The characteristic high energy velocity and total head at the outer streamlines of the exit flow are apparent. The primary mass flow as a function of primary pressure was plotted for two area ratios (Figure 19). At the lower area ratio the scatter in the data is more pronounced because of the difficulty in obtaining accurate total head readings at the lower pressures and higher mass flows. The airfoil and finger headers results are shown and indicate reasonably good correlation between orifice areas and nozzle coefficients.

Figure 20 shows horsepower required as a function of mass flow for two area ratios tested. In addition, a curve based on theoretical considerations obtained by cross plotting the results of Figure 21 is shown for comparison. The horsepower required per foot of length of primary header is shown in Figure 22 as a function of primary

pressure and area ratio. Figures 23 and 24 show variation of base pressure with height for Configurations 7 and 8, respectively. A characteristic peak in base pressure is obtained with fixed exit flap settings. The peak base pressure occurs at a height of approximately 12 inches for these configurations. The exit flaps have an appreciable effect on base pressure, especially at lower heights. As illustrated by the dotted portion of the curve in Figure 24, the base pressure still increases as the height is reduced to 6 inches. This was accomplished by setting the flaps at their optimum angle at each height. The pronounced effect of the exit flap position on the base pressure at lower heights was noted in all configurations tested.

The variation in cavity pressure as affected by height and primary pressure and exit flap angle is shown in Figures 25 through 28. By comparing Figures 24 and 27 it can be seen that improvement in base pressure, as a result of optimizing the exit flap angle at the lower heights, is generally the exact amount of improvement in the cavity pressure. Figure 28 shows the required variation in the inner and outer exit flaps as a function of height for Configuration 8. The cavity pressure, as predicted by theory, is shown in Figure 29. In comparison with experimental data the theoretically predicted cavity pressure is higher than that obtained experimentally. In previous testing of similar models (References 1 and 2) correlation between experiment and theory has been reasonably good. It is believed that the lack of correlation for this model is primarily a result of the external geometry, in particular, the overhang dimension. It appears that as a result of attempting to reduce the overall external dimensions of the ejector, there is an external interaction between the exit and inlet flow which adversely affects the cavity pressure.

Summary of Two-Dimensional Performance Data

The mass augmentation, as expected, was relatively low. Generally, the values ranged from 5 to 10, and for a given configuration remained essentially constant regardless of changes in height or primary pressure. Figure 30 is a plot of mass augmentation as a function of primary pressure for two area ratios.

The lift-power parameter is shown in Figure 31 as a function of primary pressure and area ratio at a height of 18 inches. Experimental data are plotted for area ratios of 23, 46 and 73. For comparison, curves for 122 and 231 obtained from References 1 and 2 are shown. The modified Model 1 performance has been improved only by approximately 25 per cent, because the original Model 1 performance was relatively high initially and only minor detail changes were made in the basic configuration.

Figures 32 and 33 show the efficiency as affected by height and primary pressure. The pronounced influence that height has on efficiency is a

result of increased inlet pressure recovery made possible at the lower height by higher base pressures. The effect of primary pressure is not so obvious. By definition, $\epsilon = (m/m') (V/V')^2$. It has been shown that mass augmentation remains relatively constant as primary pressure is changed. Obviously, the ratio of tertiary velocity (V) to the calculated primary velocity (V') must increase at a rapid rate initially and then tend to approach a maximum value as pressure is increased. Since the analytical expression relating tertiary velocity and primary velocity (Reference 1) contains many variables and requires an iterative process for solution, it was not possible at this time to establish relationship. An empirical correlation was attempted but meaningful results have not yet been reached. A more extensive study in this area appears warranted.

A relatively linear variation between base pressure and primary pressure is shown in Figures 34 and 35. These relationships could have been deduced from the previous data by the following reasoning:

$$P_0' \approx K_1 m \quad (\text{Figure 19})$$

$$\text{and } m/m' \approx K_2 \quad (\text{Figure 30})$$

also, for a given geometry and at these low primary pressures,

$$V/V' \approx m/m'$$

combining

$$P_0' \approx K_3 m$$

and

$$P_0' \approx K_4 V$$

The analytical expression for base pressure,

$$P_B = \frac{j}{2t} \left[\begin{array}{l} -2(t/h) (1+\cos e_1) \\ 1 - e \\ \hline -\frac{j}{h} \quad \left[1 - \frac{2}{m/m'} - \cos e_2 \right] \end{array} \right]$$

reduces to

$$P_B \approx K_5 m V$$

for a given configuration at a constant height;
therefore,

$$P_0 \approx K_6 P_B$$

A summary cross plot relating base pressure, primary pressure, area ratio and primary horsepower is shown in Figure 36. Lines of constant power peak, with respect to base pressure, at an area ratio of approximately 46. The data for area ratios 122 and 231 were taken from References 1 and 2.

A summary tabulation (Table I) of all configurations tested, run numbers and a brief description is presented on page 16. The basic data for the 2-D performance is included in Table III.

STABILITY AND CONTROL

It is apparent that the pressure under the centerbody of the recirculation systems will affect static stability and control of a vehicle. Relatively small variations in this cavity pressure, located near the perimeter of the vehicle, can produce sizeable moments in the roll and pitch plane. The stabilizing contribution of this cavity pressure was shown in a previous study (Reference 2). Also, reasonably good correlation has been obtained with the analytical expression and experimental results in previous studies. However, the cavity pressures obtained from Model 1 in this investigation do not correlate well with the theory. This effect was observed during the performance phase of testing, but because of the short study time, the stability and control model had already been fabricated. As a result, the following data show that Model 1 is generally statically unstable unless the exit flaps are varied as the height is changed.

DESCRIPTION OF MODELS AND INSTRUMENTATION

The results of tests conducted on a two-dimensional model with recirculating ejectors on opposing sides are shown in Figure 37. This model, referred to as the double ejector model, is exactly a one half scale model of the single ejector Model 1, Configuration 1. In addition, a hinge is provided where the outer wall of the ejector joins the model base which permits testing at preset values of δ . The ground board is movable in a vertical direction and can be tilted to determine the effects of a pitch (roll) angle. At any combination of height or pitch angle a vertical center board can be inserted to eliminate interactions between the left and right ejectors. This is helpful in synchronizing the performance of the two ejectors and isolating such effects as cross flow under the base. Primary air is supplied individually to the two headers from the factory air source and the headers are adjustable in location at the ejector inlet. Figure 38 shows details of the left header and primary nozzles. The overall dimensions of the model are shown in Figure 39. The instrumentation consists of an exit rake located in each ejector for measuring tertiary flow properties, static pressure taps throughout the model and a mass flow tube for determining the primary air properties. Three of the four manometer boards are shown in Figure 40 showing typical pressure gradients while the model is in operation. Approximately 200 static pressure taps are located along the length of the ground board and model base as well as completely around the perimeter of both centerbodies and along the inner walls of both ejectors. These data are entered directly into an IBM loading form, and the machine data reduction program provides read-outs as follows:

1. Static pressure at any point (lb/sq ft gage)
2. Integrated horizontal and vertical force on each component (inner walls, outer walls, centerbodies, model base and ground board) (lb/ft)

3. Total integrated normal force and side force (lb/ft)
4. Total integrated vertical force (lb/ft)
5. Pitching (rolling) moment (ft-lb/ft)
6. Velocity at each exit rake station (ft/sec)
7. Average velocity of each ejector (ft/sec)
8. Average velocity-cubed of each ejector (ft^3/sec^3)
9. Momentum flux of each ejector (lb/ft)
10. Mass flow of each ejector (slugs/sec/ft)
11. Mass augmentation of each ejector.

A plot of base pressure versus height is shown in Figure 41 for three primary pressures. Realizing that this double ejector configuration is exactly one half the size of Model 1, a direct comparison of base pressures is possible providing the height is properly scaled. Comparing Figures 23 and 41, excellent correlation is obtained between the two tests, if the height in Figure 41 is doubled.

To illustrate that the base pressure is a function of the weakest segment of the air curtain, the base pressure is plotted against a corrected height in Figure 41 (plus symbols). Normally, the height of the vehicle is referenced to the center of the base during a pitch (roll) test, but in Figure 41 the base pressure is plotted against the height of the ejector on the high side.

All of the static testing was done at heights of 5, 7 and 9 inches. Unfortunately, as was shown in Figure 41, the lift curve reaches a maximum value at 7 inches. Because of the great volume of data which must be recorded for each run (approximately 200 readings) and because of the shortness of the testing period, this condition was not detected early enough for corrective measures to be taken. As shown in Figure 24, the peak in the left curve could be virtually eliminated by proper exit flap adjustments. For the configuration tested, at 7 inches or lower, heave stability is neutral or negative. Furthermore, at 7 inches average height, as the model is pitched (rolled), one ejector will tend to follow the base pressure trend down one side of the curve and the other ejector will tend to follow down the opposite side. Over the range tested and with the configuration tested (no flaps adjustment and no undercut centerbody) the static stability properties are neutral or negative. This is further shown in Figure 42. During the performance phase of this investigation, configurations were tested which exhibited reasonably good static stability properties.

Correcting these data to half scale, the dotted line shown in Figure 42 represents the anticipated stability for Model 1, Configuration 8. It is shown from the slope of the moment curve that relatively high static stability properties are obtainable. From the slope of the lift curve, Figure 24, a high degree of heave stability is also predicted.

The effect on pitching (rolling) moment as the ejectors are tilted (θ) is shown in Figure 43. It is concluded that control by ejector tilt will be practical only on small vehicles with relatively high base pressures. Structural considerations limit the size of ejector assemblies which can be moved, and the control effectiveness deteriorates at low base pressures (low mass flux of the tertiary air).

Control by a differential throttling of the primary air to ejector assemblies on opposite sides of the vehicle is shown in Figure 44. It is anticipated that varying the primary pressure in conjunction with exit flap angle will provide an extremely effective control moment in the pitch and roll plane. In addition, inlet flaps discussed in the following section show an additional possibility of obtaining a control moment from the base pressure distribution (Figure 45).

The basic data for the stability and control tests is presented in Table II.

SKIRTS AND TRUNKS

It is not anticipated that flexible extensions to the inlet or exit of the recirculating ejector will improve performance to the degree that has been accomplished for the annular jet concept. However, because of the apparent success of this approach with the annular jet configuration a series of tests was conducted to determine its feasibility as related to the best ejectorjet configurations. Previous investigation of skirts or trunks on ejector recirculation models had not provided any significant improvement. These tests were done on configurations of relatively high area ratios, and hence high mass augmentation ratios, while the current configurations being investigated have low area ratios.

Existing models were modified to incorporate the various inlet and exit configurations, and in each case a base-reference run was made prior to the modification. Model 5 (Reference 2) was tested with various combinations of inlet and exit skirts and trunks as shown in Figures 46 through 50. It was also tested in a reverse flow direction with and without extensions as shown in Figure 46. The base-reference run was substandard in performance, but with trunks located at the exit (adjacent to base) the base pressure was increased in direct proportion to the length of trunk. However, the best performance with this configuration (Configuration 15) was not equal to the conventional Model 5 configuration (Configuration 11).

The improvement in performance for all skirted Model 5 configurations (12 through 17) was relatively low, and with some configurations the addition of skirts was detrimental to performance.

Figures 51 through 54 show various configurations of Model 1 which were tested. Exit skirts or trunks are ineffective and at low heights are detrimental. Conversely, inlet skirts and trunks are generally beneficial. In particular, the inner-inlet skirt, Configuration 24, provided a significant improvement in base pressure at the higher heights. Figure 55 shows the effect of an inlet flap on base pressure over a height range. The basic ejector curve was verified with a check run; however, evidently the exit flap positions were not adjusted properly for maximum performance over this height range. For this reason, it is probably more representative to compare the plot of P_B -vs-h for the inlet flap (Configuration 24) with the exit flap as shown in Figure 55. Figure 56 shows the result of a similar test to that shown in Figure 55, but the basic ejector data were obtained from the new modified Model 1. Again, the effect of an inner inlet extension is shown to be effective at the higher heights. It is estimated that there is an optimum angular setting of both the exit flaps and inner inlet skirt which would provide improved performance over the entire height range.

The basic data for the skirts and trunks tests is presented in Table IV.

SURFACE ROUGHNESS

Previous tests indicate that surface roughness can influence performance. Figure 57 shows three combinations of surface irregularities which were tested in the two-dimensional tunnel with Model 1. Figure 58 is a comparison of base pressure for the three surface roughness models and the basic ejector over a smooth surface. It is difficult to comprehend that the irregular surfaces could actually improve the base pressure at the higher heights, as shown. More probably, at the higher heights, the relative height of the irregularity is small and therefore has little effect on the base pressure. At the lower heights the condition causes a reduction in base pressure.

These data are difficult to interpret because of the two-dimensional nature of the test device. It is apparent that the flow under a vehicle will not be the same, under these conditions, as the flow which is confined by side walls in the test device. For this reason, the results are considered to provide trends only and it is recommended that future testing of this type should provide for the three-dimensional effects.

EVALUATION

As a result of this investigation the following conclusions, recommendations and anticipated performance estimates of the modified (proposed) MCTV are presented.

PERFORMANCE

The new modified Model 1 ejector configuration provides superior lifting capability over any previous configuration. To obtain the maximum performance over a height range of 6 to 24 inches, it is necessary to adjust the exit flap angle as height is varied.

STABILITY

Model 1, as tested in the stability and control tunnel, was not stable. Previous investigations have shown that a relatively high degree of inherent static stability can be obtained with the ejectijet concept. Further, results of the performance testing of this investigation show that the cavity pressure (the dominating factor in determining stability characteristics) can be directly controlled through the use of exit flaps. It is therefore concluded that adequate static stability can be provided either by (1) a detail change in the ejector configuration which results in inherent static stability over the entire height range, or by (2) remote control of the exit flaps with height, to provide artificial stability.

CONTROL

Adequate moments in the pitch and roll planes can be obtained by either a differential throttling of the primary pressure or differential control of the exit flaps, or both. Moment in the yaw plane (directional control) can best be obtained by a thrust vector control. The proposed engine for the MCTV has approximately 150 pounds of residual thrust which must be compensated for in a hovering attitude. This magnitude of thrust reacting at a proper lever arm will produce a sufficient amount of yaw control.

MANEUVER

Maneuver forces are low and expensive in power to provide, as in any GEM vehicle. Careful attention should be given to this parameter in the proposed modification. It appears that a propulsive system, separate from the lift system, will be the only satisfactory solution.

SKIRTS AND TRUNKS

The addition of an extension to the inner-inlet of the ejector improves the performance at higher heights for low area ratio (low mass

augmentation) recirculation ejectors. For the best configuration tested, a significant improvement in base pressure was obtained at heights above 18 inches. At 12 inches or lower the performance was the same or less than without the skirt. Other combinations of inlet and exit skirts and trunks were tested, but do not appear to be feasible.

SURFACE ROUGHNESS

It is difficult to conclude what effect surface roughness will have on a full size vehicle. The data obtained to date are from two-dimensional tests, small-scale models, and the low efficiency ejectors on the original MCTV. At low heights, where the relative height of the surface irregularity is large, a degradation in performance is anticipated. At higher heights the effect on base pressure appears to be negligible.

OVERLOAD CAPABILITY

The lifting capability of the ejectijet concept is reduced appreciably at very low heights. It would seem desirable to be able to travel at minimum height (minimum power) when the ground surface is smooth enough to permit. Preliminary discussions with General Motors personnel indicate that there is a mutual compatibility between their Hovair concept and the Martin ejectijet principle. Incorporation of these Hovair pads in the modified MCTV would permit an extremely high overload capability (limited by vehicle structural considerations), facilitate the ground handling problem, and provide retractable-self adjusting landing gear for any terrain.

PRELIMINARY PERFORMANCE ESTIMATES

Figure 59 indicates the proposed change in the plan form of the MCTV. To minimize sharp corners in the ejectors and compound curvatures, the modification shown is a compromise between the vehicle performance and manufacturing costs. It is necessary to have a continuous curtain around the perimeter of the vehicle with a minimum of inactive sections. With the proposed modification six identical ejectors would be fabricated, three for the front and three for the rear. In this way, an approximate elliptical planform is obtained with a minimum of modification. Figure 60 is a sketch of the proposed rework, showing the ejectors fixed in place (no variable θ), a very low vehicle silhouette, large contiguous area for payload and retractable Hovair pads. Figure 61 shows the two-dimensional performance obtainable from the modification. The curves plotted are from actual experimental data but have not been corrected for any three-dimensional or surface roughness effects which may be detrimental. It is obvious then, from the difference between the lift curve and empty weight of the vehicle, that an appropriate margin of performance is provided. The following

is a tabulation of the anticipated two-dimensional performance of the modified MCTV.

Weight, empty	= 2,500 lb
Lift at 18 inches	= 5,300 lb
Lift at 12 inches	= 7,200 lb
Maximum overload capability	= 20,000 lb (Hovair pads)
Base pressure at 18 inches	= 22.5 psfg
Base pressure at 12 inches	= 30.0 psfg
Primary mass flow	= 28 lb/sec
Primary pressure	= 7 psig
Horsepower	= 560
Maximum forward speed	= 25 mph
Maximum grade	= 10%

BIBLIOGRAPHY

1. Vinson, P., "Recirculation Principle for Ground Effect Machines," OR 2907, Martin Company, Orlando, Florida
2. Ortell, A., "Recirculation Principle for Ground Effect Machine, Two-Dimensional Tests," OR 2907, Martin Company, Orlando, Florida

TABLE I

<u>Configuration</u>	<u>Run Numbers</u>	<u>Description</u>
1	101 - 108	Original Model 1, Original Header, vary center body location
2	201 - 207	
3	301 - 307	
4	401 - 407	
5	501 - 703	Original Model 1, flush centerbody
6	801 - 805	Original Model 1, undercut centerbody
7	901 - 920	New Model 1, Airfoil Header, AR = 46
8	1001 - 1036	New Model 1, Airfoil Header, AR = 23
9	1101 - 1123	New Model 1, Finger Header, AR = 46
10	1201 - 1202	Original Model 1, Multi-Nozzle Header
11	1319 - 1327	Model 5, Base Run
12	1401 - 1406	Model 5, Exit Trunks
13	1501 - 1506	Model 5, Mod. Centerbody and Exit Flaps
14	1601 - 1606	Model 5, Exit Trunks
15	1701 - 1703	Model 5, Reverse Flow Base Run
16	1801 - 1802	Model 5, Reverse Flow, Exit Trunk, Small
17	1803 - 1804	Model 5, Reverse Flow, Exit Trunk, Large
18	1901 - 1909	Original Model 1, Base Run
19	2052, 2053, 2054, 2010 - 2015	Original Model 1, 12" Inner Exit Skirts, $\delta_L = 30^\circ$
20	2116 - 2121, 2155, 2156, 2157	Original Model 1, 12" Inner Exit Skirts, $\delta_L = 40^\circ$
21	2222 - 2224, 2249, 2251	Original Model 1, 12" Inner Exit Skirts, $\delta_L = 20^\circ$

TABLE I (cont'd)

<u>Configuration</u>	<u>Run Numbers</u>	<u>Description</u>
22	2325 - 2330	Original Model 1, Inlet Trunk, Large
23	2431 - 2436	Original Model 1, Inlet Trunk, Small
24	2537 - 2542	Original Model 1, Inner Inlet Skirt
25	2643 - 2648	Original Model 1, Outer Inlet Skirt
9	2701 - 2708	New Model 1, Base Run
26	2801 - 2806	New Model 1, Inner Inlet Skirt (check of Configuration 24)
18	2901 - 2909	Original Model 1, Ground Board - Grating
18	3010 - 3012, 3019 - 3024	Original Model 1, Ground Board - Simulated Grass
18	3113 - 3118 3125 - 3127	Original Model 1, Ground Board - Random Blocks

TABLE II
STABILITY AND CONTROL

Run	<i>h</i> (inches)	<i>P</i> (psi)	α (°)	β	Exit Flaps	\bar{P}_B (gauge)	\bar{M} (gauge)	\bar{L} (gauge)	Tertiary Flow m/m_1'	m_1	m_2	m_3	R
1	7	5	5	0	+5 -5 0	20.3	4.8	1/4	4.2	4.0	11.9	11.2	
2	7	10	10			40.1	13.8	233	5.9	5.7	11.3	10.8	
3	7	20	20			63.6	43.4	359	7.9	7.3	10.0	9.7	
4	5	10	10			36.0	21.9	210	6.1	5.7	11.7	10.7	
5	5		-1.8			29.0	66.6	188	5.6	4.8	10.7	9.1	
6	5		0.5			34.7	13.1	205	6.3	5.7	11.9	10.8	
7	5		1.7			26.6	51.4	169	5.4	5.3	10.2	10.0	
8	7		-3.5			31.6	15.6	177	5.5	5.6	10.4	10.6	
9			-1.75			34.7	18.5	199	5.7	5.5	10.8	10.4	
10			3.5			32.4	11.6	185	6.0	5.3	11.4	9.9	
11			2.34			36.0	13.5	212	6.0	5.4	11.3	10.3	
12			1.2			37.5	10.4	222	5.9	5.5	11.2	10.4	
13			0			23.4	12.6	133	5.2	4.9	9.8	9.2	
14			-3.5			23.0	-2.6	135	4.9	5.0	9.3	9.4	
15			-1.75			26.6	6.6	154	5.1	5.2	9.7	9.8	
16			5.82			13.5	63.8	92	4.7	4.3	8.9	8.1	
17			1.68			14.9	68.6	102	5.3	4.4	10.0	8.4	
18			3.5			17.5	29.3	117	5.1	4.5	9.7	8.5	
19			1.2			24.5	11.2	140	5.2	4.8	9.9	9.2	
20			0			37.0	1.0	213	5.6	5.7	11.3	10.3	
21			1/2			38.8	-2.3	226	5.7	6.0	12.3	10.3	

STABILITY AND CONTROL

RUN	h (INCHES)	b'	R	α (°)	β	EXIT FLAPS	\bar{F}_B (lb/ft)	M (lb/ft)	TERTIARY FLOW	m/m'
	L	R	δ_L	δ_R	δ_f		m_L	m_R	L	R
22	7	7	1/3	0	+5	-5	0	38.0	-9.3	2.22
23		5	1/5		+5	-5		28.0	-25.0	1/3.0
24		10	1/0		+1	-9		36.5	1/5.9	1/2.8
25		10	1/0		-3	-1/3		35.5	1/3.3	1/1.0
26		10	1/0		-7	-1/7		35.2	2/3.0	1/0.2
27		10	1/0		+9	+1		36.1	1/3.5	1/0.9
28	12	5	5		-3.5	+3.5	-10	7.7	9.6	4/1
29	12	10	1/0					16.7	3/1.6	9/0
30	12	1/2	1/5					23.0	1/2.4	5/6
31	14	10	1/0					12.0	1/1.5	7/5
32	14	1/5	1/5					18.0	1/4.6	10/9
50	12	-	-5		-	+4.7	1/2	3.3	8.6	-
51	12	-	1/0					16.6	-	-
52	12	-	1/5					29.6	-	-
53	14	-	5					6.1	-	-
54	14	-	1/0					13.0	-	-
55	14	-	1/5					19.8	-	-
56	16	-	5					5.4	-	-
57	16	-	1/0					11.7	-	-
58	16	-	1/5					17.3	-	-
59	12	5	5		-4.6	+4.6	1/2	9.5		

STABILITY AND CONTROL

Run	h (inches)	θ'	α (°)	β	Exit	Flaps	\bar{P}_B (psig)	M_1 (lb/ft)	L	Terrain Flow	m_p'
		L	R		δ_i	δ_f			L	R	
60	12	10	0	-4.6	+4.6	12	3.3	19.0			
61	12	1.5	1.5	-4.6	+4.6	12		27.5			
62	9	5	5	-10.0	+10.0	15		16.7			
63	10	10		-10.0	+10.0	15		35.0			
64	15	15		-10.0	+10.0	15		51.0			
65	5	5		0	0	9		14.2	-9.2	9.1	4.1
66	10	10		0	0	11.5		34.0	-22.9	18.7	5.9
67	15	15		0	0	11.5		49.0	-46.9	26.7	7.1
70	5	5		+4	-7	0		16.0	-1.0	8.6	3.9
71	10	10						31.0	-8.2	16.4	5.5
72	15	15						44.5	-21.0	22.8	6.6
73	10	10						28.0	-1.0	15.6	5.4

TABLE III
2-D PERFORMANCE

RUN	Config	Area Ratio	Exit Flaps Inner Outer Inches	h	P_0' (PSIG) (inches)	η' (PSIG)	P_B' (PSIG)	P_c (PSIG)	η/m' (PSIG)	P_{01}' (PSIG)	Press. Recover.	ϵ (%)	P_B/P_{01} (%)
101	-	-	-	-	-	-	-	-	-	-	-	-	-
102	1	7.3	-	18	4.5	1.37	82.4	111.4	-	-	.47	7.7	-
103	1	-	-	-	4.0	1.26	78.5	102.5	-	-	.51	7.8	-
104	1	-	-	-	3.4	1.11	58.7	86.8	-	-	.50	7.5	-
105	1	-	-	-	2.8	1.03	48.1	75.8	-	-	.50	7.5	-
106	1	-	-	-	2.2	.84	36.0	58.5	-	-	.46	6.7	-
107	1	-	-	-	1.6	.72	26.6	44.1	-	-	.45	6.5	-
108	1	-	-	-	1.0	.55	13.8	28.4	-	-	.45	6.5	-
201	2	-	-	-	1.0	.55	13.8	28.8	-	-	.46	6.6	-
202	2	-	-	-	1.6	.71	26.2	43.6	-	-	.45	6.5	-
203	2	-	-	-	2.2	.83	35.7	50.1	-	-	.46	6.6	-
204	2	-	-	-	2.8	1.03	48.0	74.7	-	-	.46	6.6	-
205	2	-	-	-	3.4	1.11	58.3	85.5	-	-	.46	6.6	-
206	2	-	-	-	4.0	1.26	71.4	99.5	-	-	.46	6.6	-
207	2	-	-	-	4.5	1.39	84.1	112.0	-	-	.47	7.7	-
301	3	-	-	-	10	.55	13.8	24.8	-	-	.28	5.6	-
302	3	-	-	-	16	.71	26.3	38.7	-	-	.27	5.7	-
303	3	-	-	-	2.2	.83	35.7	50.4	-	-	.32	6.1	-
304	3	-	-	-	2.8	1.03	48.0	63.9	-	-	.32	6.2	-
305	3	-	-	-	3.4	1.11	58.3	76.5	-	-	.34	6.7	-
306	3	-	-	-	4.0	1.26	72.0	86.0	-	-	.35	6.5	-

2-D PERFORMANCE

RUN	CONFIG.	AREA RATIO	ELAETS	P_0'	m'	H_P	P_B	η/m'	\bar{P}_o^3	PRESS RECOVERY	ϵ	P_B/\bar{P}_o^3
			INNER	(PSIG)	(INCHES)	(LB/FT)	(PSFg)	—	(PSFg)	(%)	—	—
306	3	7.3	—	1.8	40	1.26	72.0	86.0	—	.35	6.5	—
401	4	—	—	10	.55	13.8	25.2	—	.25	5.7	—	—
402	4	—	—	16	.71	26.3	36.9	—	.25	5.5	—	—
403	4	—	—	22	.83	35.7	51.1	—	.33	6.9	—	—
404	4	—	—	28	1.03	48.0	70.1	—	.34	7.0	—	—
405	4	—	—	34	1.11	58.3	82.0	—	.35	7.2	—	—
406	4	—	—	40	1.26	72.0	95.5	—	.35	7.3	—	—
407	4	—	—	45	1.39	84.1	107.5	—	.35	7.4	—	—
501	5	3.5	40	44	1.40	83.4	102.2	—	.70	—	—	—
502	5	—	40	1.27	72.2	96.0	—	.73	—	—	—	—
503	5	—	35	1.13	60.4	86.6	—	.74	—	—	—	—
504	5	—	28	1.00	48.0	69.8	—	.6.9	—	—	—	—
505	5	—	22	.85	36.2	55.4	—	.6.6	—	—	—	—
506	5	—	16	.71	26.3	42.3	—	.6.3	—	—	—	—
507	5	—	10	.54	13.6	27.0	—	.6.2	—	—	—	—
508	5	—	4.5	1.38	83.3	113.8	—	7.8	—	—	—	—
509	5	—	28	1.02	48.1	72.0	—	7.1	—	—	—	—
510	5	—	10	.53	13.2	26.1	—	6.1	—	—	—	—
601	5	—	4.5	1.38	83.4	120.7	—	8.3	—	—	—	—
602	5	—	28	1.02	47.5	73.5	—	7.4	—	—	—	—
603	5	—	10	.53	13.4	27.9	—	6.5	—	—	—	—

2-D PERFORMANCE

RUN	CONFIG AREA RATIO	INNER FLAPS	EXIT OUT-ER (INCHES)	P_0' (psig)	\dot{m}' (lb/sec/ft) (lb/sec/ft)	P_B (psfg)	ρ_c (psfg)	m/m' T_{03} (psfg) Recovery (%)	PRES. ϵ (psfg) Recovery (%)	P_B/ρ_c^2
604	5	73	35	40	18	40	1.26	74.6	103.5	-
605	5					35	1.16	61.3	94.6	-
606	5					22	.84	26.4	58.5	-
607	5					16	.69	43.2	-	6.8
608	5									3.6
609	5									3.6
610	5									3.1
611	5									7.0
612	5									8.3
613	5									9.0
614	5									8.5
615	5									8.1
616	5									5.8
701	5									8.8
702	5									8.0
703	5									5.3
801	6									7.6
802	6									8.2
803	6									8.5
804	6									8.7
805	6									9.1

2-D PERFORMANCE

RUN	CONFIG	AREA RATIO	EXIT FLAPS	h	P_0'	m'	ρ_0'	ρ_e	m/m'	$P_{0,3}$	Press.	ϵ	$P_{0,3}/P_{0,2}$	
		(KHE3)	(PS19)	(KHE3)	(PS19)	(KHE3)	(PS19)	(PS19)	-	(PS19)	Recom.	(%)	(%)	
901	7	46.7	24.5	4.3	1.8	15.5	.93	35.1	50.7	4.4	8.3	1.2		
902						15.5	.74	35.1	55.7	7.6	8.2	6.6	.60	
903						15.8	1.03	36.1	44.0	9.4	6.2		.32	
904						15.7	1.05	35.8	58.8	8.1	7.4		.53	
905						10.5	.79	21.0	37.7	5.2	8.0		.46	
906						5.3	.54	8.2	18.4	2.4	8.0		.41	
907						3.3	.39	11.2	8.5				.61	
908						3.2	.39	3.8	10.3	1.5	2.9		.34	
909	↓		↓	↓	↓	5.4	.54	8.4	18.4	2.4	8.2		.42	
910	-	-	-	-	-	-	-	-	-	-	-		-	
911	7	46.7	24.5	4.3	1.8	10.2	.80	20.1	40.0	4.8	7.8		.50	
912						24	3.0	.39	3.6	6.3	.7	7.0		.24
913						24	5.6	.54	8.7	11.7	1.1	7.5		.24
914						24	10.4	.78	20.4	22.0	2.0	6.4		.26
915						12	4.0	.41	3.9	12.1	0	8.8		.42
916						12	5.2	.53	8.1	22.5	0	9.2		.49
917						12	10.5	.79	20.8	44.5	1.0	8.0		.54
918						12	15.2	1.01	34.2	64.0	1.8	8.4		.63
919						6	15.6	1.02	35.0	59.3	-19.0	7.4		.48
920						6	12.9	.92	28.1	45.3	-16.0	7.5		.46
921	↓		↓	↓	↓	6	10.5	.79	20.7	34.6	-19.0	7.9		.44

2-D PERFORMANCE

Run	Config	Area Ratio	Inner	Outer	Flaps	β	P_a'	m'	$40'$	P_c	m/m'	\overline{P}_{03}	Press.	ϵ	P_{03}/\overline{P}_{03}
			(inches)	(inches)	(psig)	(lb/ft ²)	(psig)	(psig)	(psig)	(psig)	-	(psig)	(% of Recurr.)	(%)	(%)
922	7	46.7	24.5	43	6	8.1	.68	14.9	27.0	-11.0	8.2		.44	2.8	
923					6	5.4	1.53	8.4	17.1	-7.0	8.3				
924					6	3.3	.40	4.1	9.4	-4.5	8.2		.40	2.6	
925					24	15.5	1.01	34.4	35.0	3.1	5.9		.34	2.3	
926	▼		▼	▼	24	13.0	.87	29.1	28.7	2.2	6.2		.24	4.8	
1001	8	23	37	36	8	17.0	1.97	65.8	95.6	14.0	5.0		.53	7.7	
1002					14.3	1.79	53.4	82.2	12.0	5.2			.54	7.6	
1003					10.9	1.49	36.7	63.3	8.0	5.4			.52	7.5	
1004					8.1	1.29	27.8	42.4	4.0	5.4			.46	6.8	
1005					5.6	1.04	16.8	33.7	4.5	5.6			.43	6.8	
1006					3.2	1.78	7.7	18.9	2.8	5.4			.38	6.4	
1007					2.4	17.0	1.96	65.8	52.5	12.0	3.8		.29	5.1	
1008					14.5	1.75	53.4	46.2	10.0	4.0			.29	5.2	
1009					3.3	.80	8.3	12.1	2.7	4.5			.25	4.7	
1010					5.6	1.02	16.5	30.7	4.5	4.4			.25	5.1	
1011					8.3	1.27	27.9	28.3	5.9	3.7			.24	4.9	
1012					11.5	1.51	38.8	38.6	7.9	4.1			.28	5.4	
1013					12	17.5	1.96	65.8	109.5	12.0	5.5		.73	6.7	
1014					12	14.4	1.76	53.4	91.4	10.0	5.7		.72	6.4	
1015					12	11.5	1.52	38.8	75.9	7.6	5.8		.73	6.6	
1016	▼	33	21	12	18.0	1.96	65.8	121.0	19.8	5.2			.68	7.4	

2-D PERFORMANCE

Run	Config Ratio	Area	Exit Flaps	h	P_0'	$\frac{P_0}{P_0'}$	P_c	η/m'	\overline{P}_0^3	Press.	ϵ	$P_0/\frac{P_0'}{(1-\epsilon)}$
			INNER	OUTER	(inches)	(psig)	(lb/ft ²)	(psig)	(psig)	RECOVERY	(%)	(%)
1017	8	23	3.3	2.1	1/2	1.42	1.72	53.4	97.9	16.2	5.3	6.0
1018						11.5	1.53	38.8	80.8	13.0	5.4	6.2
1019						7.5	1.23	25.1	58.4	9.4	5.5	5.1
1020						5.1	1.05	17.1	43.5	7.6	5.5	4.7
1021						3.2	0.80	8.1	26.0	4.7	5.5	4.4
1022			3.7	3.6		7.7	1.26	26.3	54.8	5.7	6.0	6.4
1023						5.8	1.03	17.9	41.3	4.5	6.2	6.4
1024						3.3	0.82	8.5	24.7	2.7	6.2	6.0
1025						6	7.5	1.25	35.5	46.7	-11.7	5.1
1026						6.2	1.07	18.9	35.9	-9.4	5.0	6.0
1027						3.2	0.80	8.1	20.2	-4.5	5.0	5.9
1028						14.1	1.93	62.1	102.0	-15.8	5.1	4.1
1029						11.8	1.76	50.2	89.0	-16.7	5.2	3.6
1030						10.0	1.53	38.6	69.6	-13.5	5.1	3.6
1031						15.0	1.96	45.7	142.4	20.7	5.3	5.2
1032						12.0	1.75	50.3	120.0	12.5	5.9	5.1
1033						10.0	1.52	38.6	99.3	14.4	5.5	4.3
1034						7.7	1.24	25.9	70.0	11.7	5.8	5.0
1035						5.8	1.07	17.9	51.6	9.4	5.6	4.7
1036						3.2	0.79	7.9	31.0	5.8	5.8	4.9

2-D PERFORMANCE

RUN	CONFIG.	AREA RATIO	EXIT INNER	FLAPS OUTER	h (INCHES)	P_0' (PSIG)	m' (lb/ft ²)	ρ_B (psfg)	ρ_c (psfg)	m_{in}' (psfg)	$\frac{P_{O_2}}{P_{O_1}}$	PRESS. RECOVERY (%)	$\frac{P_{O_2}}{(P_{O_1})^{2/3}}$
1101	9	46	37	36	18	17.5							
1102													
1103													
1104													
1105													
1106													
1107													
1108													
1109													
1110													
1111													
1112													
1113													
1114													
1115													
1116													
1117													
1118													
1119													
1120													
1121													

2-D PERFORMANCE

Run	Config Area	Exit Flaps	h	P_0'	m'	P_0	P_c	m/m'	P_{c3}	Press.	E	P_0 / P_{c3}
		INNER	OUTER	(INCHES)	(psig)	(lb/ft ²)	(psig)	(psig)	(psig)	-	(%)	(%)
1122	9	46	37	36	/8	4.4						
1123	9	46	37	36	/8	2.2						
1201	10	73	32.5	6.5	/2	10			27.0			
1202	10	73	32.5	6.5	/2	30			69.1			

TABLE IV
SKIRTS AND TRUNKS

RUN	CONFIG	AREA	EXIT	FLAPS	<i>h</i>	<i>P_{0'}</i>	<i>m'</i>	<i>H_{0'}</i>	<i>P_c</i>	<i>m/m'</i>	<i>P₀₃</i>	<i>E</i>	<i>P_{c3}</i>	<i>E₃</i>
1319	1/1	2.30		(WASHED OUT)	17	17	3.7	.00468	6.86	8.55	—	(postg)	(postg)	(postg)
1320					17	17	3.0	.00406	5.20	6.3	1.35			
1321					17	17	2.0	.00315	3.19	4.95	1.35			
1322					12	12	3.7	.00466	6.86	10.3	-1.45			
1323					12	12	3.0	.00401	5.35	9.0	-1.5			
1324					12	12	2.0	.00308	3.22	6.75	-1.5			
1325					6	6	3.7	.00466	6.87	13.5	1.35			
1326					6	6	3.0	.00401	5.35	13.0	1.2			
1327					6	6	2.0	.00308	3.22	8.1	1.85			
1401	1/2	2.30			17	2.0	.00308	3.22	4.1	1.9				
1402					17	3.0	.00395	5.38	5.85	1.4				
1403					17	4.0	.00482	7.87	7.2	1.6				
1404					12	2.0	.00308	3.22	6.75	0				
1405					12	3.0	.00395	5.37	9.0	-4.5				
1406					12	3.9	.00469	7.56	12.6	0				
1501	1/2	2.30			12	2.0	.00311	3.22	6.75	—				
1502					12	3.0	.00395	5.00	10.35	—				
1503					12	3.9	.00472	7.55	12.6	—				
1504					17	2.0	.00308	3.28	3.15	—				
1505					17	3.0	.00395	5.48	4.5	—				
1506					17	3.9	.00472	7.55	5.4	—				

SKIRTS AND TRUNKS

RUN	CONFIG	AREA	EXIT	FLAPS	<i>h'</i>	<i>P_{0'}</i>	<i>m'</i>	<i>P₀</i>	<i>P</i>	<i>m'/m₁'</i>	<i>P₀/P₀'</i>	<i>P₀/P₀'</i> (%)
NUMBER			INNER	OUTER	(inches)	(PSIG)	(PSIG)	(PSIG)	(PSIG)	(PSIG)	(PSIG)	(PSIG)
1601	14	230			17		20	.003605	3.35	3.6	1.3	
1602					17		30	.003935	5.48	4.95	1.3	
1603					17		38.5	.004466	7.52	5.45	1.3	
1604					12		20	.00311	3.28	4.95	1.3	
1605					12		30	.003935	5.48	7.9	1.3	
1606					12		40	.00482	7.9	10.35	1.3	
1701	15	230										
1702					6		36	.00448	3.9	-2.6		
1703					17		36	.00445	9.9	-5.2		
1801	16				12		35	.00454	2.6	-.5		
1802					17		35	.00451	3.9	-2.6		
1803					12		35	.00445	3.12	-2.3		
1804					17		35	.00443	6.5	-2.9		

SKIRTS AND TRUNKS

RUN	CONFIG	AREA RATIO	EXIT FLAPS	4 INCHES OUTER	6 INCHES INNER	P_0' (PSIG)	H_P' (in/ft)	P_E (PSIG)	$\frac{P_0}{P_{SRE}}$ (%)	$\frac{E}{E_{SRE}}$ (%)
1901	18	73		12		10	.0246	21.6	29.7	-1.7
1902	1			12		20	.0360	48.2	50.9	-4.4
1903				12		30	.0472	77.8	68.0	-8.0
1904				18		10	.0246	21.6	13.5	2.3
1905				18		20	.0360	48.2	24.3	3.7
1906				18		30	.0472	77.8	32.9	5.0
1907				24		10	.0247	21.3	10.4	2.0
1908				24		20	.0364	47.8	19.8	3.9
1909				24		30	.0476	77.0	27.0	5.3
2052	19	73		12		10		24.8		
2053				12		20		47.7		
2054				12		30		68.5		
2010				18		10	.0246	21.6	-5	
2011				18		20	.0360	39.6	-1.5	
2012				18		30	.0472	51.3	-4.8	
2013				24		10	.0247	10.8	3.2	
2014				24		20	.0362	18.5	4.9	
2015				24		30	.0474	25.2	7.0	

SKIRTS AND TRUNKS

RUN	CONFIG	AREA	EXIT FLAPS	h'	P_0'	\dot{m}'	P_0	\dot{m}/m_1	P_0^3	\dot{m}_3/m_1	$P_0/\frac{P_0}{\rho_{STC}}$
2155	20	73		12	10				19.4		
2156				12	20				37.0		
2157				12	30				55.0		
2116				18	10	.0847			18.9	.3	
2117				18	20	.0364			35.8	.9	
2118				18	30	.0476			38.7	2.1	
2119				24	10	.0247			10.4	2.3	
2120				24	20	.0364			18.9	4.6	
2121	↓		→	24	30	.0476			24.3	6.5	
2249	21	73		12	10				25.2		
2250				12	20				49.2		
2251				12	30				70.3		
2222				18	10	.0247			19.4	3.2	
2223				18	20	.0364			33.3	6.0	
2224	↓		→	18	30	.0476			44.6	8.7	
2325	22	73		18	10	.0250			24.6	.7	
2326				18	20	.0368			46.3	0	
2327				18	30	.0482			62.4	-.9	
2328				24	10	.0250			14.6	1.7	
2329				24	20	.0368			27.7	3.3	
2330	1		↓	24	30	.0492			40.2	5.7	

SKIRTS AND TRUNKS

RUN	CONFIG	AREA RATIO	EXIT FLAPS	b'	b''	m'	H'	P_B	η_{m1}	\bar{P}_0	E
			INNER	OUTER	INCHES	INCHES	16/SCC	4/ET	PSFC	PSFC	(%)
2431	23	73			18		10	.0250		19.8	0
2432					18		20	.0368		41.8	-1.2
2433					18		30	.0482		61.2	-2.8
2434					24		10	.0250		11.7	.5
2435					24		20	.0368		23.4	2.9
2436					24		30	.0482		34.6	5.0
2537	24	73			18		10	.0250		24.1	-7
2538					18		20	.0368		46.3	-2.9
2539					18		30	.0482		63.8	-4.6
2540					24		10	.0250		12.6	1.7
2541					24		20	.0368		25.9	3.5
2542					24		30	.0482		36.9	4.8
2643	25	73			18		10	.0250		15.8	
2644					18		20	.0368		17.5	
2645					18		30	.0482		38.3	
2646					24		10	.0250		8.1	
2647					24		20	.0368		16.2	
2648					24		30	.0482		23.9	

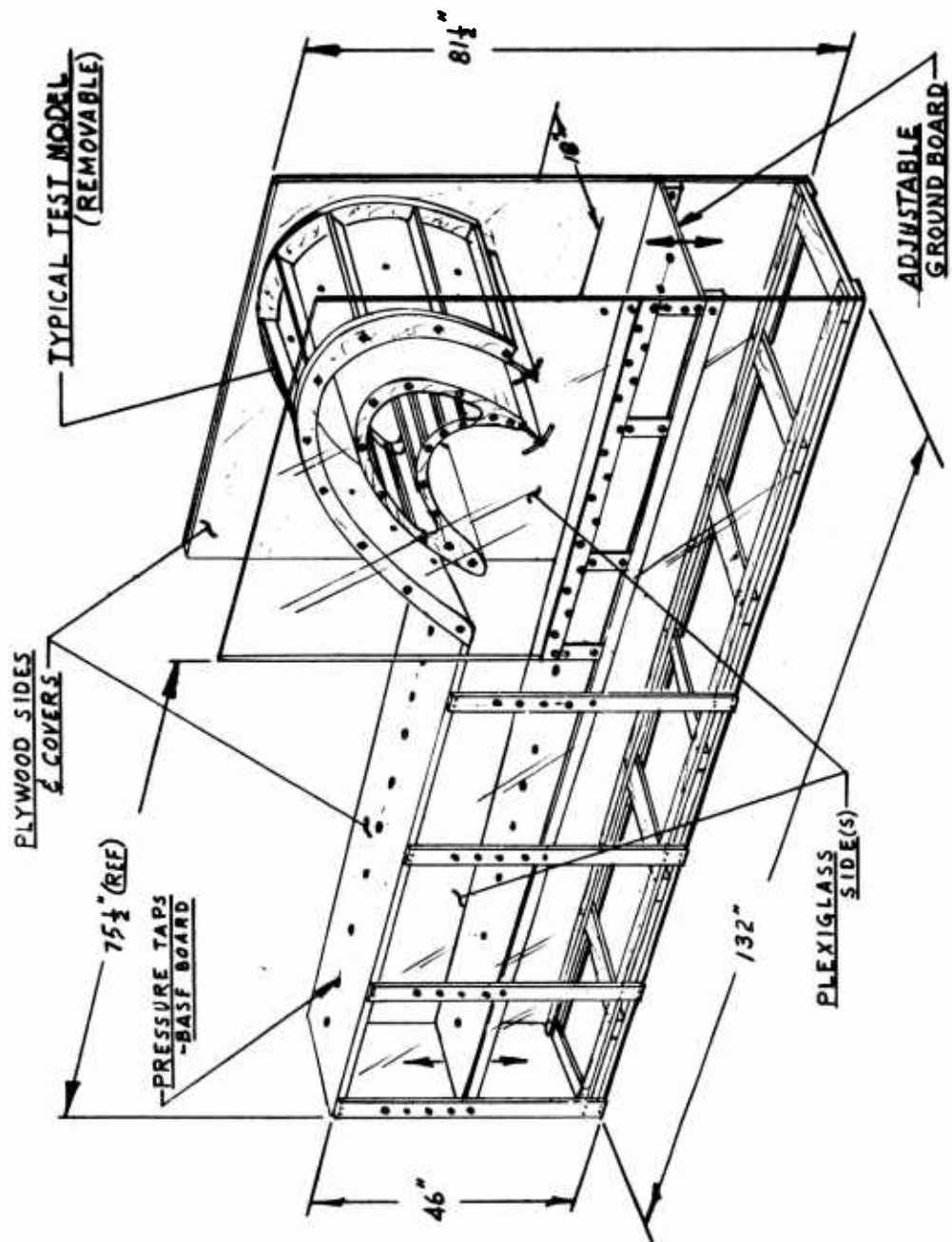


Figure 1. Two-Dimensional Test Device

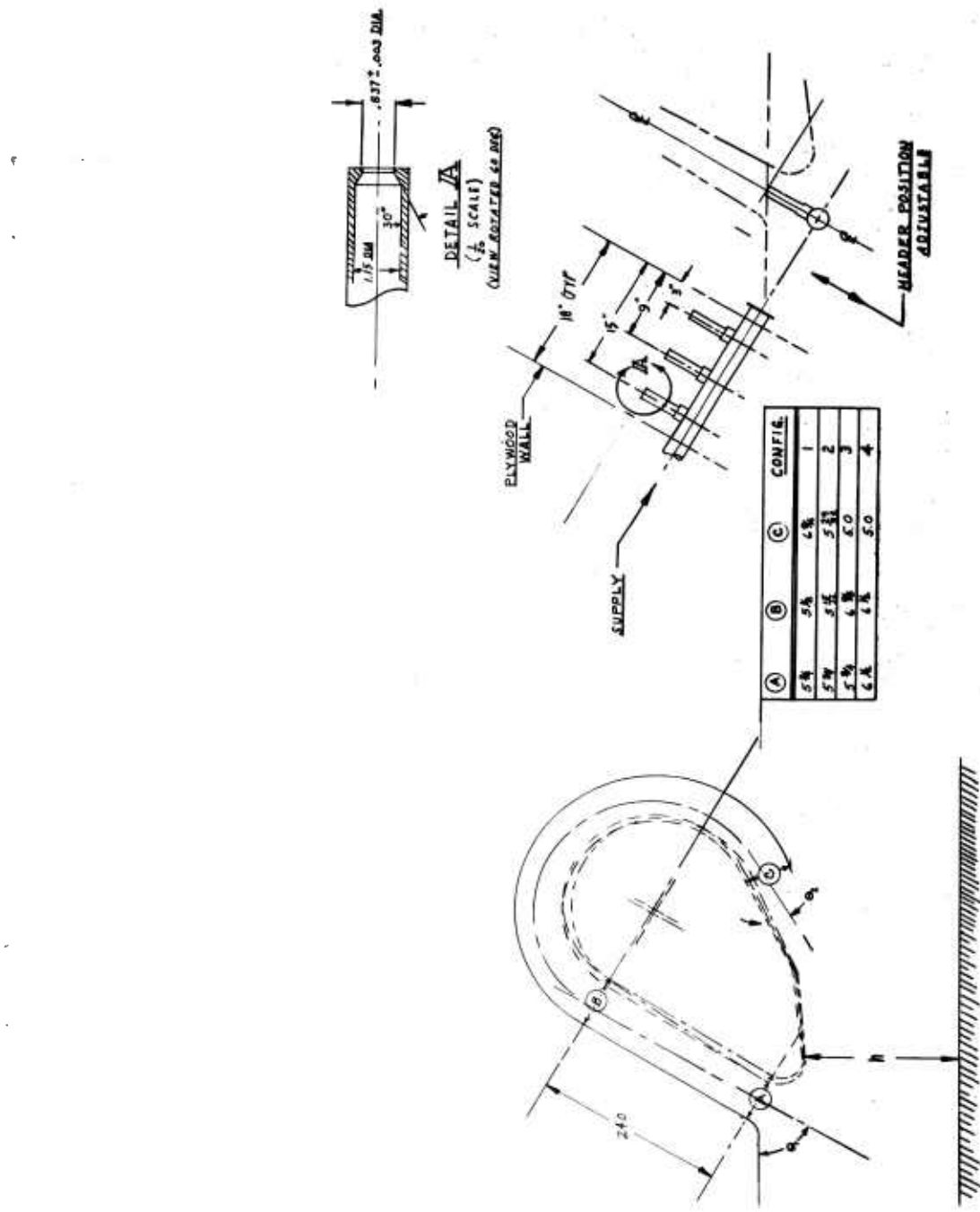


Figure 2. Original Model 1, Configurations 1-4, Sketch.

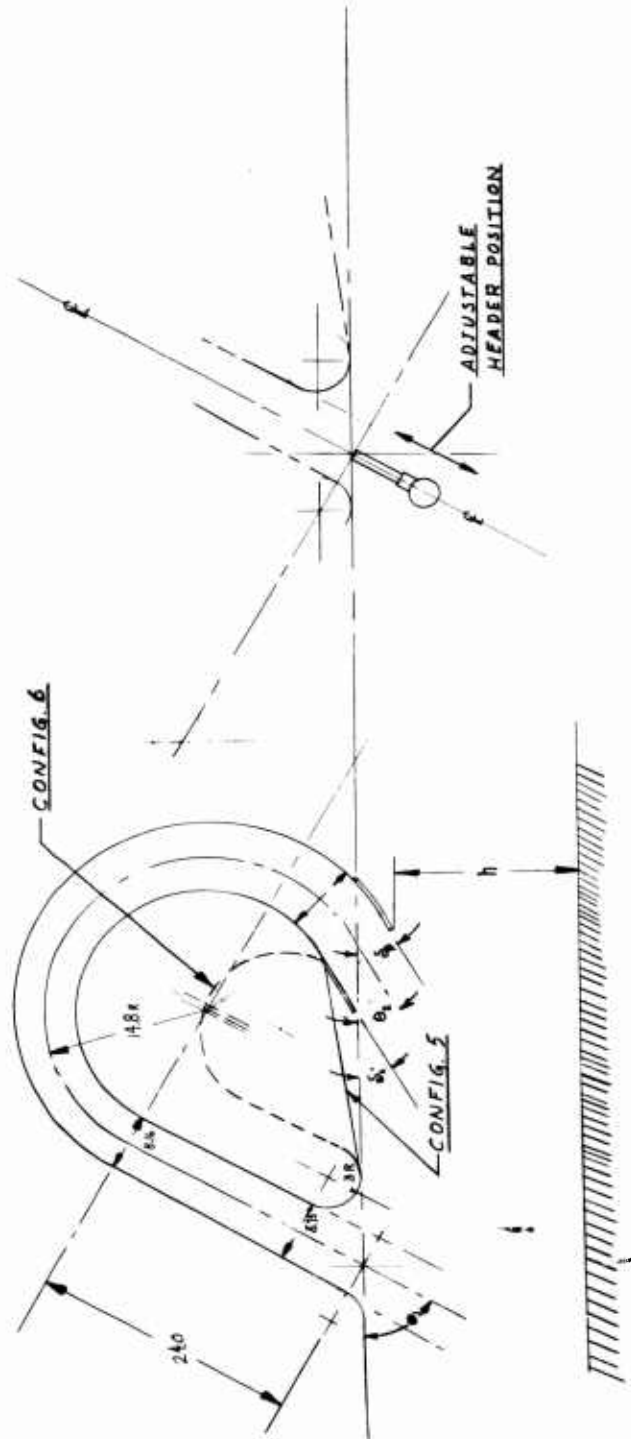


Figure 3. Original Model 1, Configurations 5 and 6, Sketch.

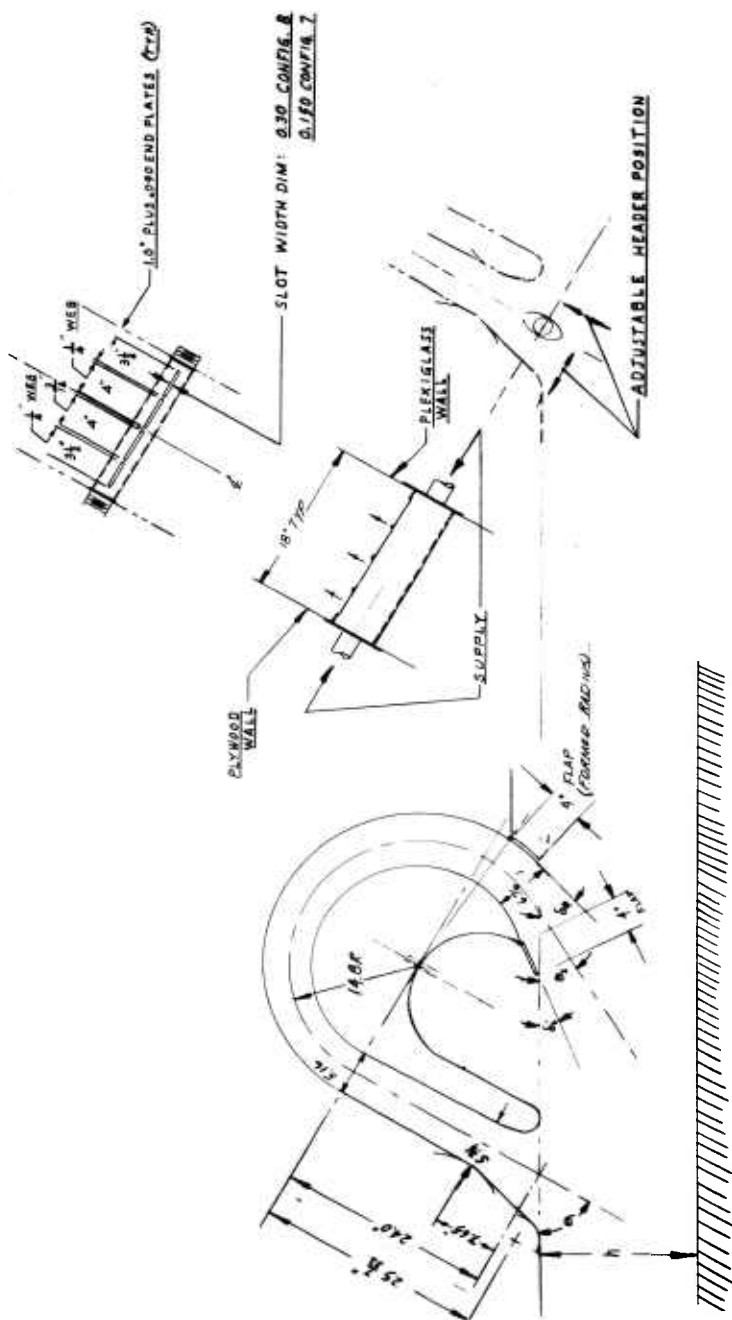


Figure 4. Modified Model 1, Configurations 7 and 8, Sketch.

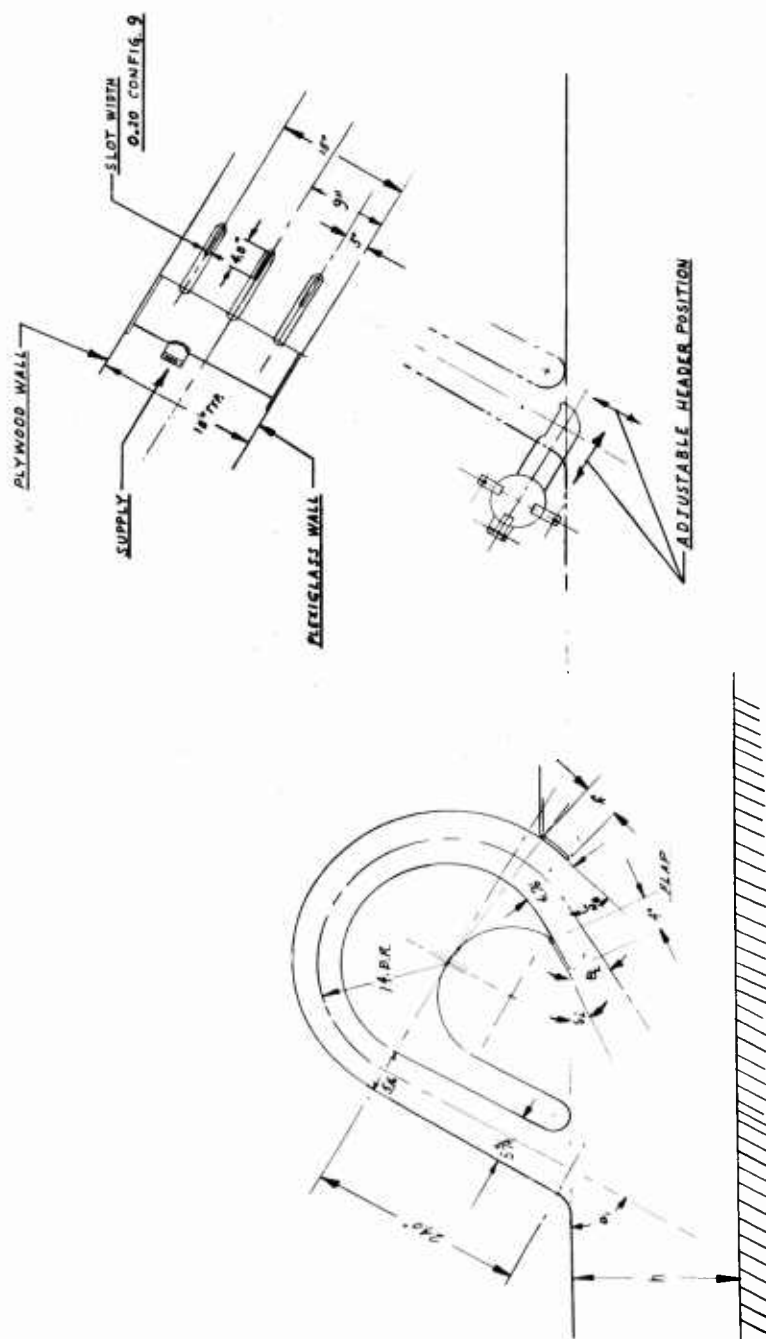


Figure 5. Modified Model 1, Configuration 9, Sketch.



Figure 6. Typical Test Installation.

Figure 7. Modified Model 1.



0190-37688-X

Figure 8. Airfoil Header and Inlet Rake.





Figure 9. Exit Flaps and Rakes.

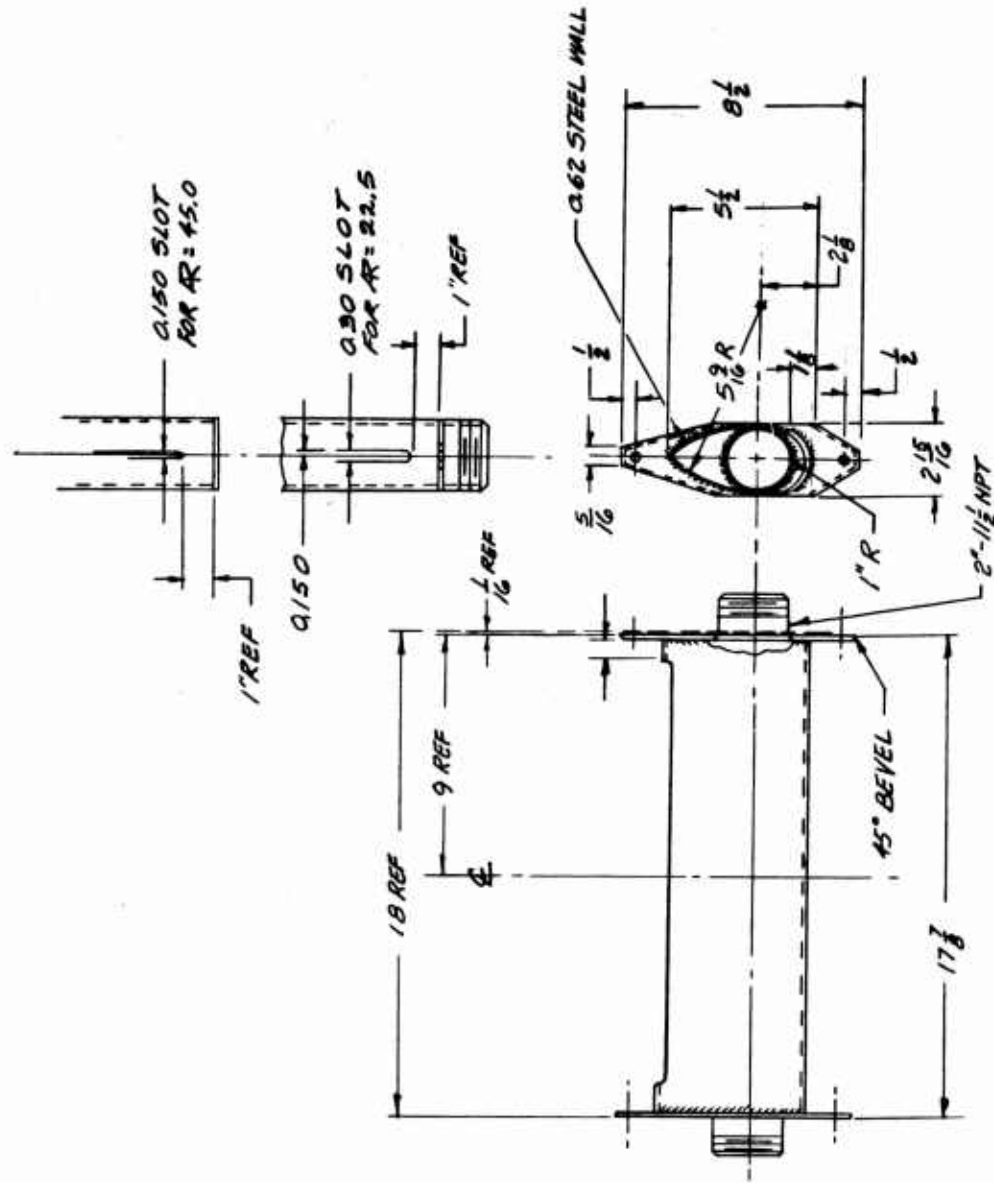


Figure 10. Airfoil Header, Sketch.

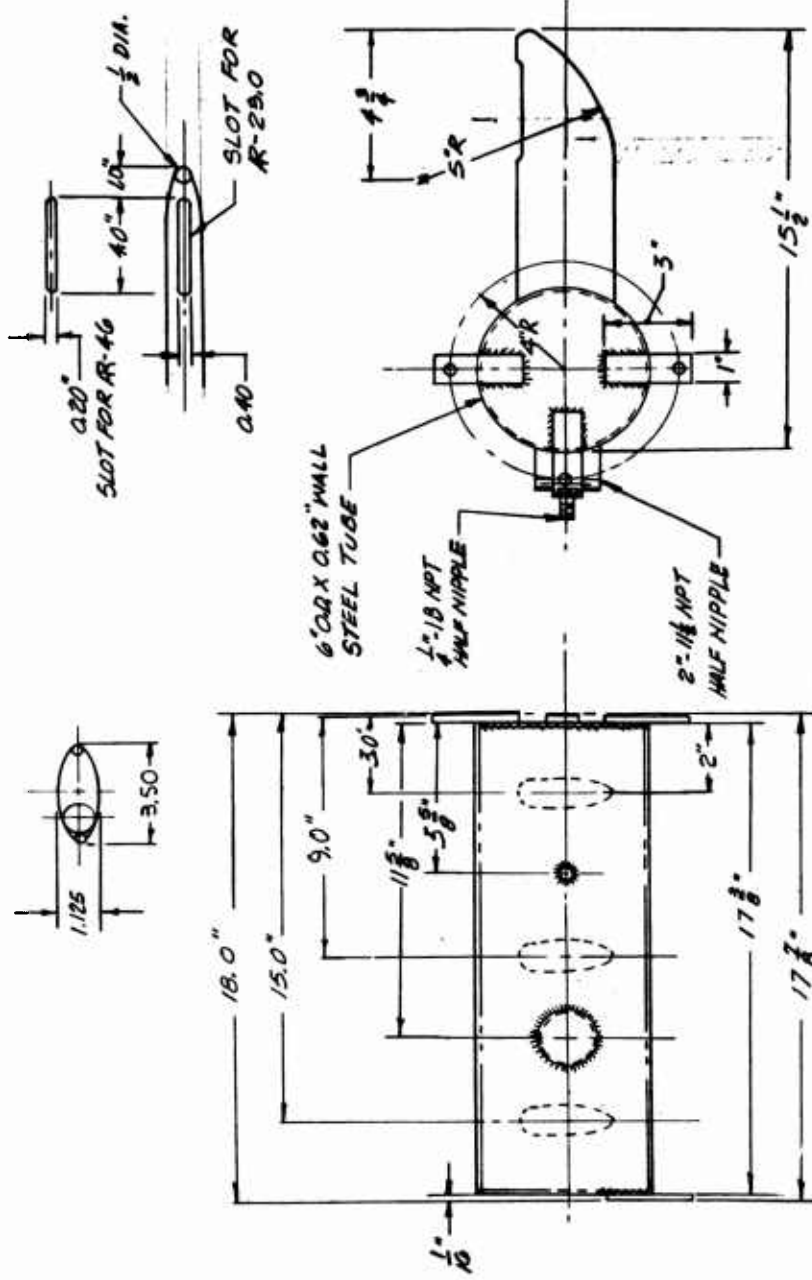
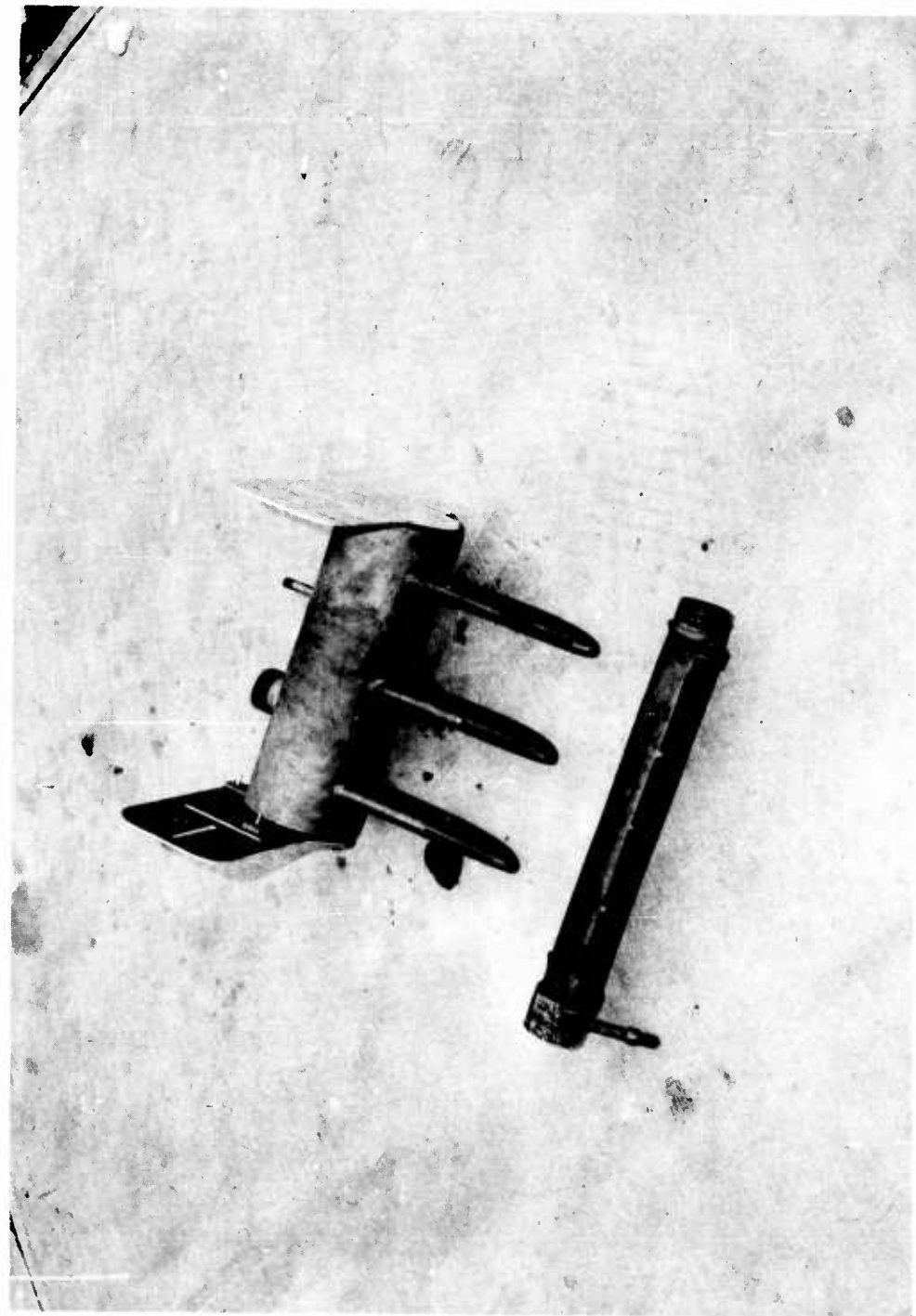


Figure 11. Finger Header, Sketch.

Figure 12. Primary Headers.



OJ93-33278-X

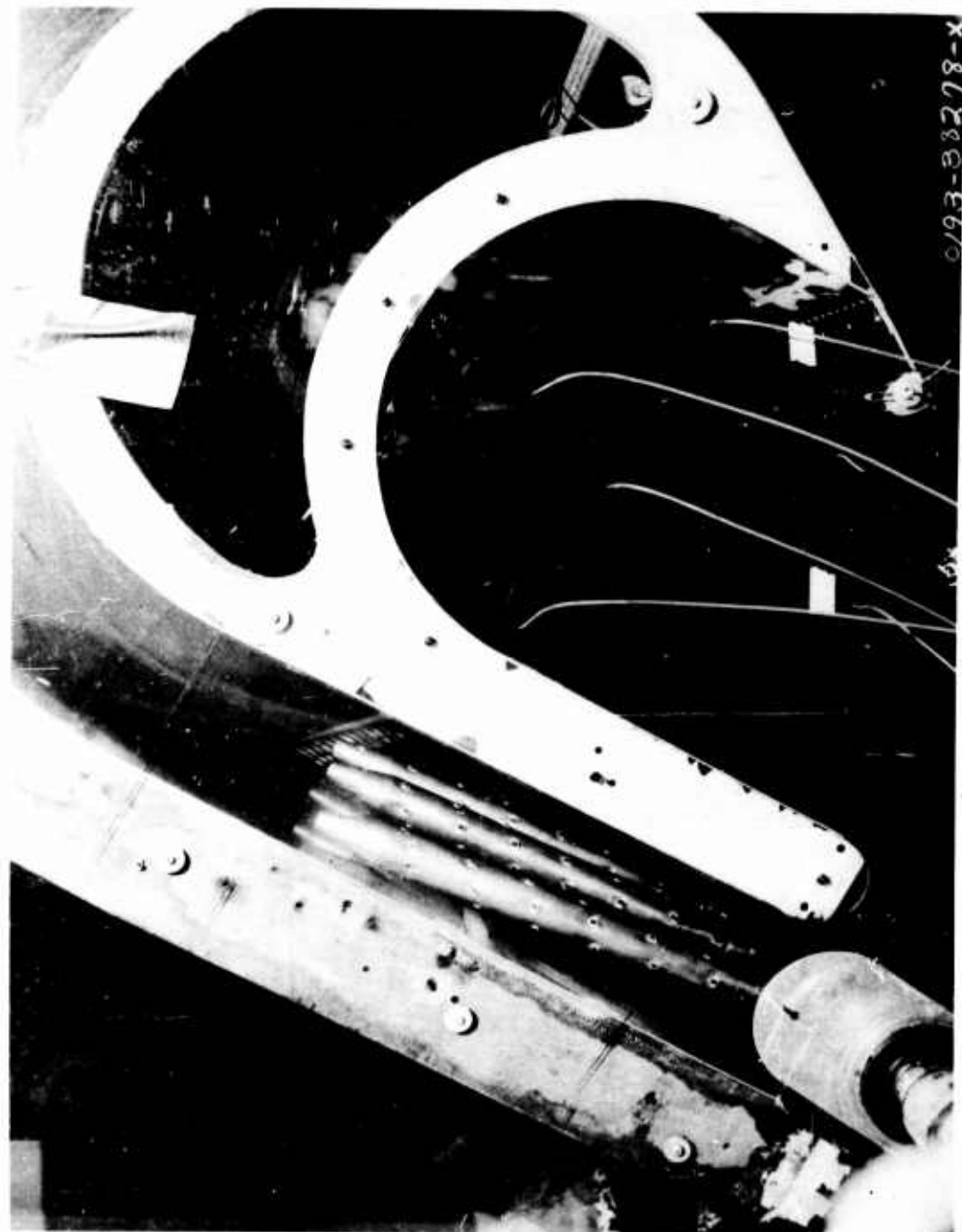


Figure 13. Multiple Nozzle Headers.

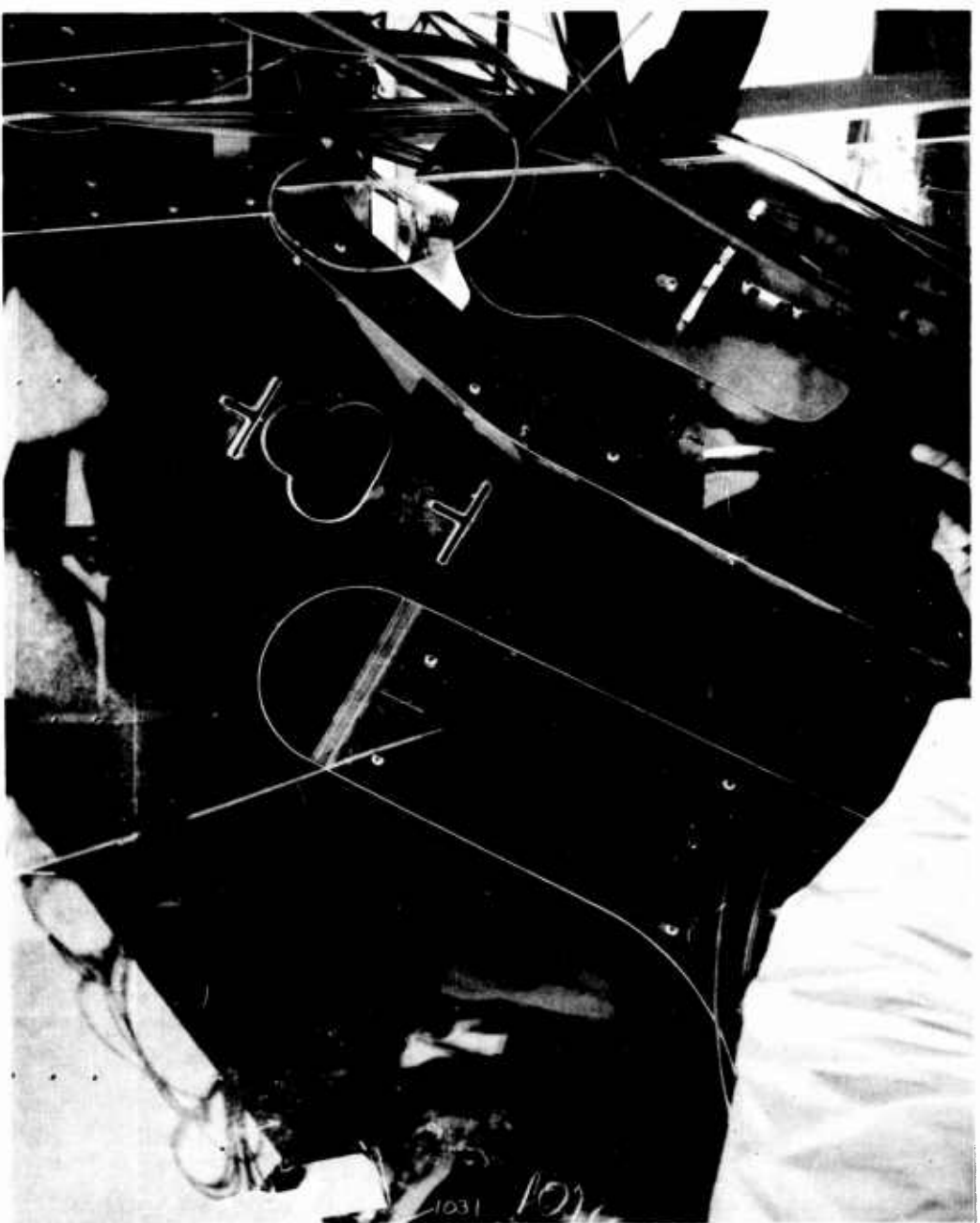


Figure 14. Finger Header, Installed.

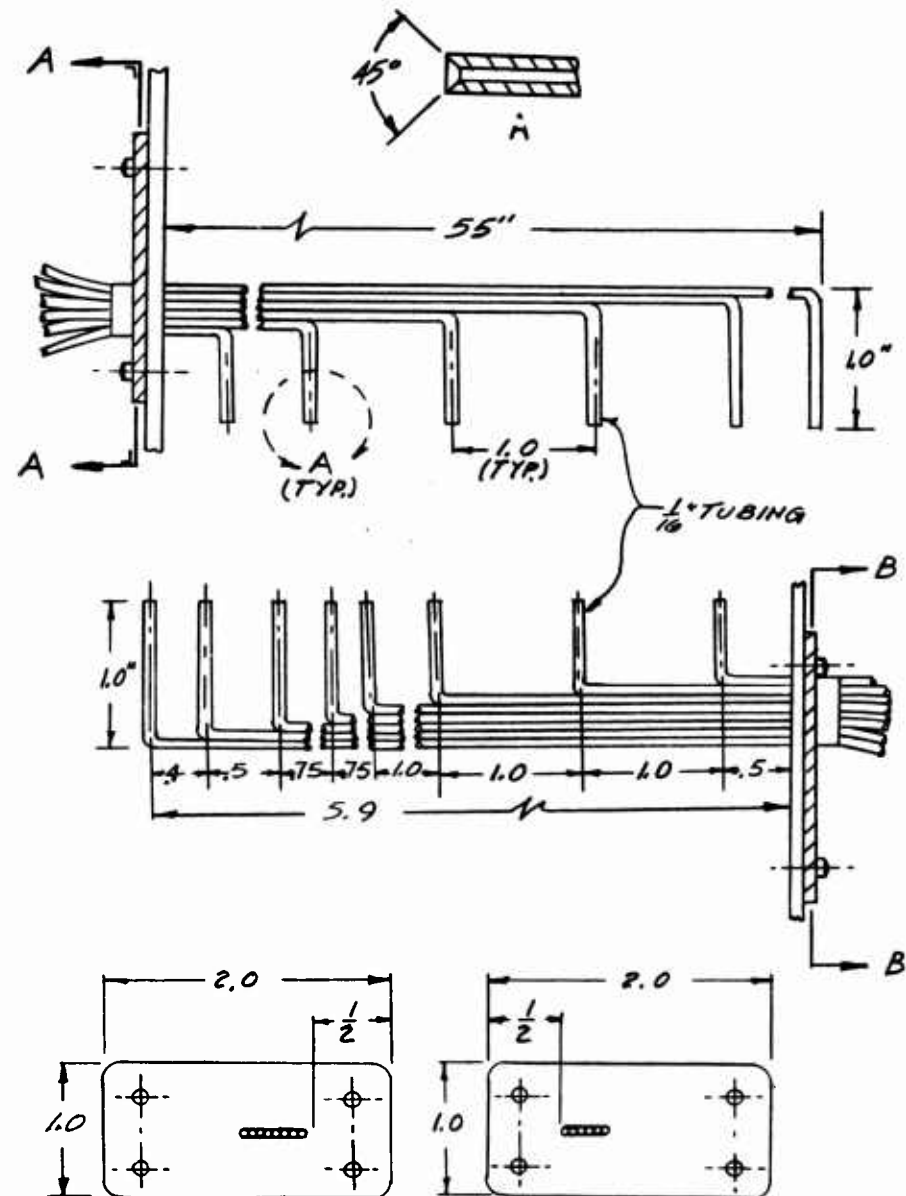


Figure 15. Rakes, Sketch

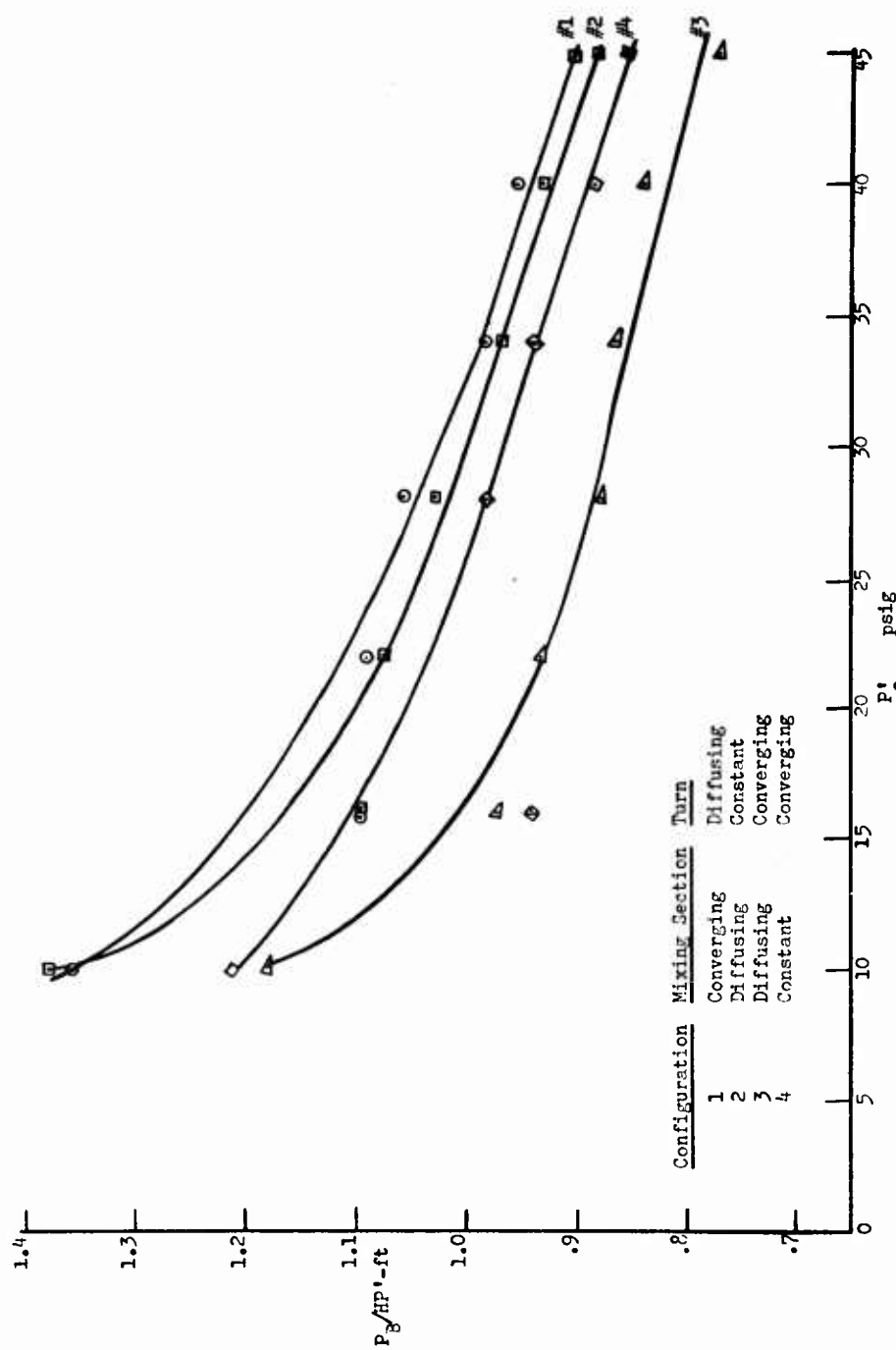


Figure 16. Original Model 1, Center-body Location.

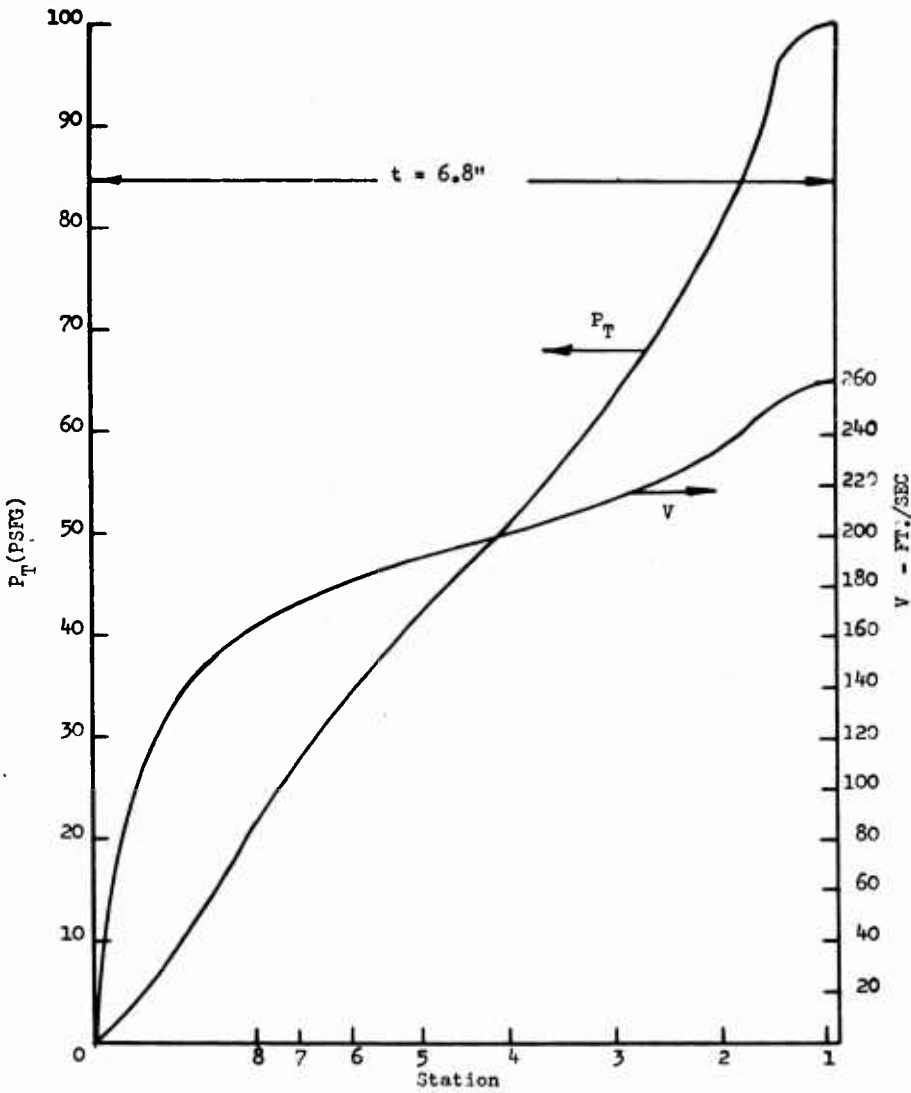


Figure 17. Typical Testing Velocity and Total Head Profiles.

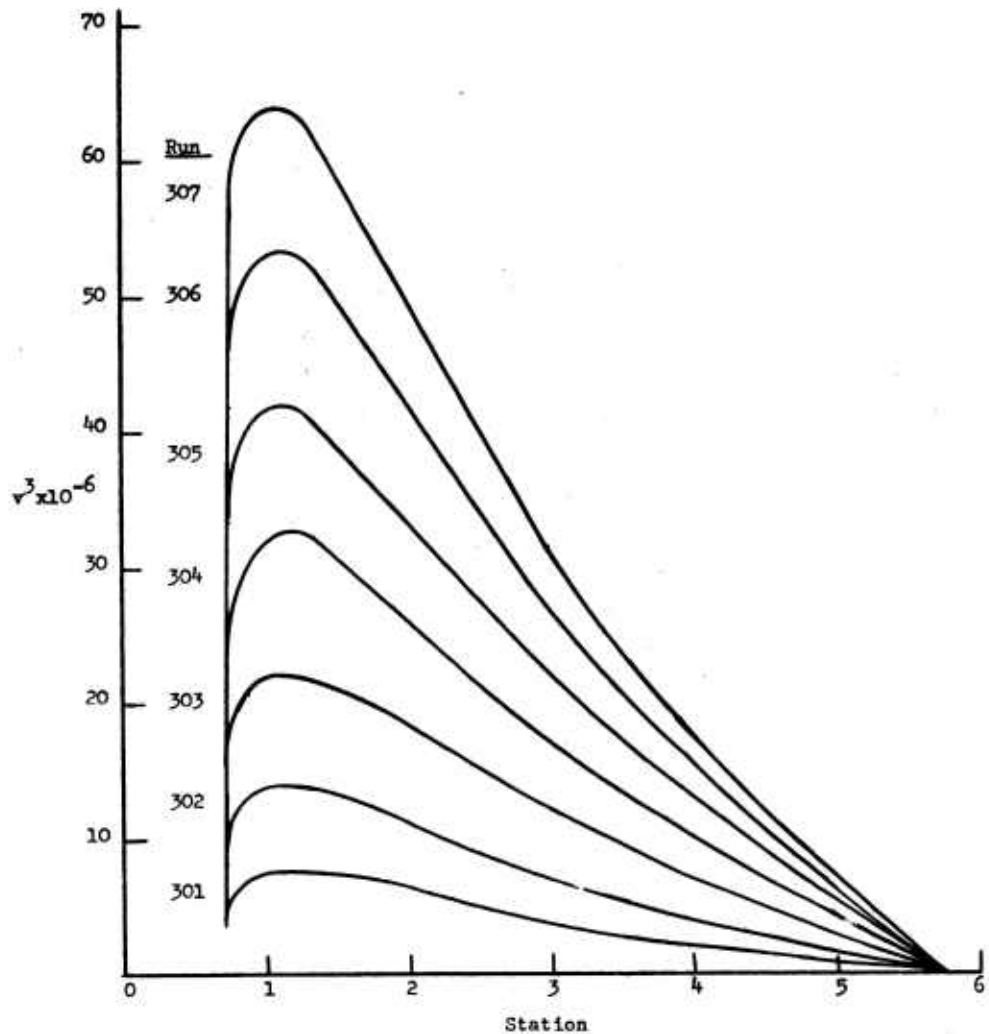


Figure 18. Typical Testing Velocity Cubed Profiles

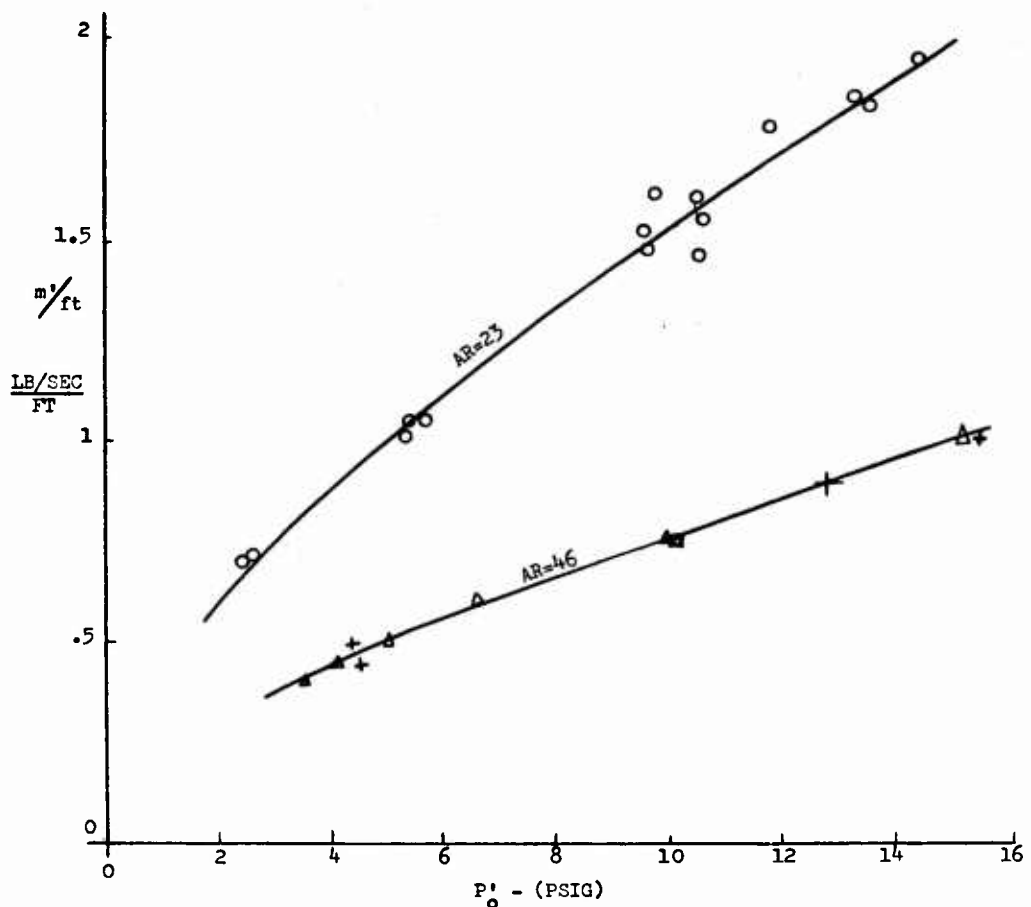


Figure 19. Mass Flow -vs- Primary Pressure
Configurations 7, 8, 9.

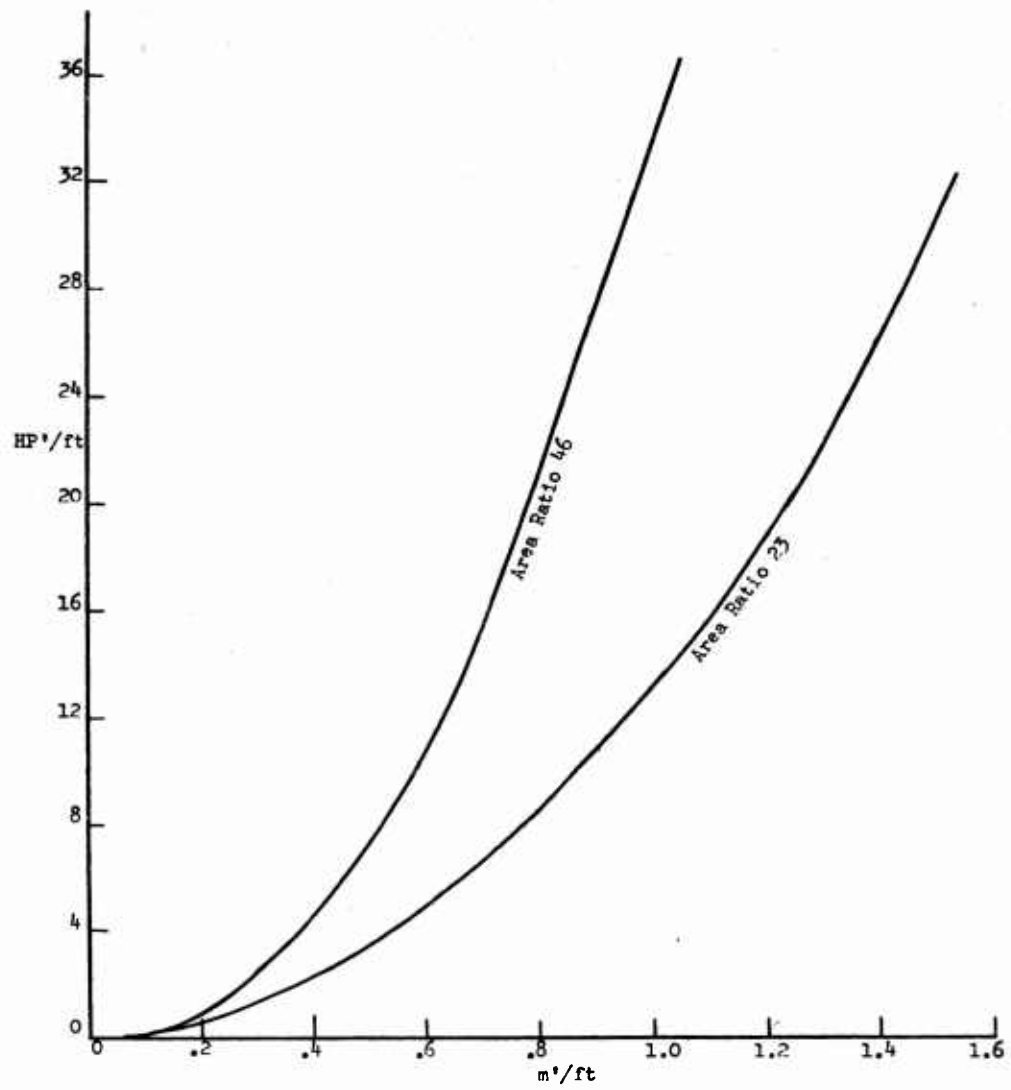


Figure 20. Primary Horsepower -vs- Mass Flow,
Configuration 7, 8, 9.

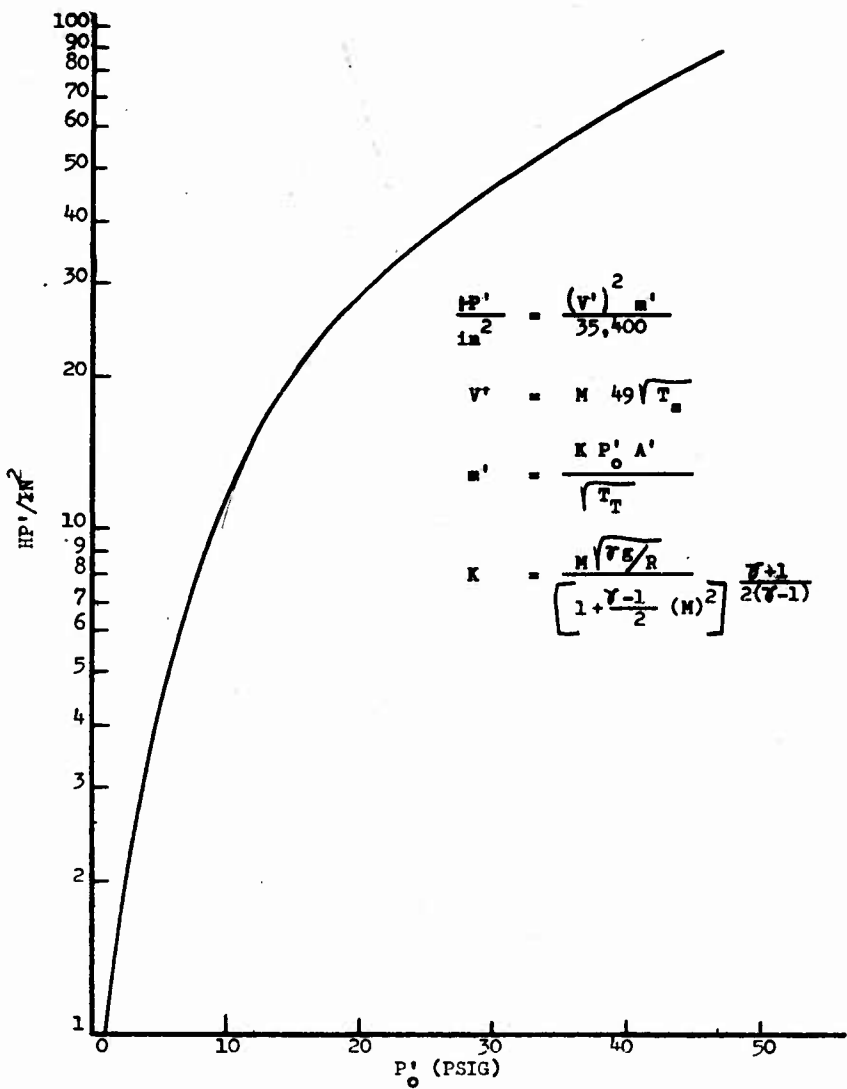


Figure 21. Primary Horsepower -vs- Mass Flow,
Theory.

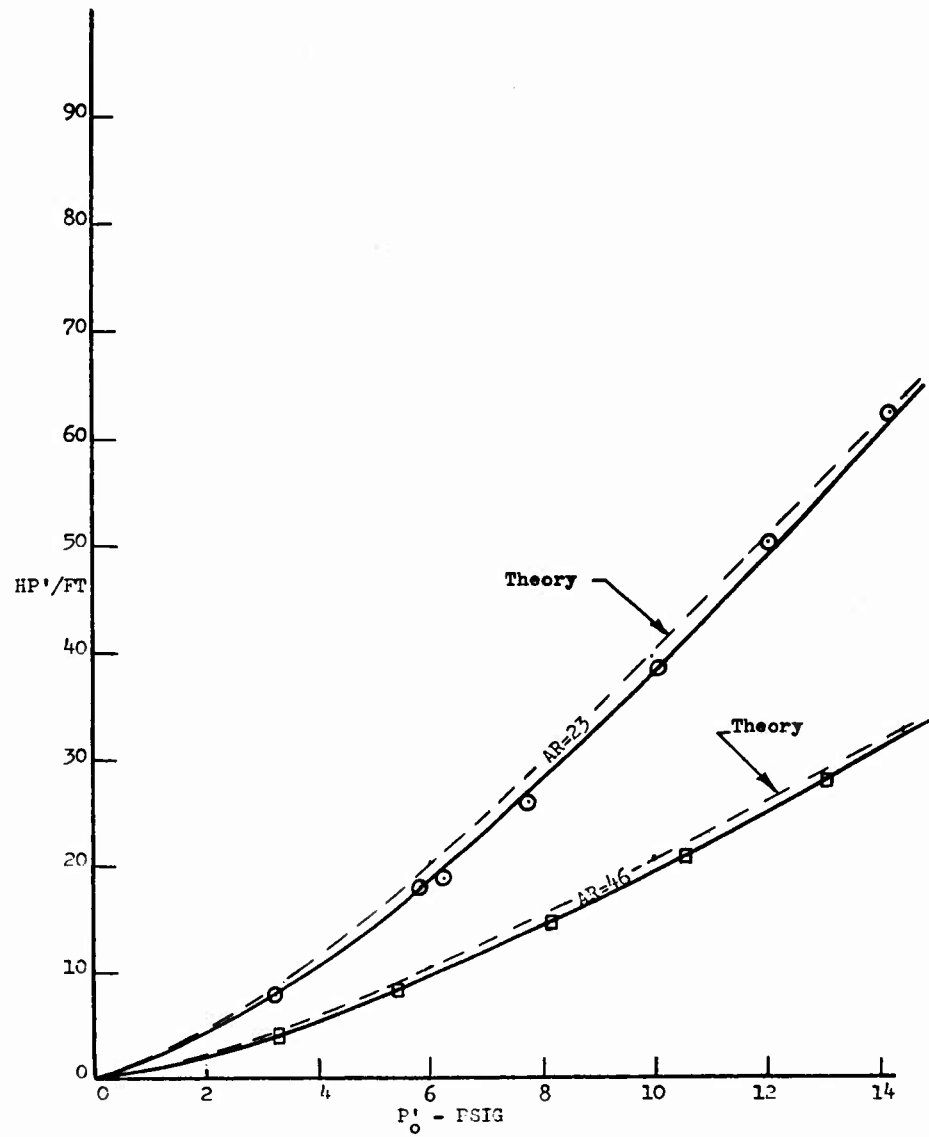


Figure 22. Primary Horsepower - vs. Primary Pressure for Configuration 7, 8 and 9.

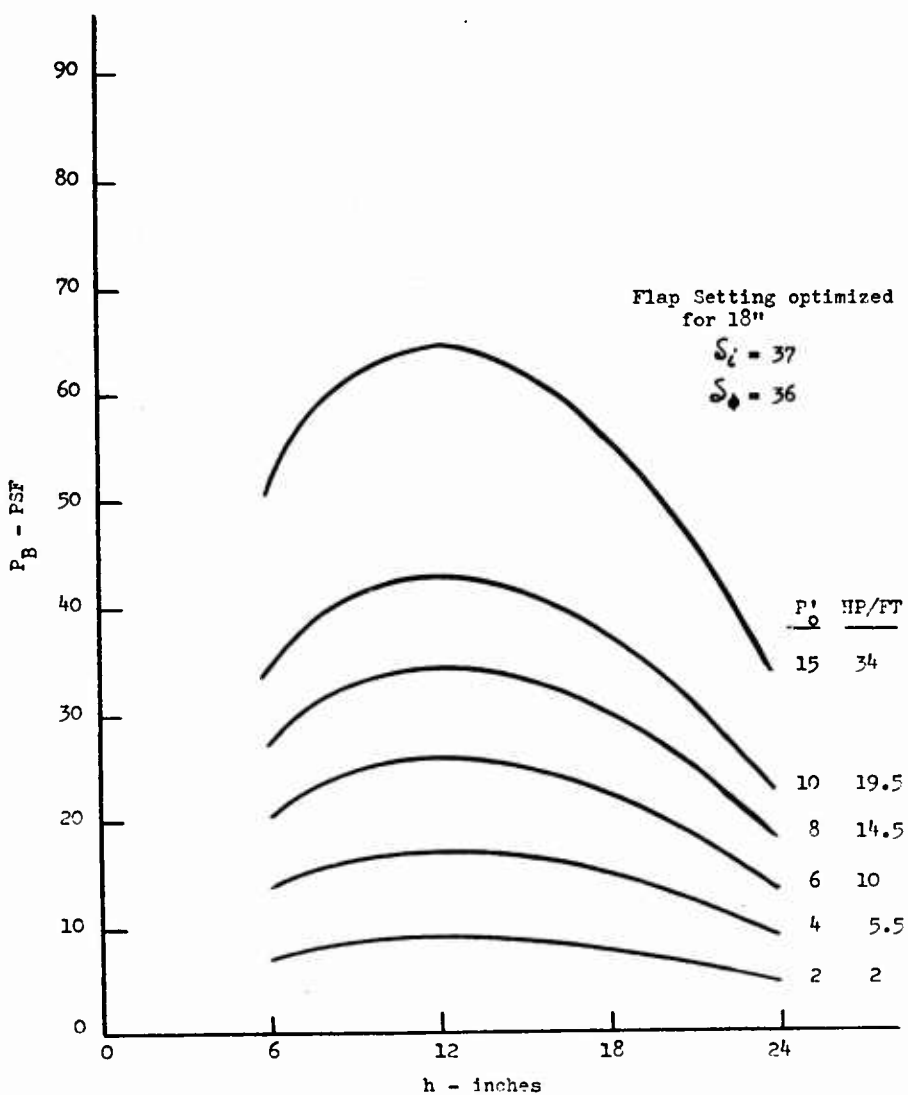


Figure 23. Base Pressure - vs. - Height for Configuration 7.

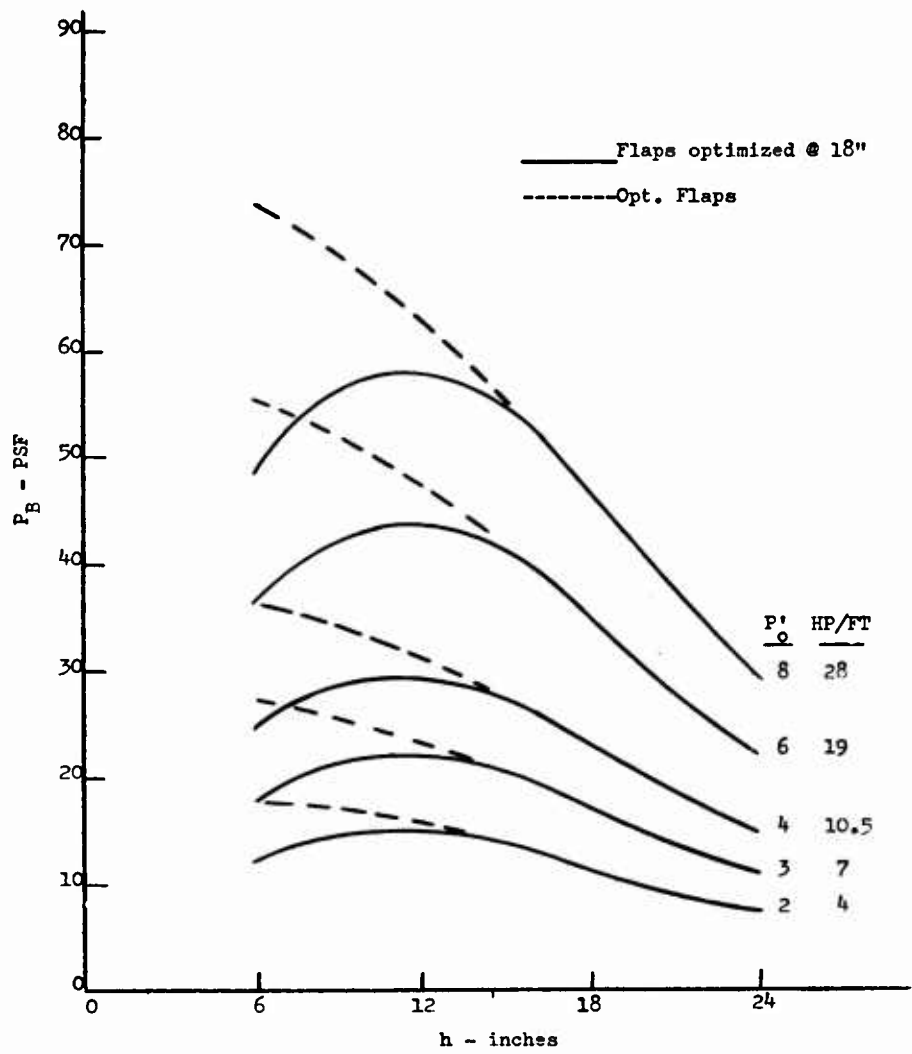


Figure 24. Base Pressure -vs- Height for Configuration 8.

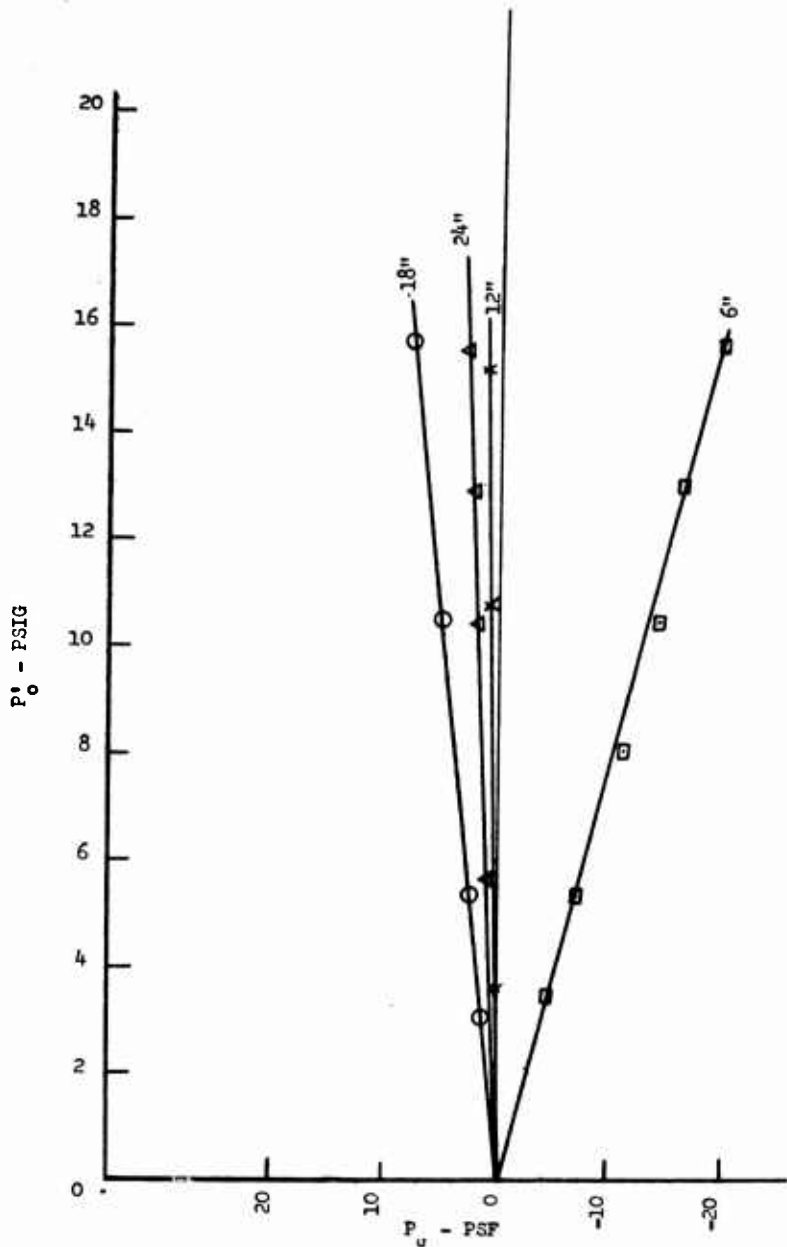


Figure 25. Cavity Pressure -vs- Primary Pressure for Configuration 7.

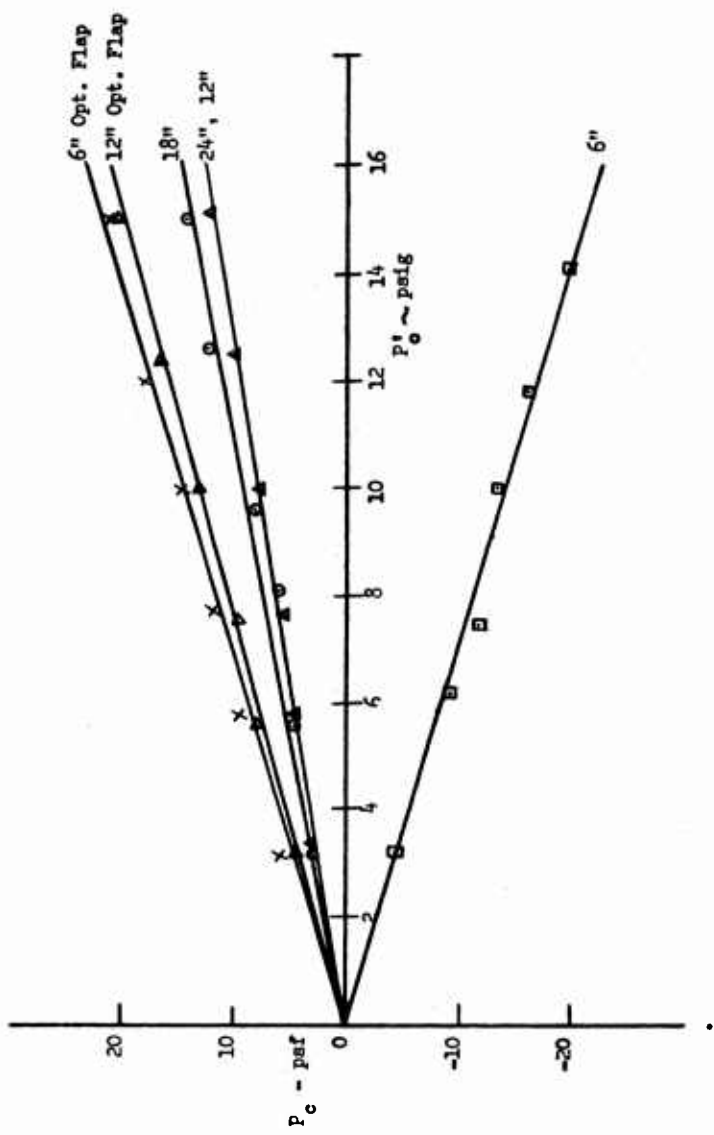


Figure 26. Cavity Pressure -vs- Primary Pressure,
Configuration 8.

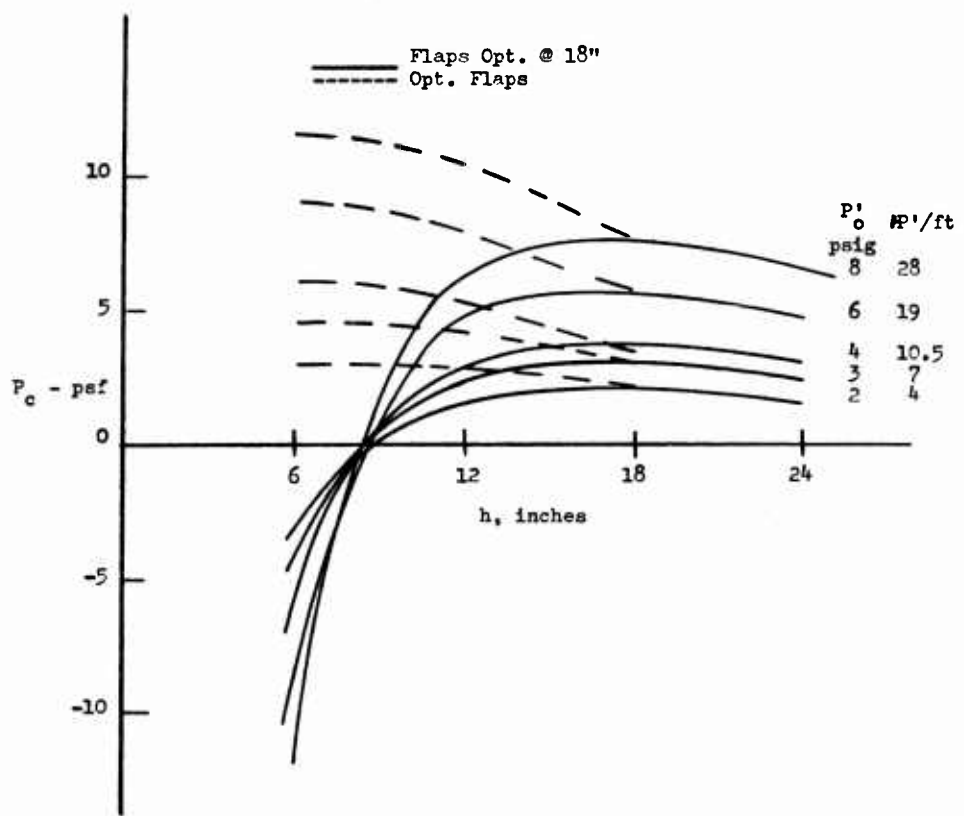


Figure 27. Cavity Pressure -vs- Height, Configuration 8

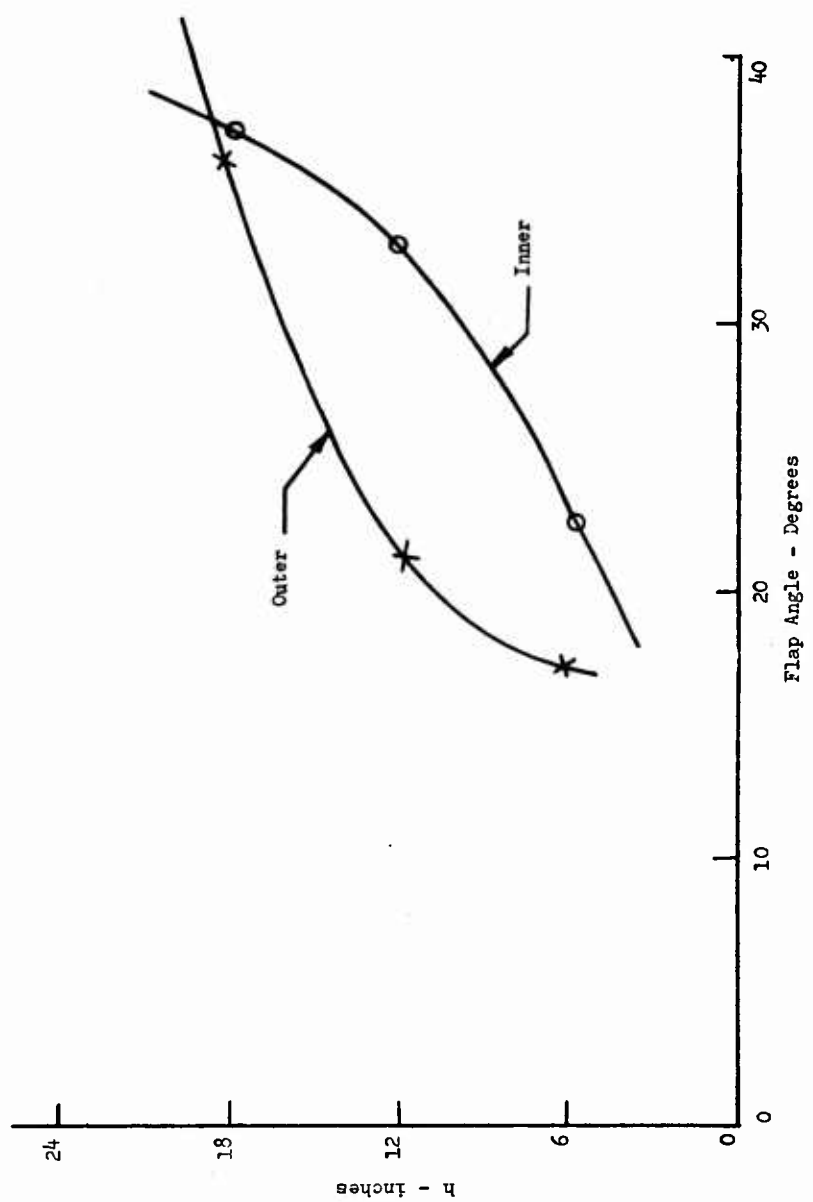


Figure 28. Optimum Exit Flap Angle,
Configuration 8.

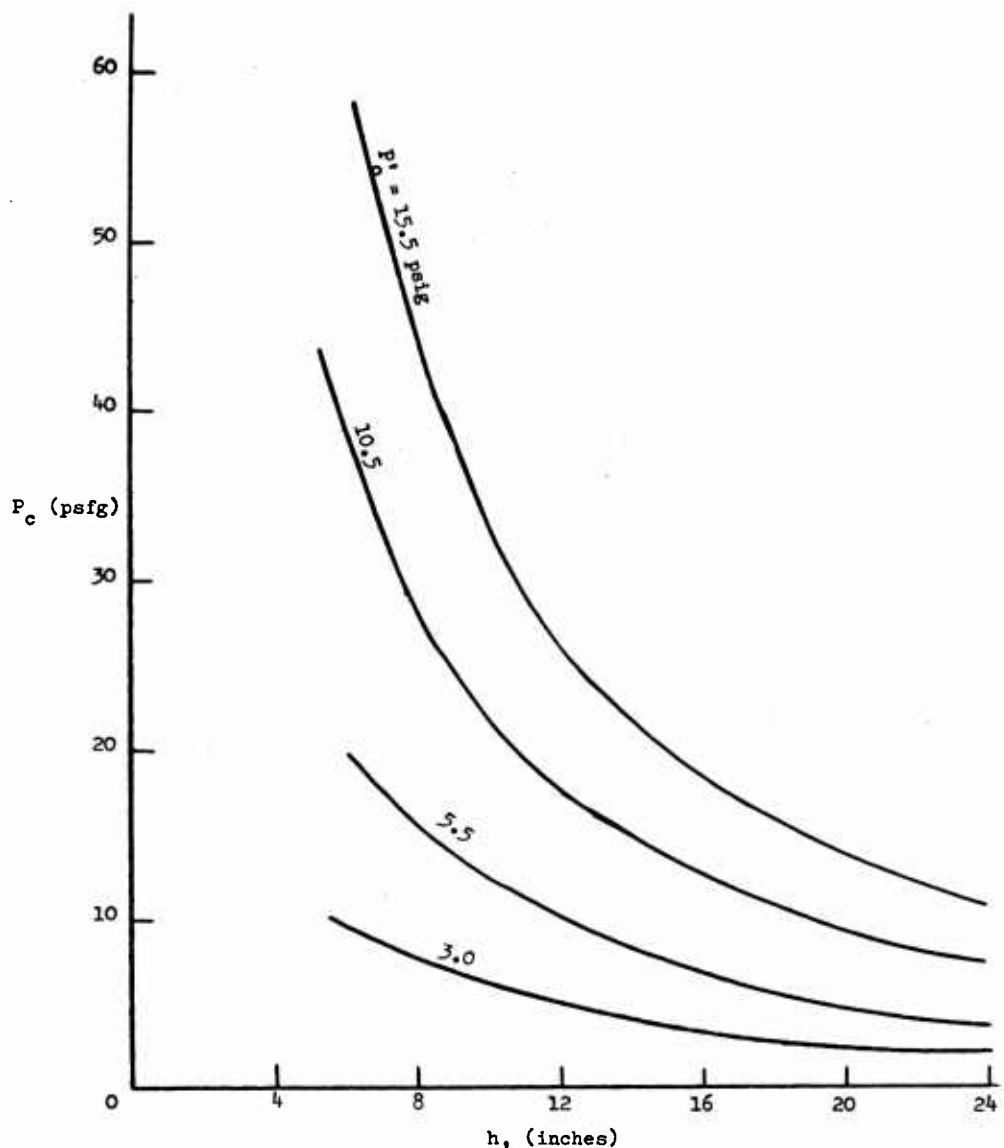


Figure 29. Cavity Pressure -vs- Height,
Theory, Configuration 7.

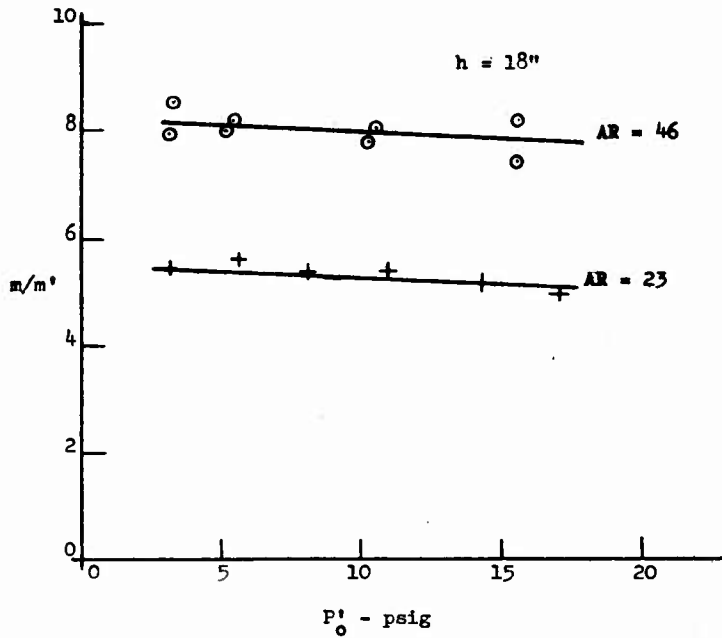


Figure 30. Mass Augmentation -vs- Primary Pressure, Configuration 8, 9.

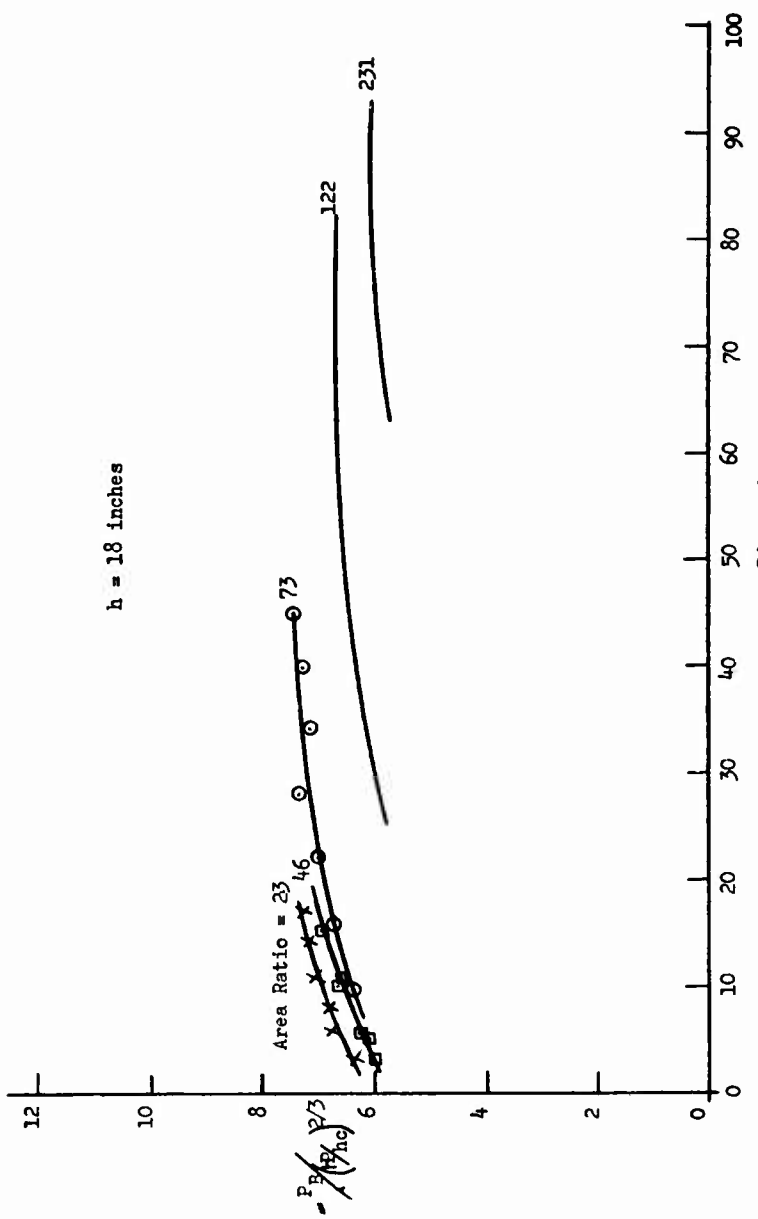


Figure 31. Lift-Power Parameter -vs- Primary Pressure.

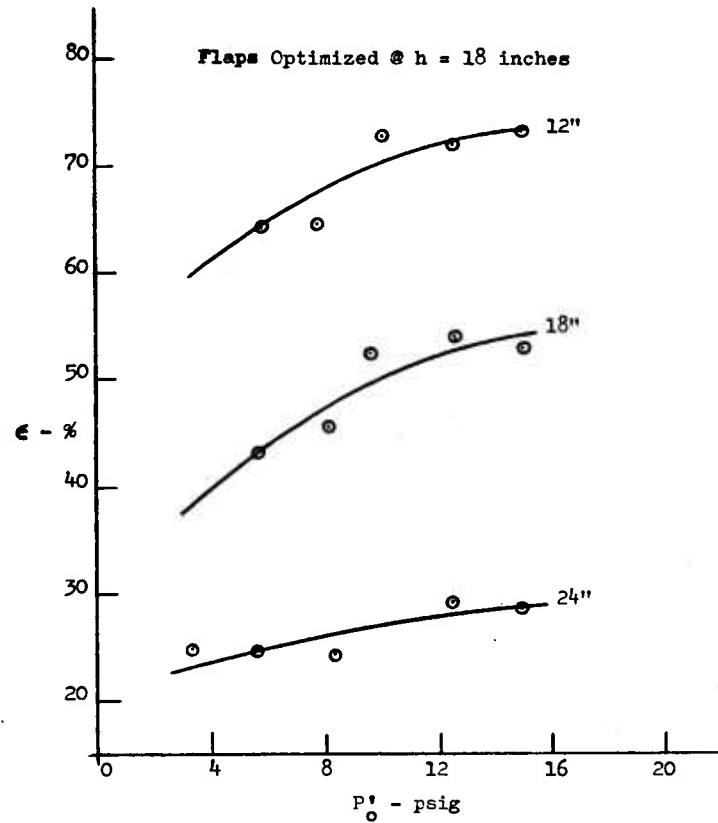


Figure 32. Efficiency -vs- Primary Pressure,
Configuration 8.

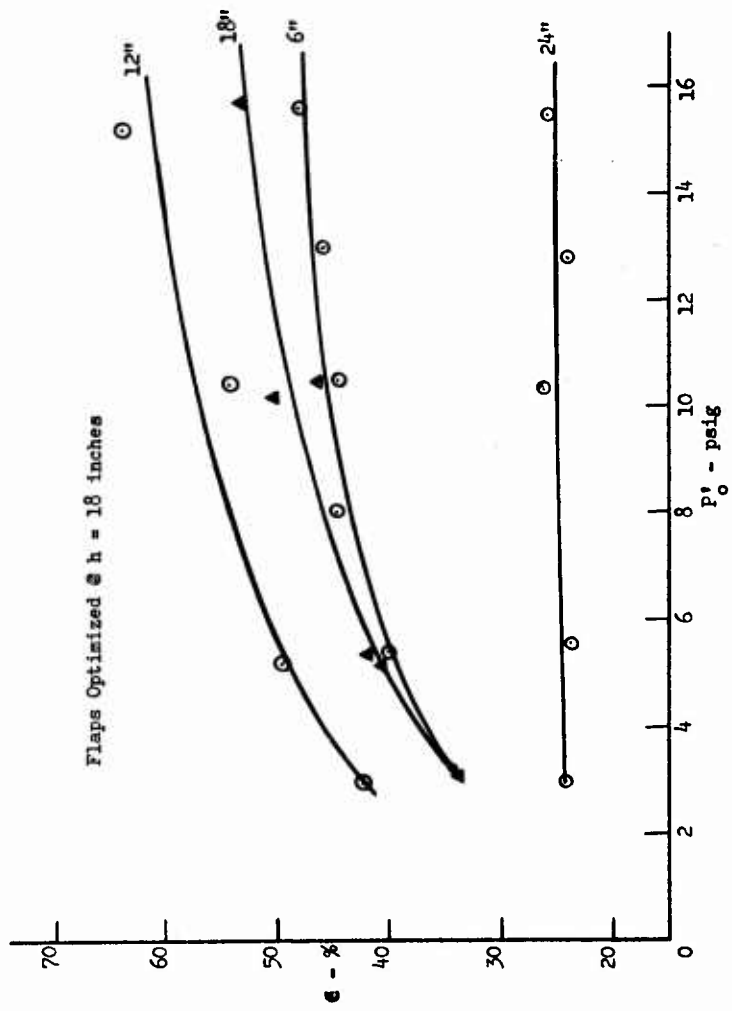


Figure 33. Efficiency -vs- Primary Pressure,
Configuration 9.

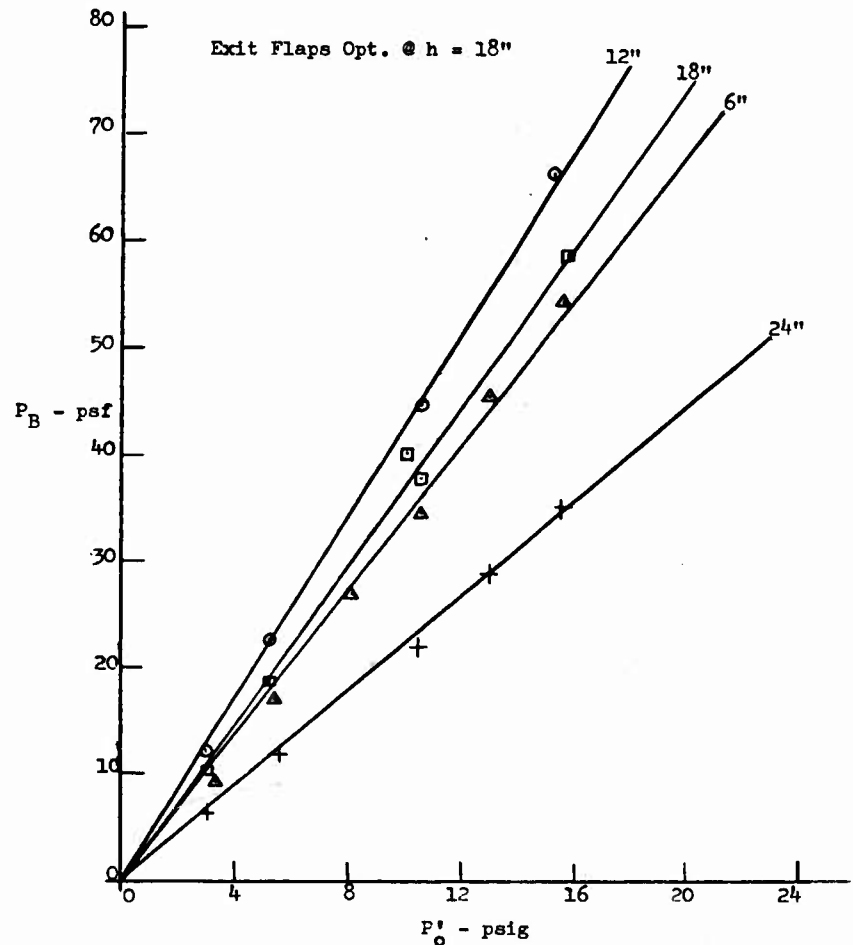


Figure 3⁴. Base Pressure -vs- Primary Pressure
Configuration 7

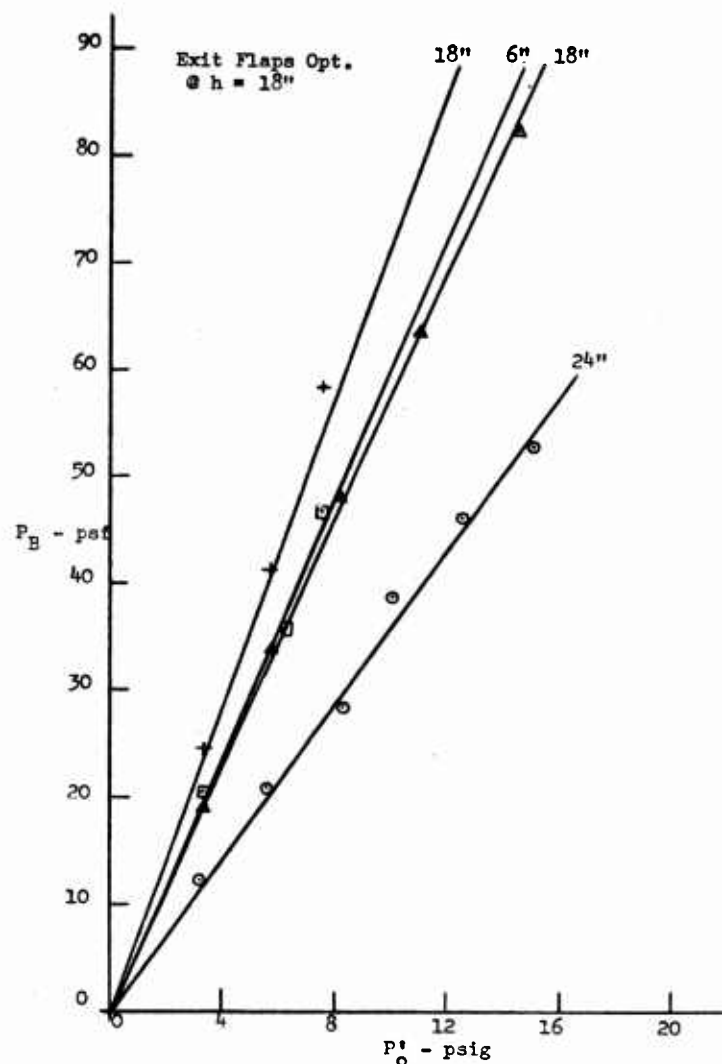


Figure 35. Base Pressure -vs- Primary Pressure,
Configuration 8

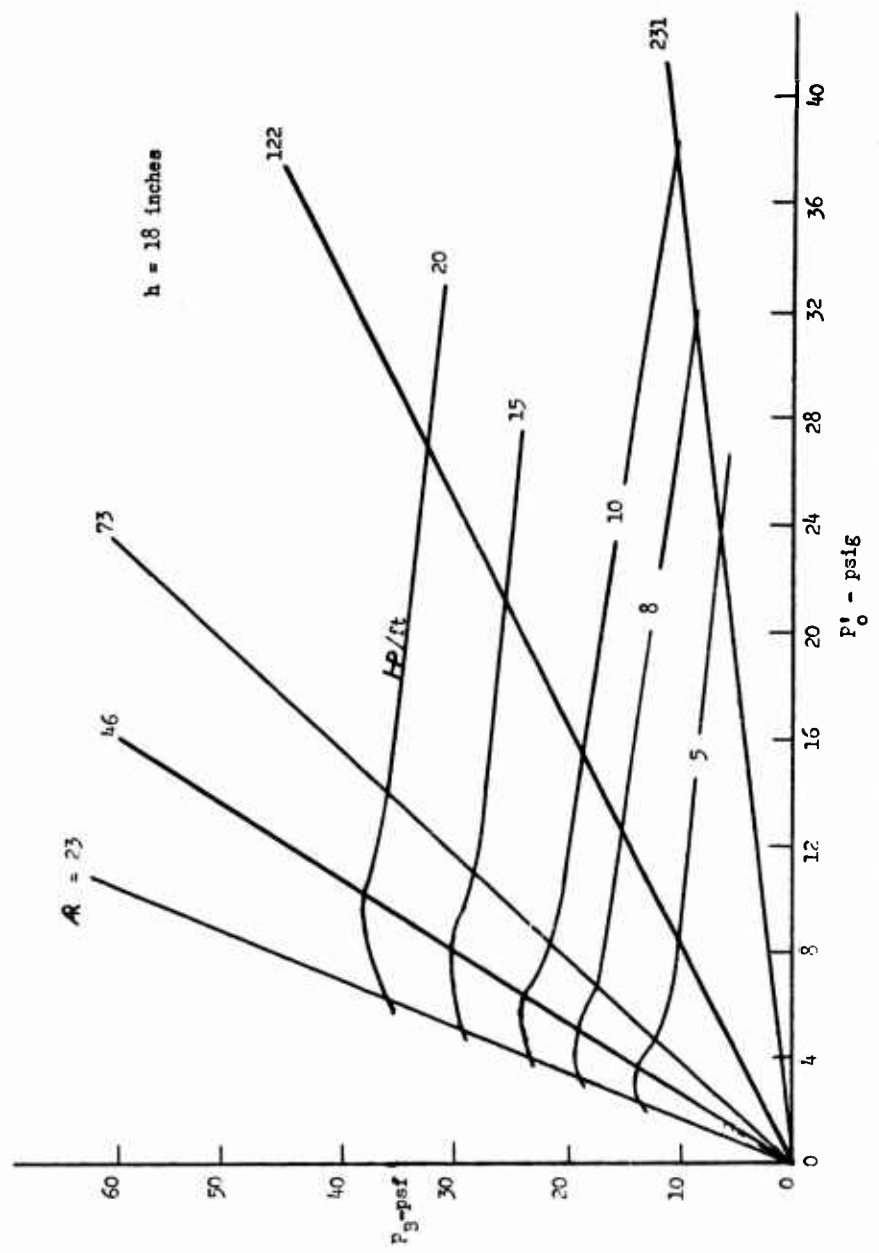


Figure 36. Base Pressure -vs- Primary Pressure, Summary



Figure 37. Stability and Control Model.



Figure 38. Lift Header, Stability and Control Model.

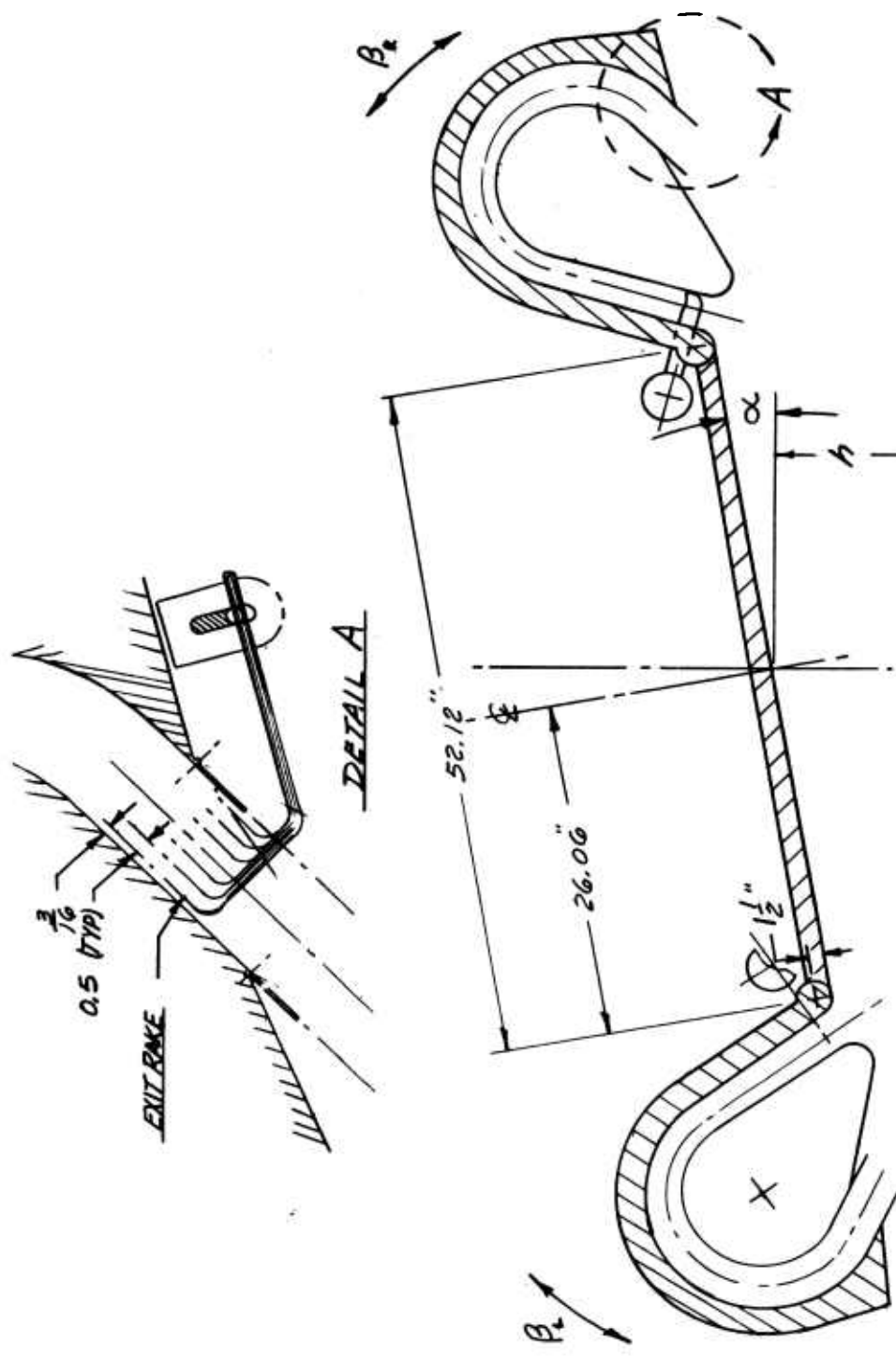


Figure 39. Stability and Control Model.

090-37485-X

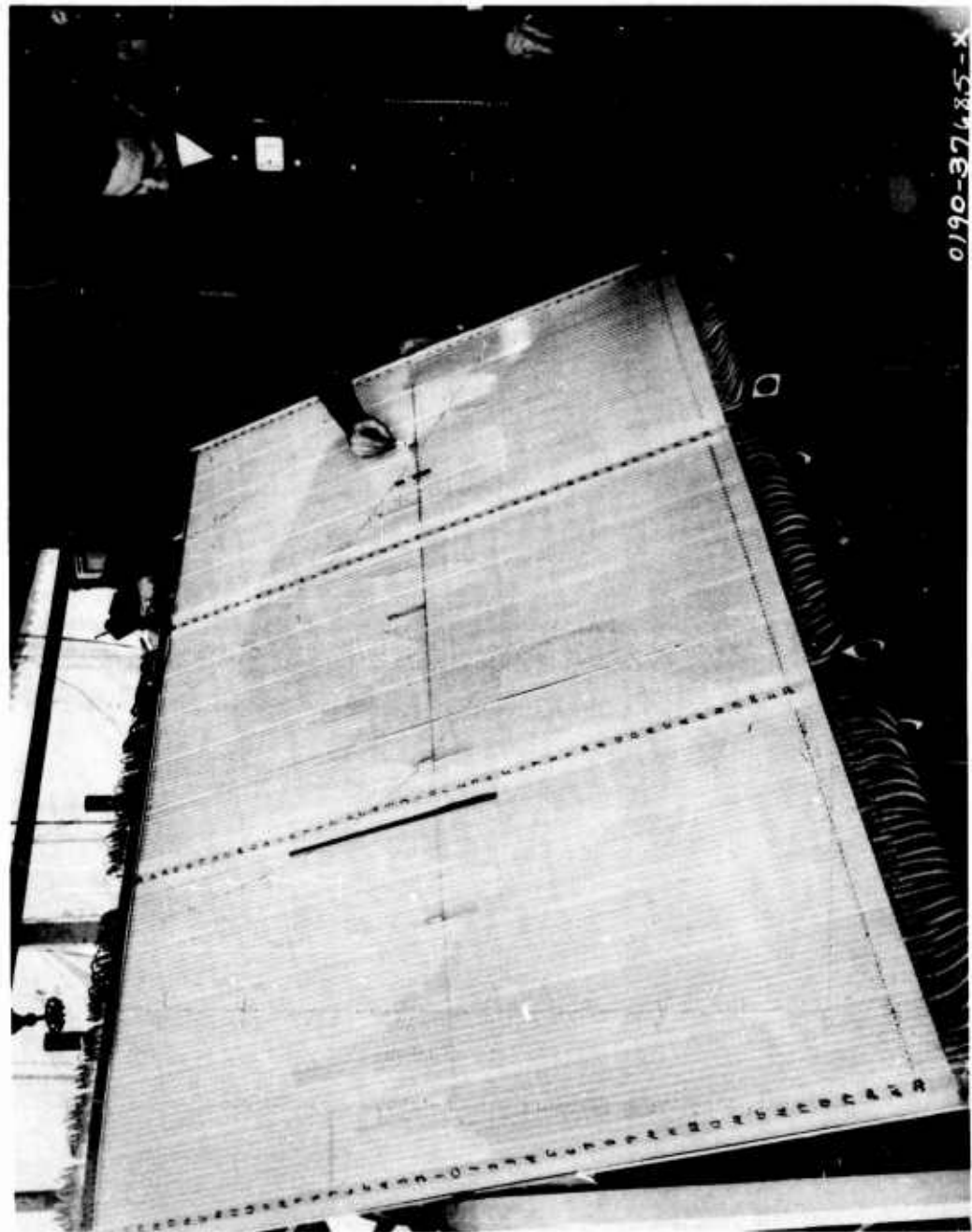


Figure 40. Manometer Board.

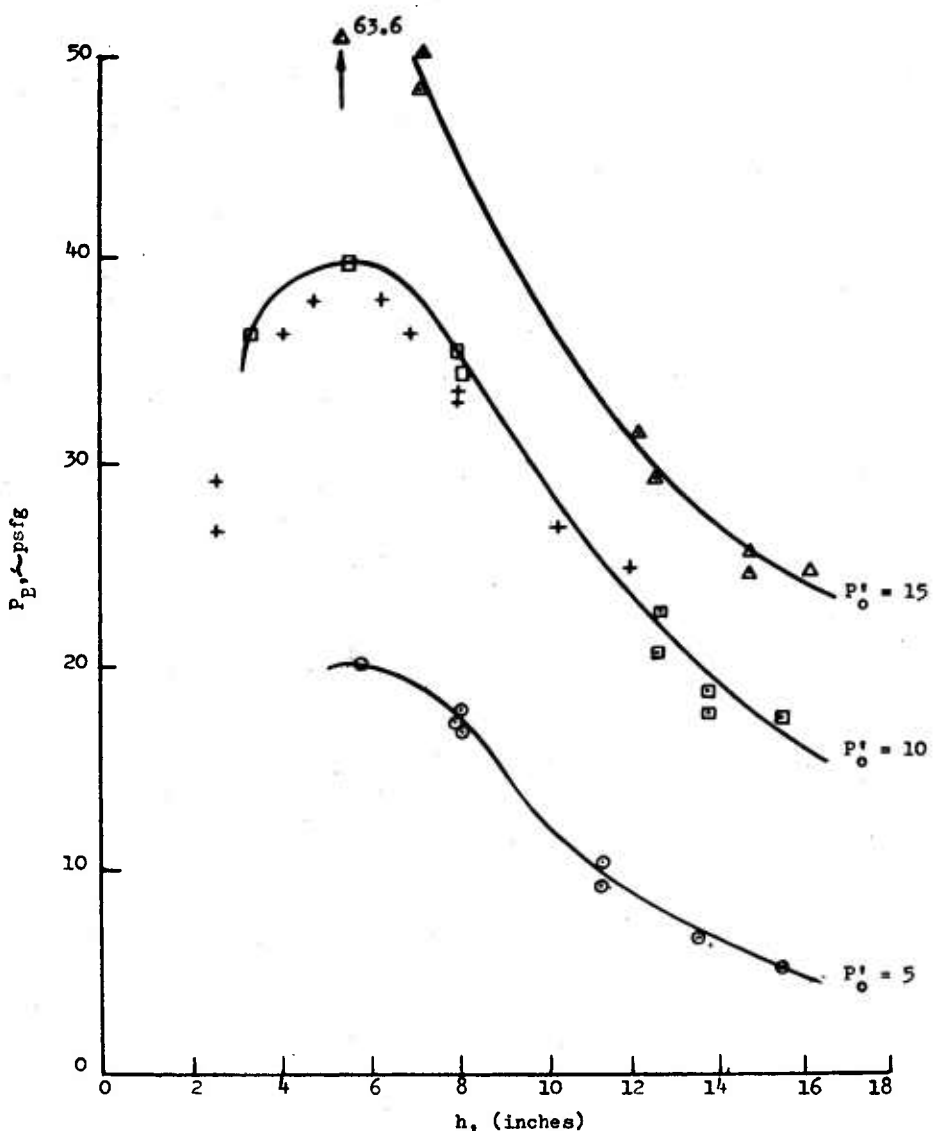


Figure 41. Base Pressure -vs- Height, Double Ejector

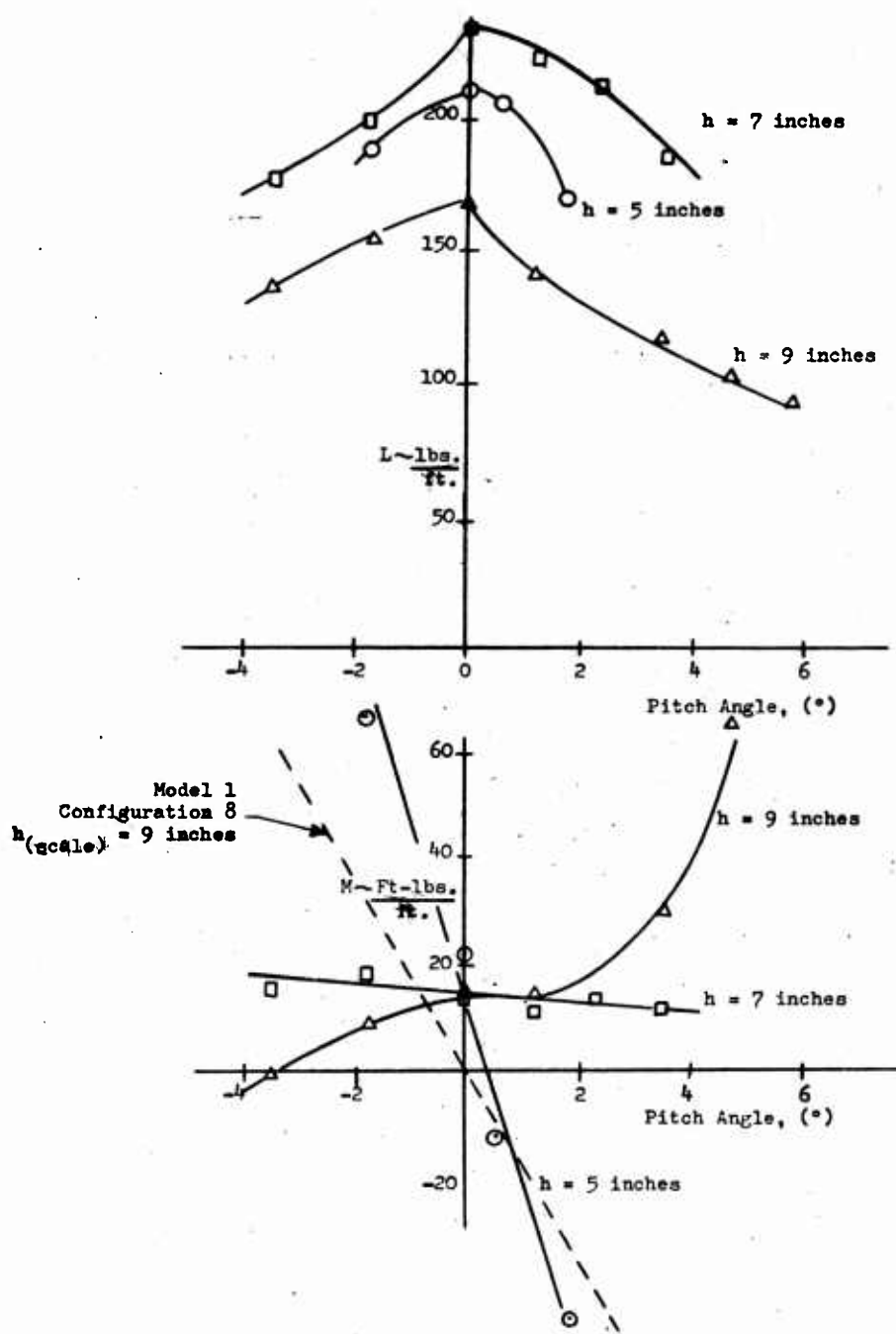


Figure 42. Lift & Moment -vs- Angle.

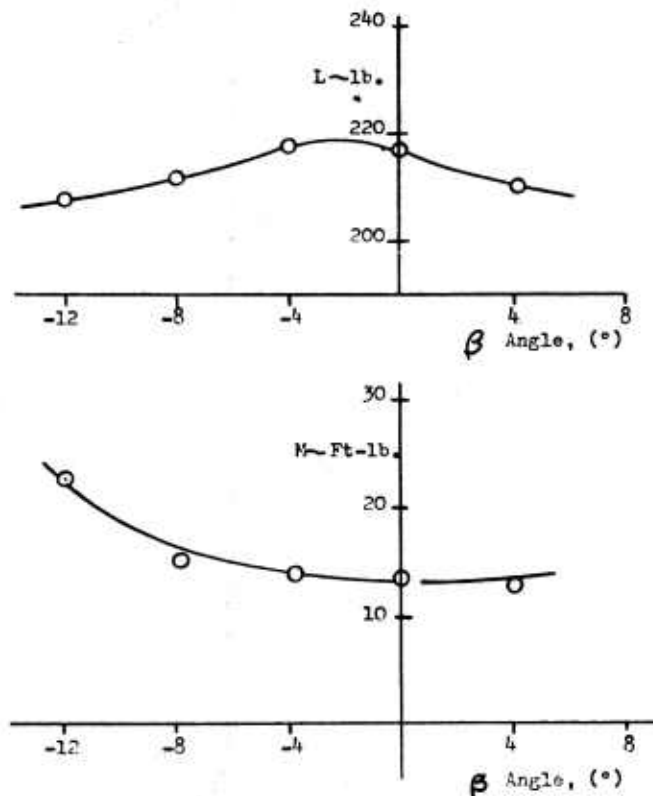


Figure 43. Control Effectiveness,
Ejector Tilt

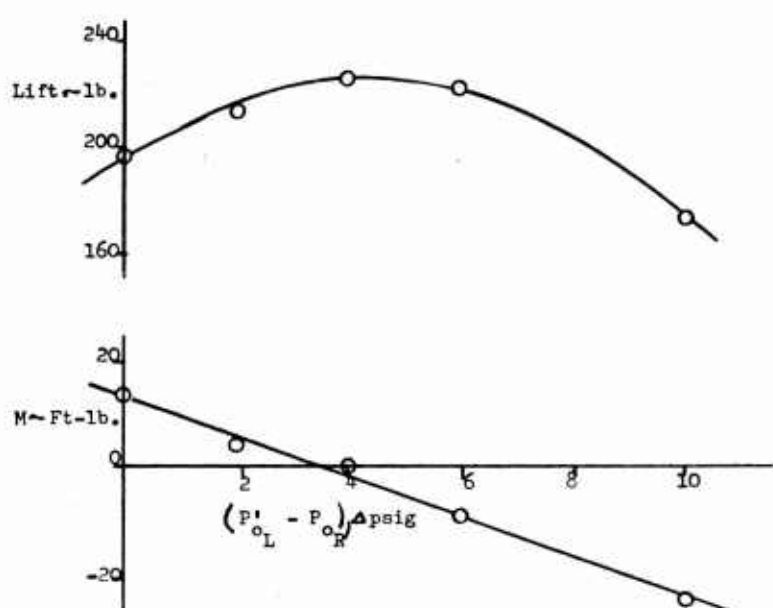


Figure 44. Control Effectiveness,
Primary Pressure

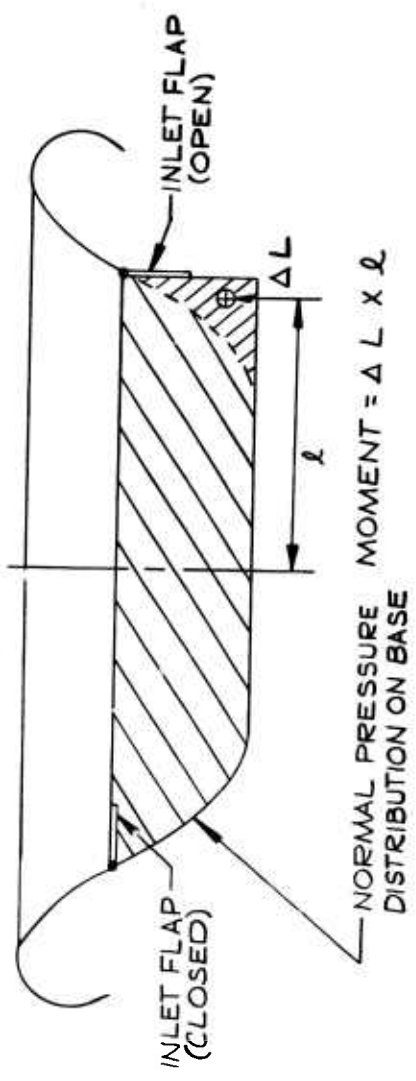


Figure 45. Control With Inlet Flaps.

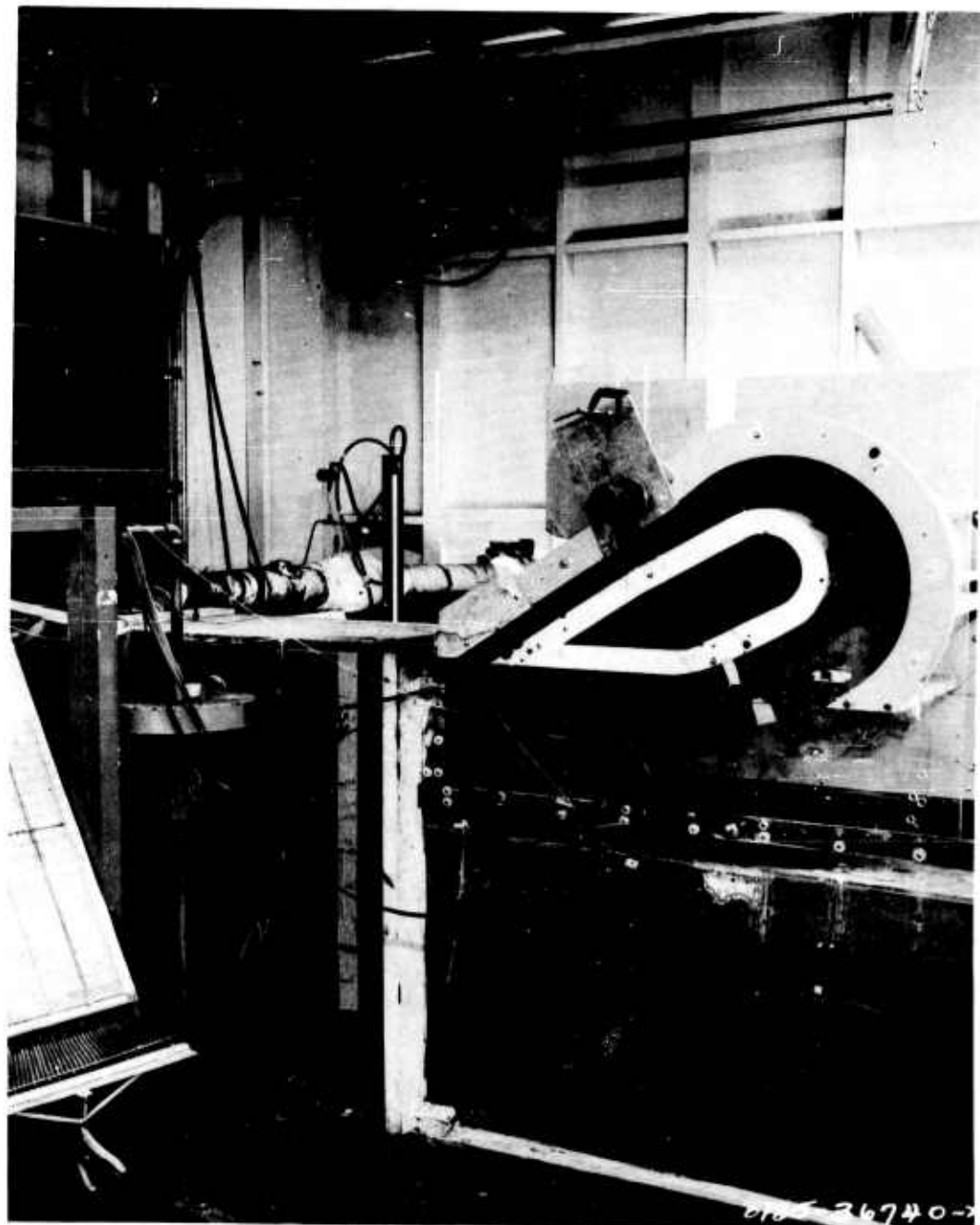


Figure 46. Model 5, Reverse Flow.

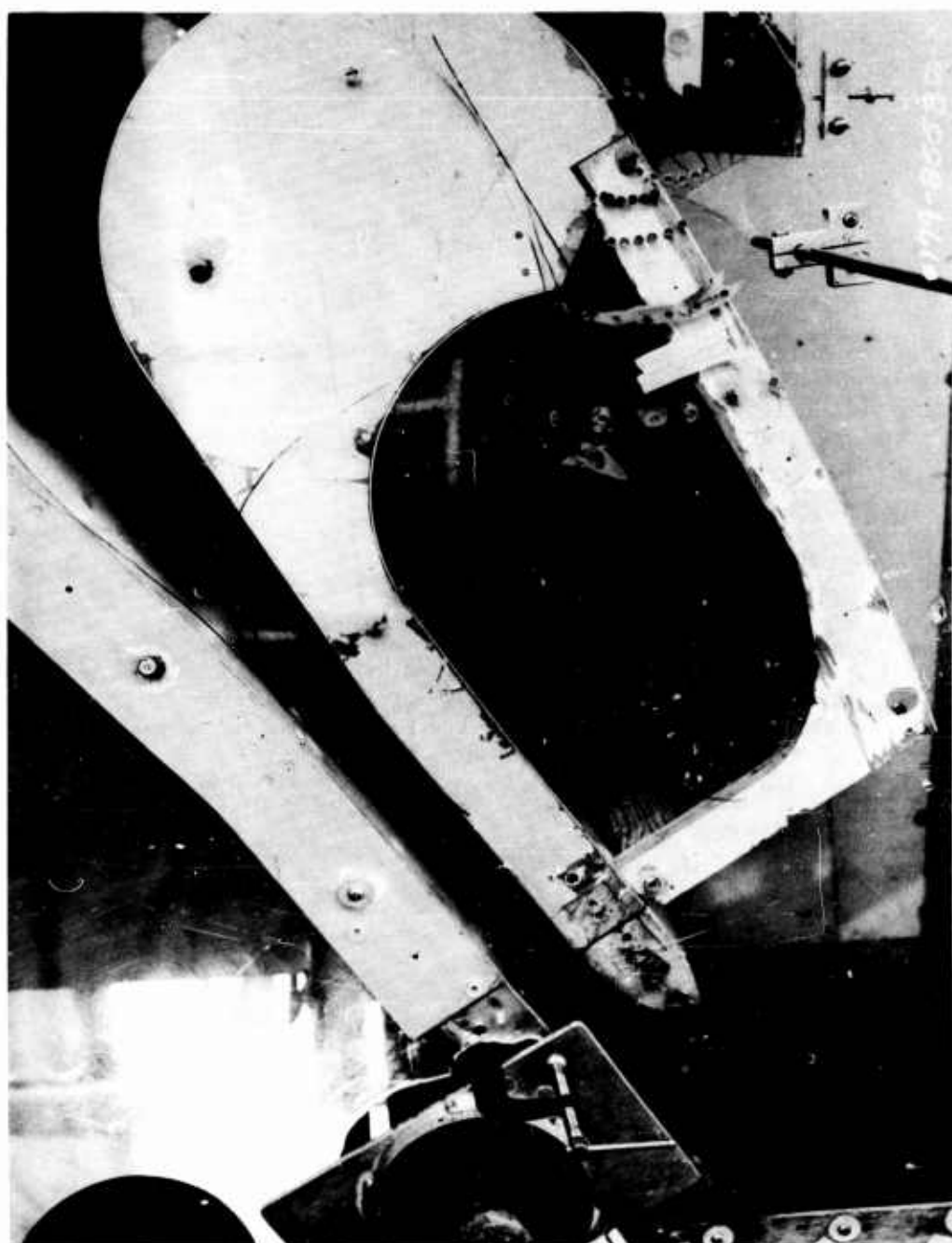


Figure 47. Model 5, Configuration 12.

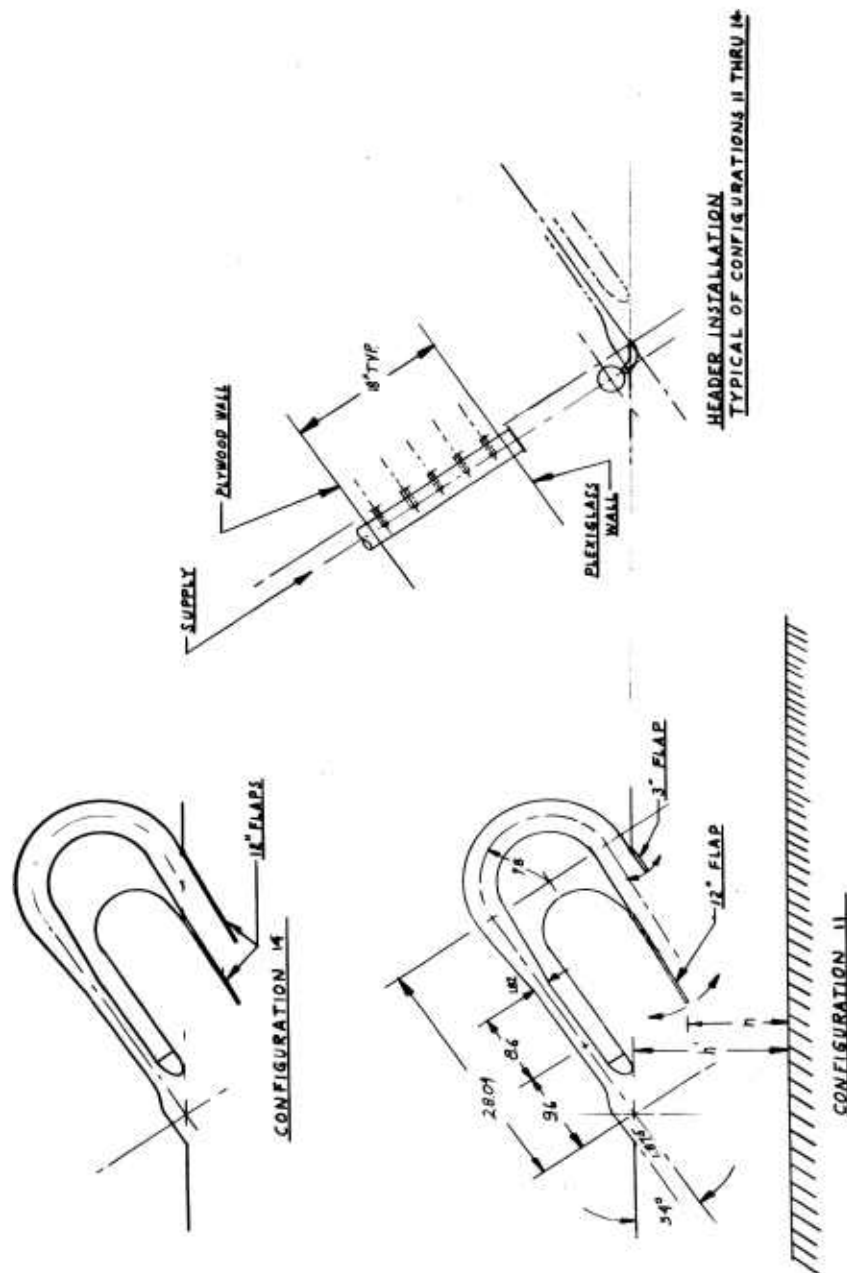


Figure 48. Model 5, Configurations 11 and 14, Sketch.

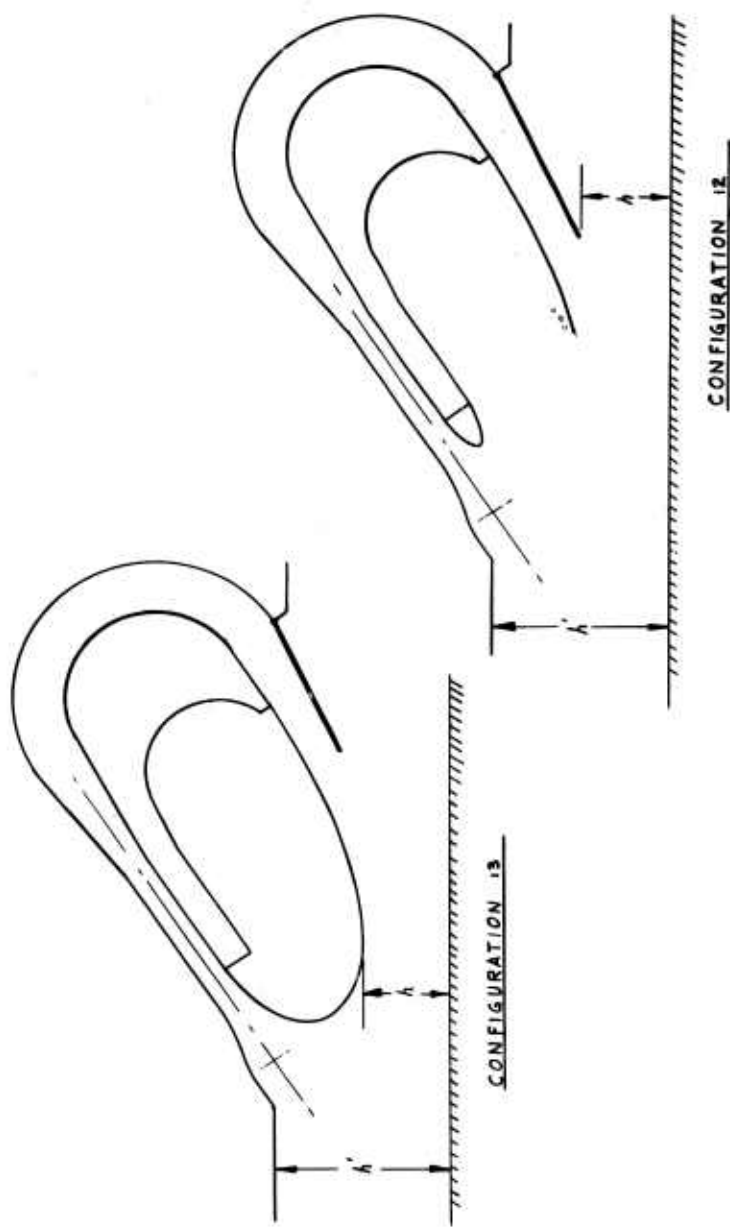


Figure 49. Model 5, Configurations 12 and 13, Sketch.

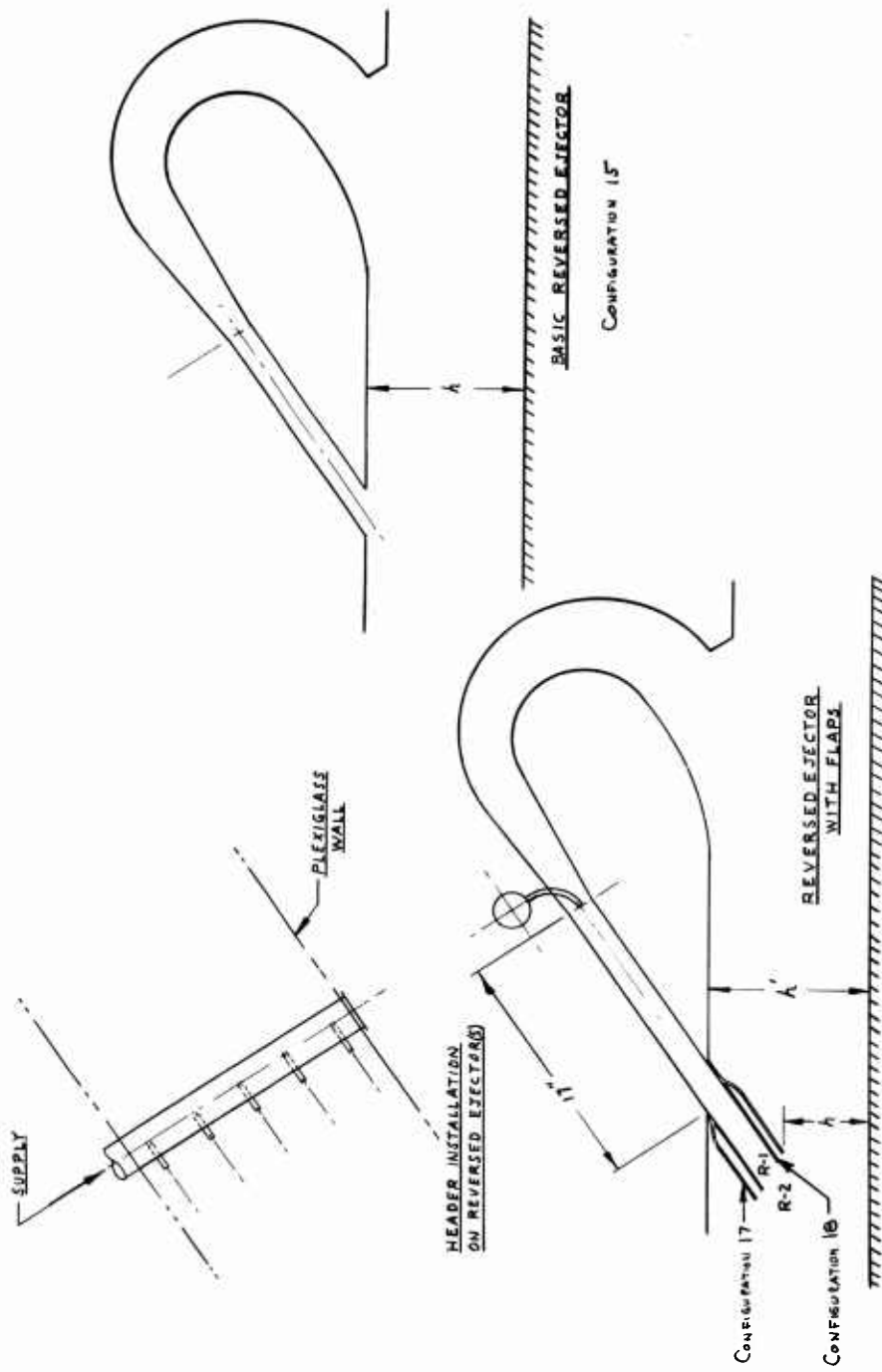


Figure 50. Model 5, Configurations 15, 16 and 17, Sketch.

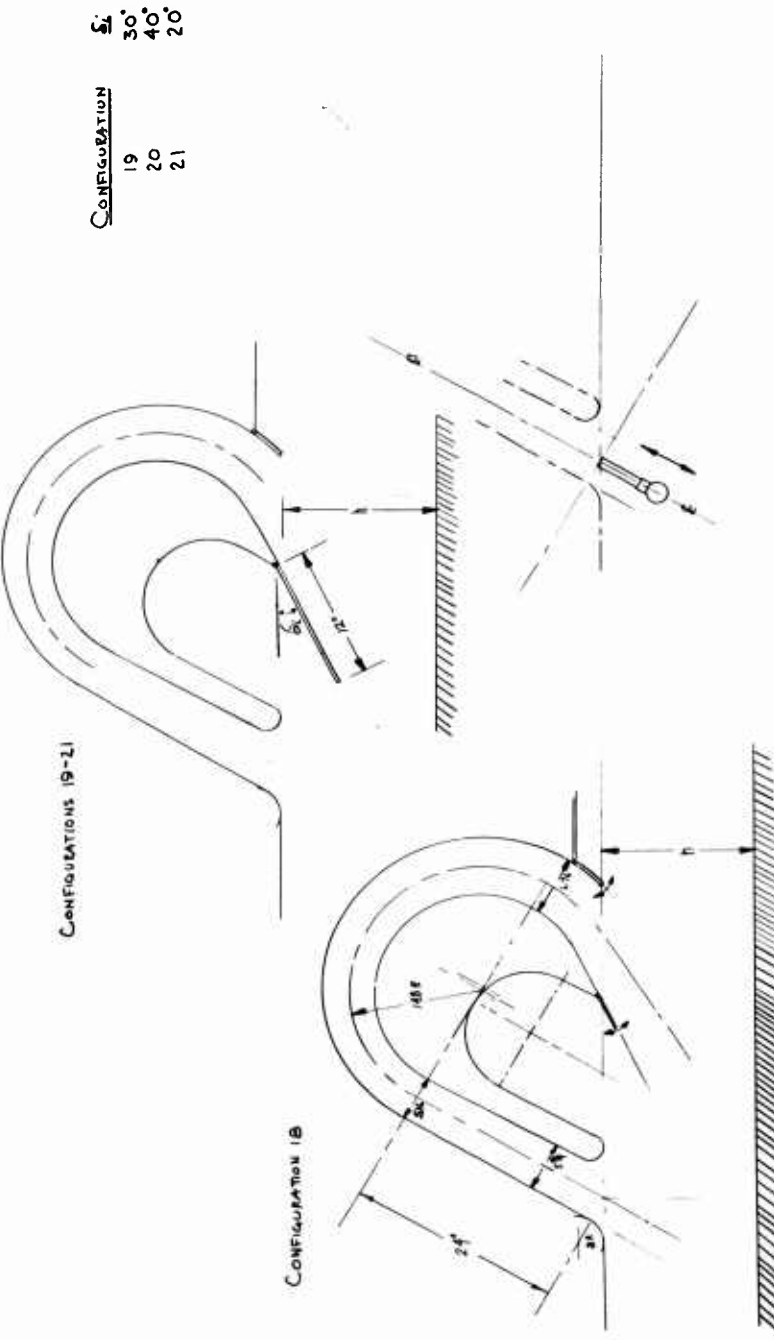


Figure 51. Model 1, Configurations 18-21, Sketch.

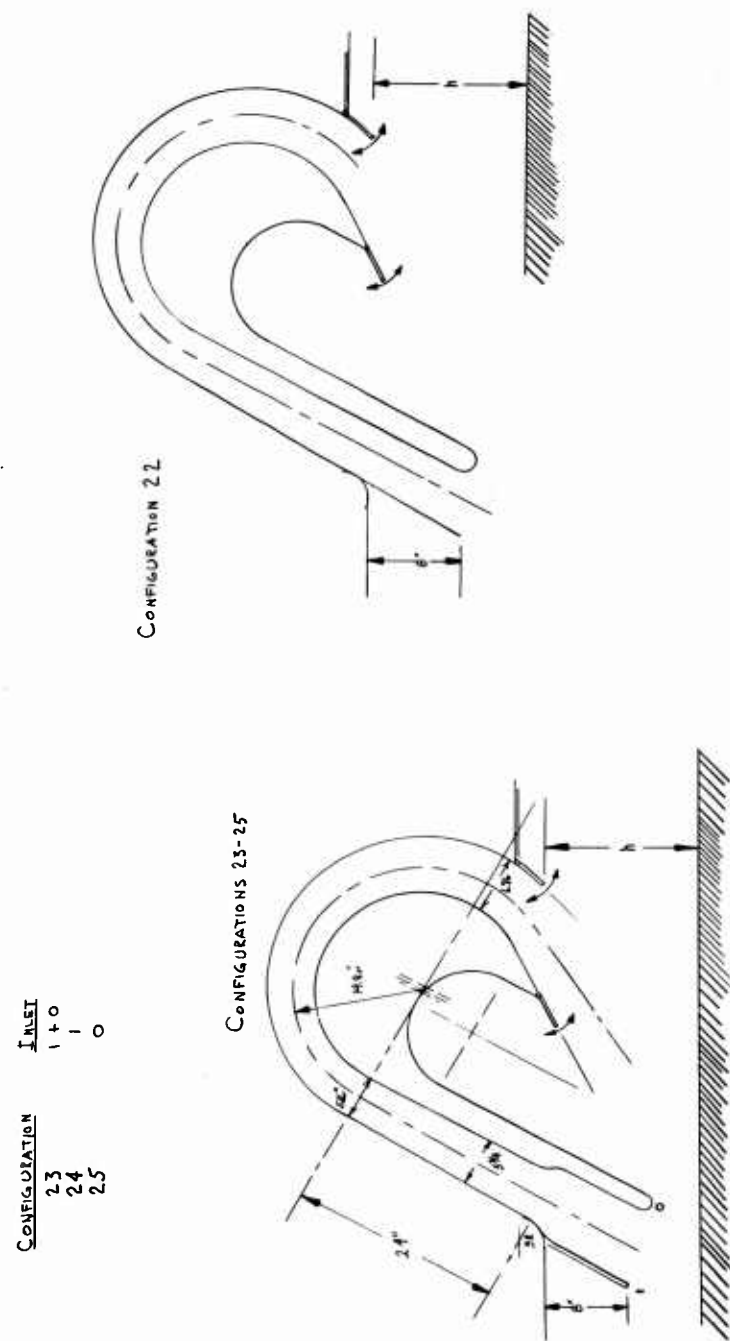
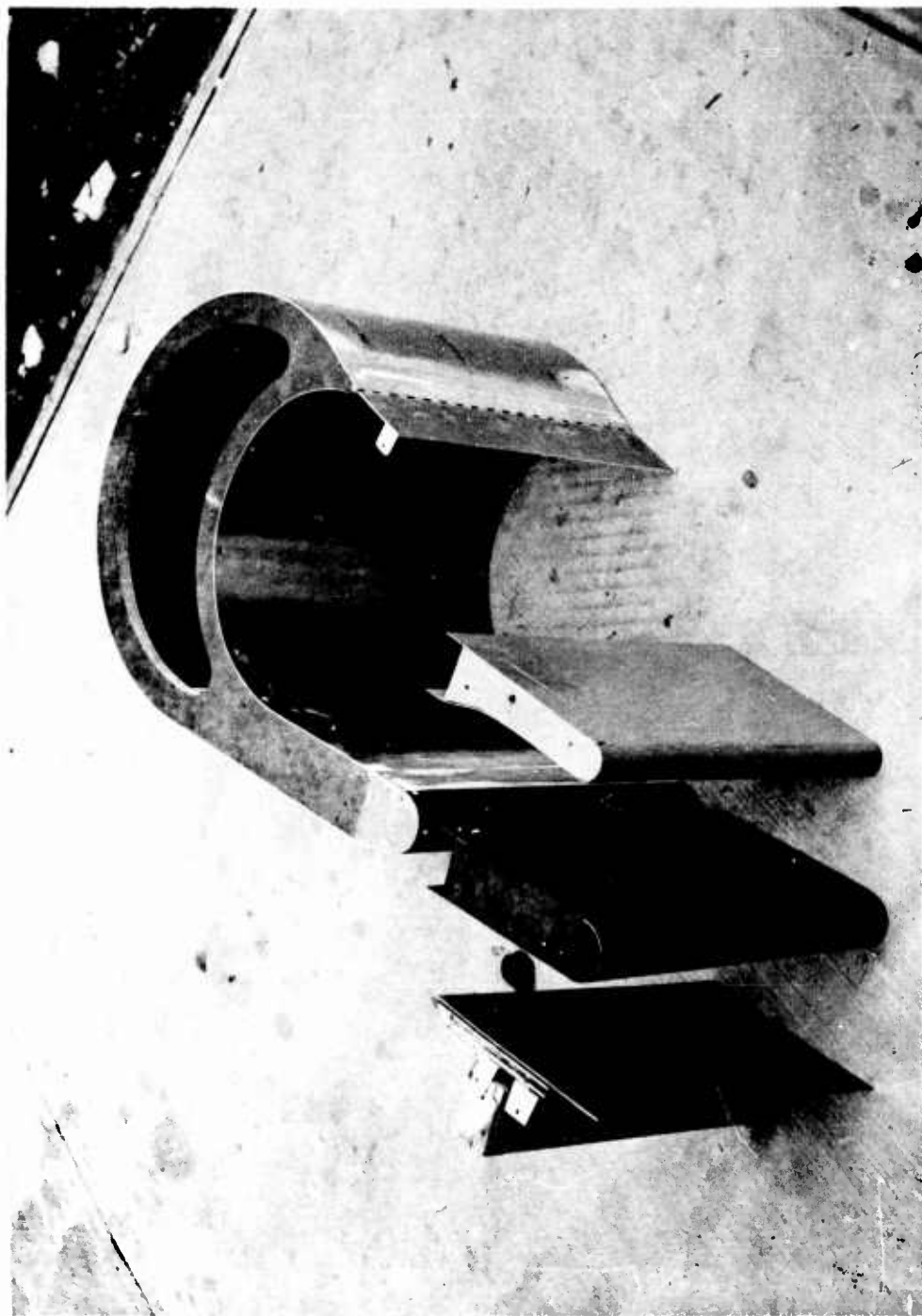


Figure 52. Model 1, Configurations 22-25, Sketch.

Figure 53. Model 1, Centerbody and Inlets.



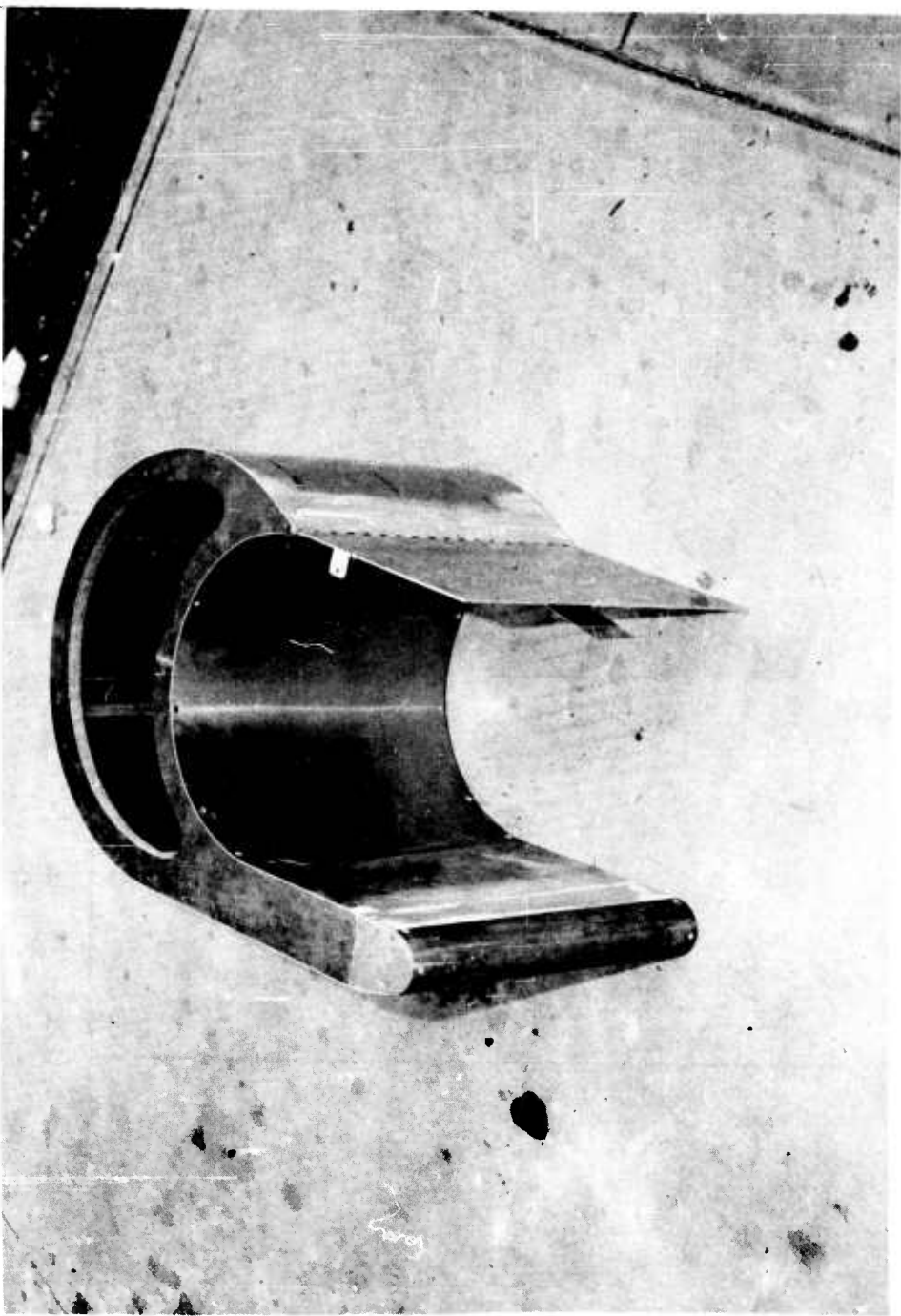


Figure 54. Model 1, Centerbody Inner Exit Skirt.

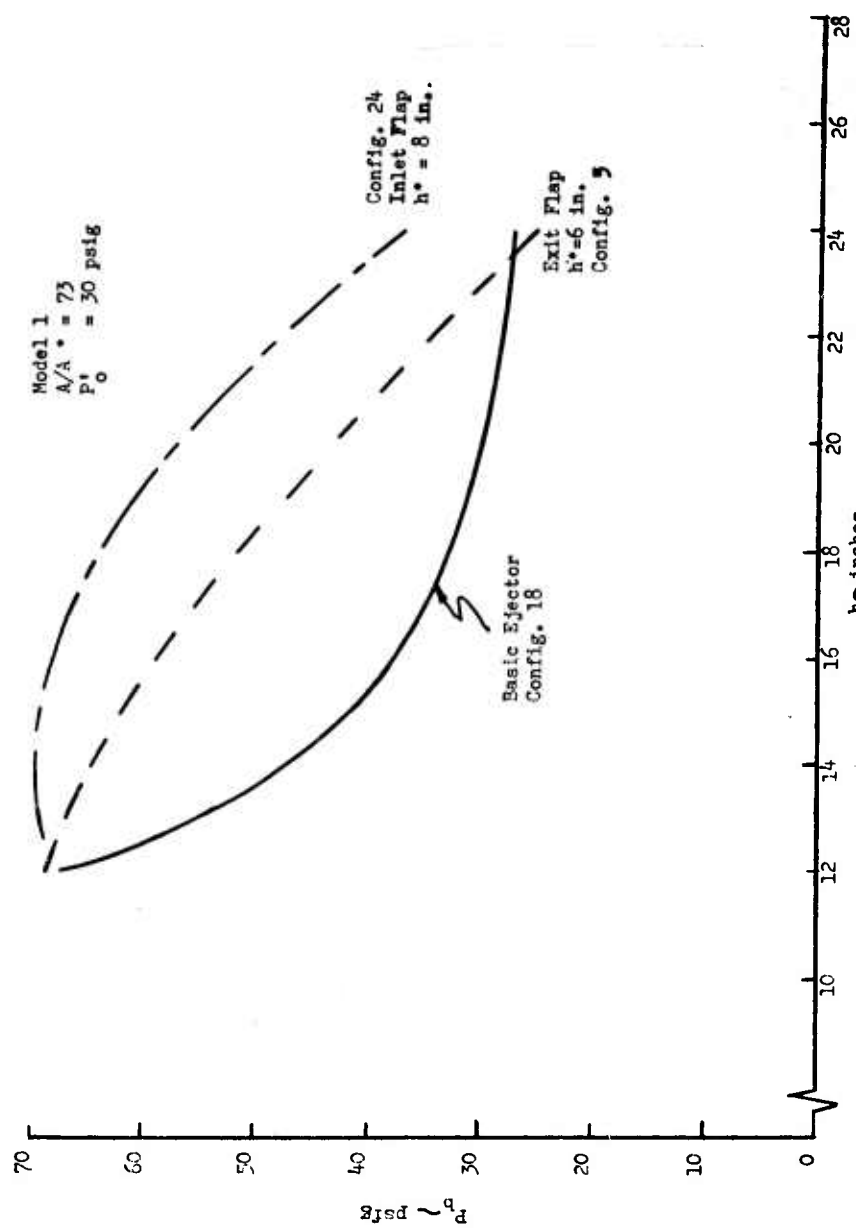


Figure 55. Base Pressure -vs- Height, Configuration 18, 24, 25.

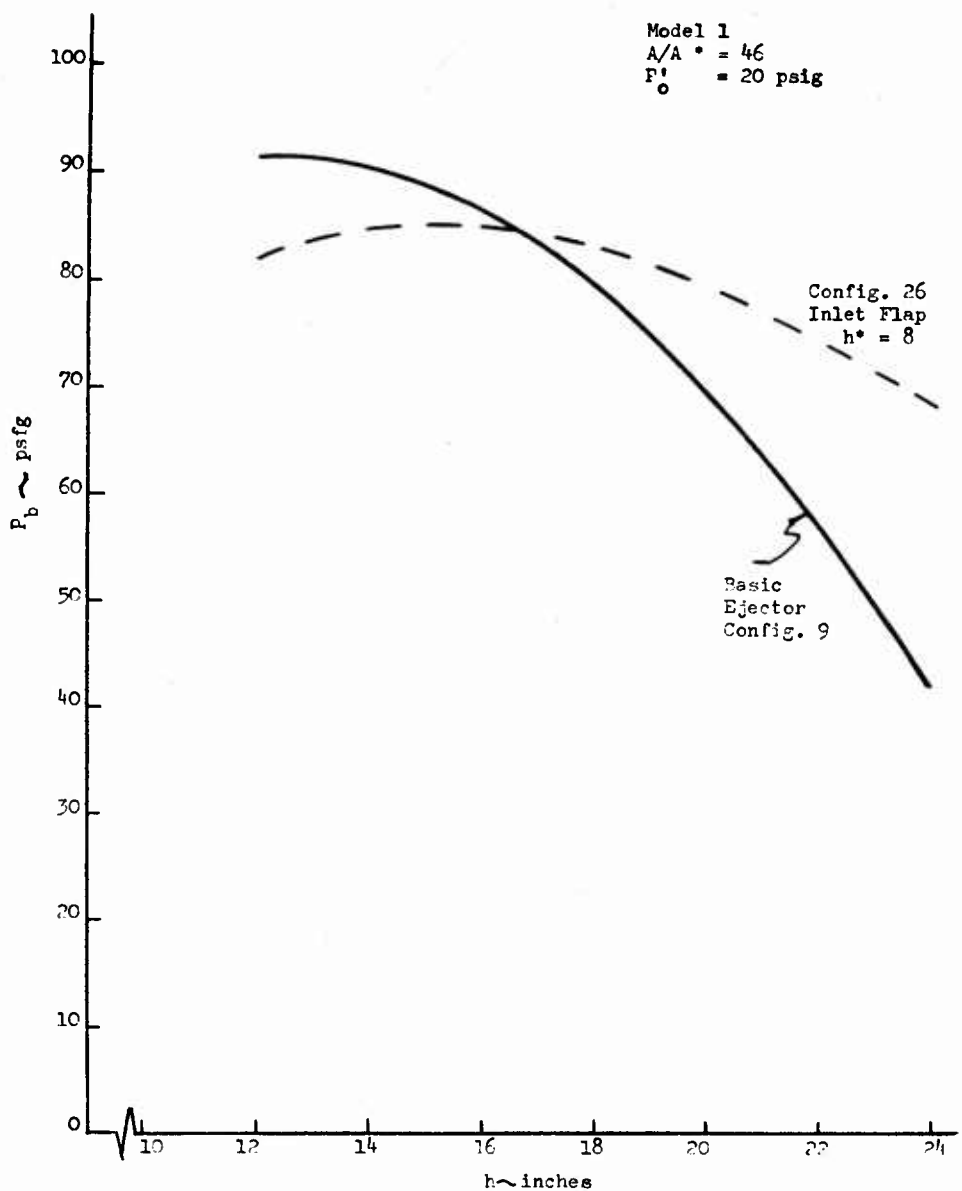


Figure 56. Base Pressure -vs- Height, Configuration 9, 26.

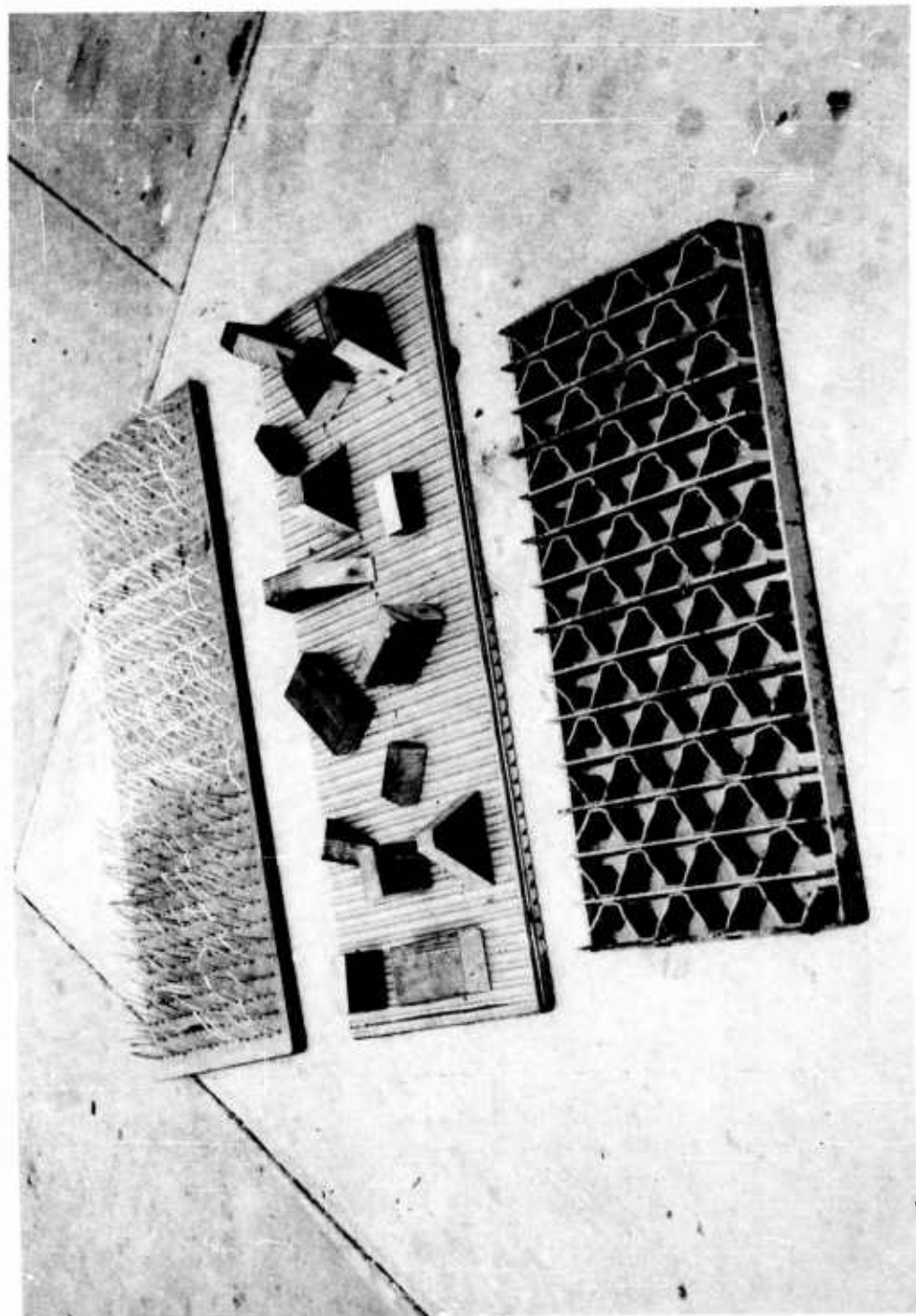


Figure 57. Surface Roughness Models.

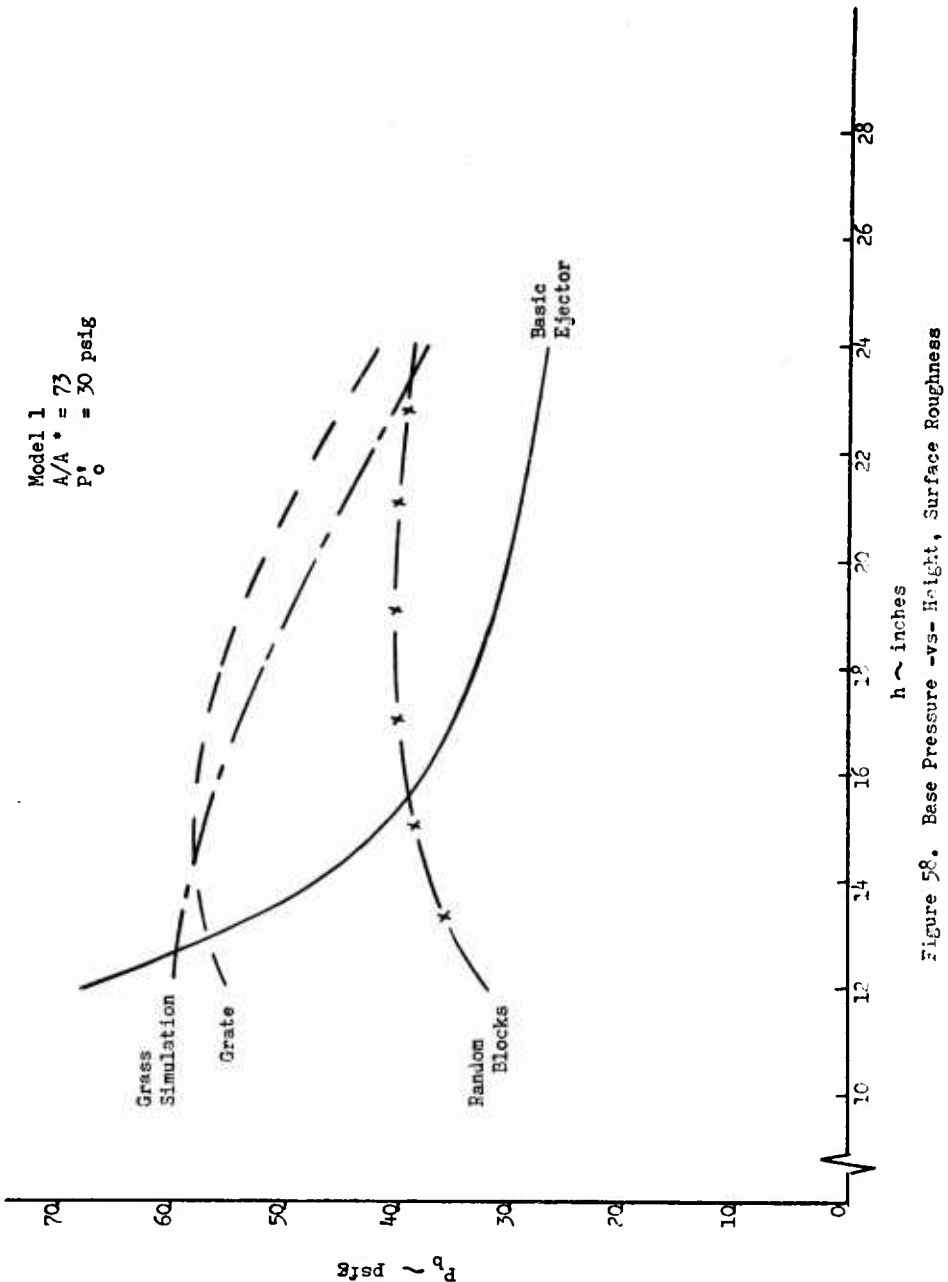


Figure 58. Base Pressure -vs- Height, Surface Roughness

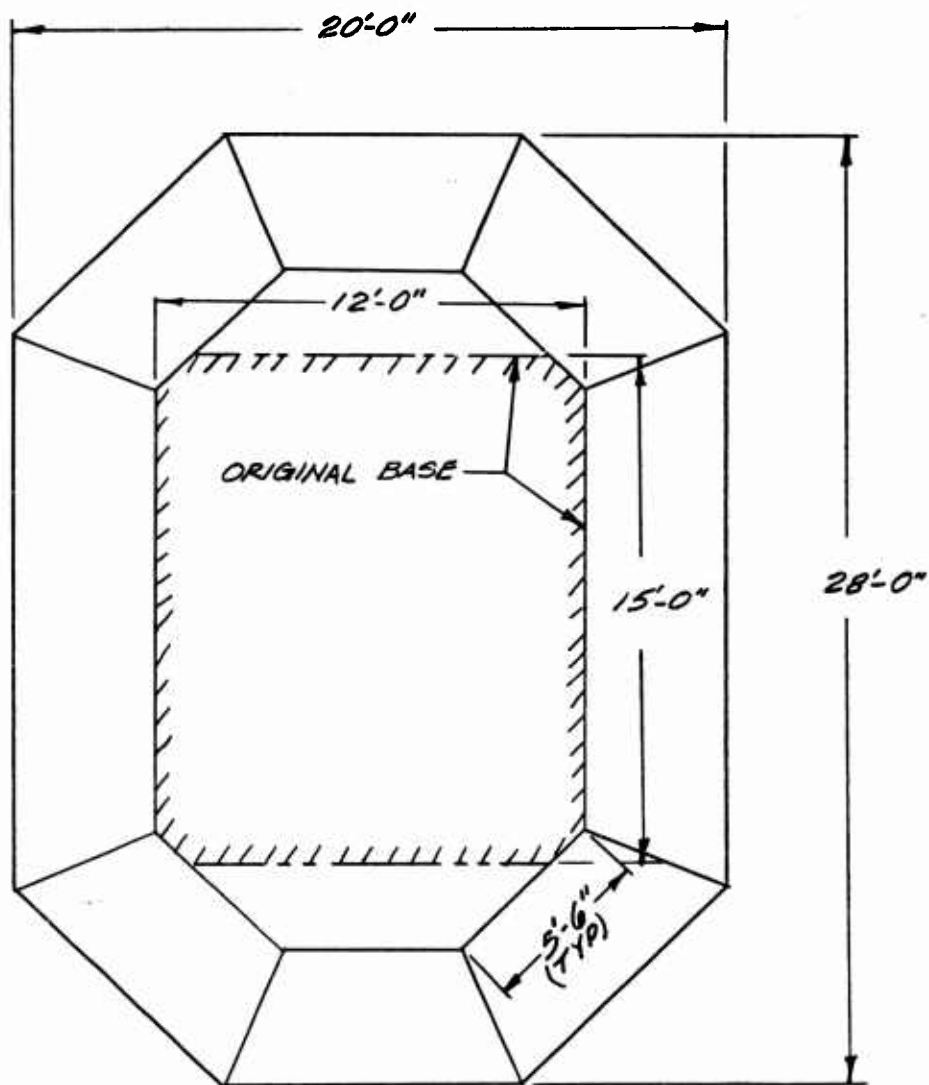


Figure 59. MCTV Base Modification, (Proposed).

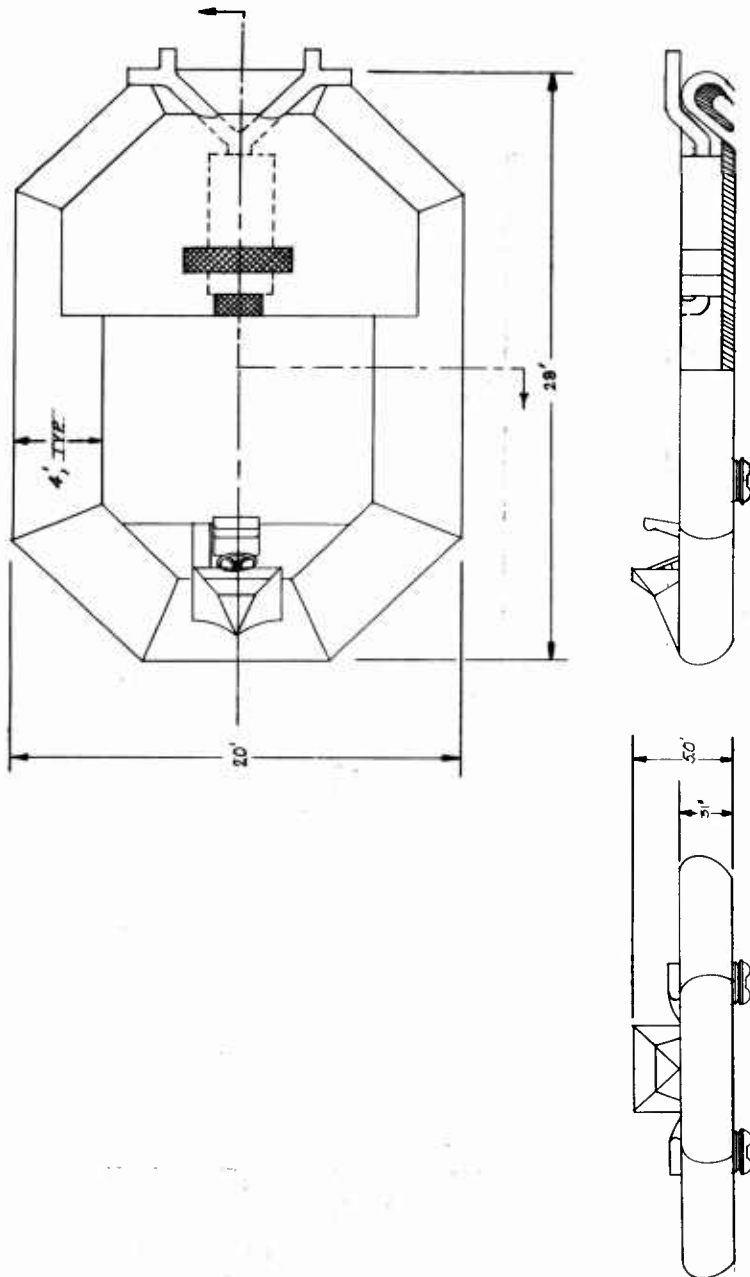


Figure 60. MCTV Modification, Sketch.

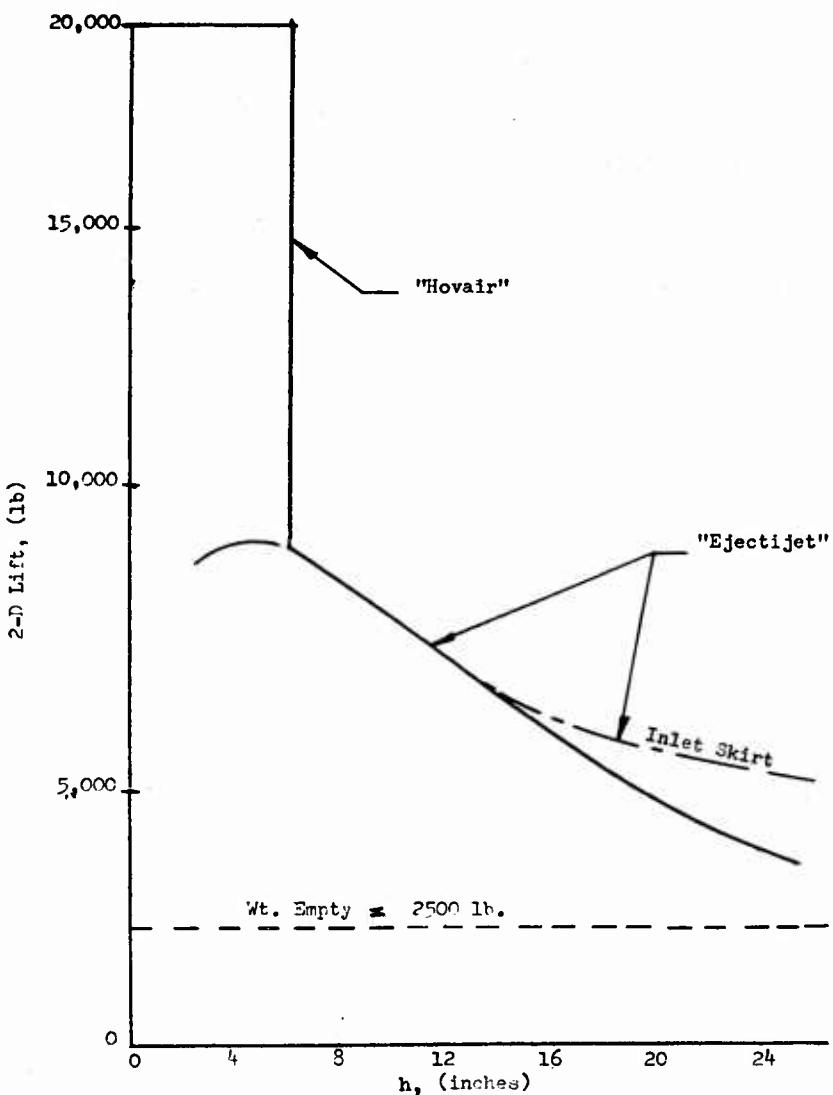


Figure 61. MCTV Modified Model 1
2-D Performance

DISTRIBUTION

Army War College	1
Aviation Test Office, Edwards AFB	1
U. S. Army Polar Research and Development Center	1
Deputy Chief of Staff for Logistics, D/A	1
The Research Analysis Corporation	1
Army Research Office, Durham	2
Office of Chief of R&D	2
Naval Air Test Center	1
Army Research Office, OCRD	1
Deputy Chief of Staff for Military Operations, D/A	1
U. S. Army Engineer Research & Development Laboratories	2
U. S. Army Tank-Automotive Center	1
The Ordnance Board	1
U. S. Army Combat Developments Command, Transportation Agency	1
U. S. Army Aviation and Surface Materiel Command	14
U. S. Army Transportation School	4
U. S. Army Transportation Research Command	68
U. S. Army Airborne, Electronics and Special Warfare Board	1
U. S. Army Research & Development Group (Europe)	2
Chief of Naval Operations	1
Bureau of Naval Weapons	2
Bureau of Supplies and Accounts, D/N	1
U. S. Naval Supply Research and Development Facility	1
U. S. Naval Postgraduate School	1
Bureau of Ships	1
U. S. Naval Ordnance Test Station	1
David Taylor Model Basin	1
Marine Corps Landing Force Development Center	1
Marine Corps Educational Center	1
U. S. Army Standardization Group, Canada	1
Canadian Army Liaison Officer, U. S. Army Transportation School	3
British Army Staff, DAQMG (Mov & Tn)	4
U. S. Army Standardization Group, U. K.	1
Langley Research Center, NASA	2

Manned Spacecraft Center, NASA	1
Ames Research Center, NASA	2
Lewis Research Center, NASA	1
NASA Representative, Scientific and Technical Information Facility	1
U. S. Government Printing Office	1
Defense Documentation Center	10
U. S. Army Medical Research & Development Command	1
Human Resources Research Office	2
Office of the Asst. Sec. of Defense for R&E	1
U. S. Maritime Administration	1
Human Engineering Laboratory	1
U. S. Army Mobility Command	3
U. S. Strike Command	1
U. S. Army Materiel Command	4
Chief of Naval Research	3

Martin Company, Orlando Division, 1. Aerodynamics
Orlando, Fla., RECIRCULATION PRINCIPLE FOR GROUND EFFECT MACHINES:
INVESTIGATION OF IMPROVEMENTS BY
MAJOR MODIFICATIONS TO MCTV,
K. Cossairt, Report No. CR3159,
TRECOM Technical Report 63-27,
July 1963, pp. Incl. illus. and
tables (Contract DA 44-177-AMC-9(T)
Task 1D021701A04804.

Unclassified Report

Analytical studies and experimental
investigations were conducted to
(over)

Martin Company, Orlando Division, 1. Aerodynamics
Orlando, Fla., RECIRCULATION PRINCIPLE FOR GROUND EFFECT MACHINES:
INVESTIGATION OF IMPROVEMENTS BY
MAJOR MODIFICATIONS TO MCTV,
K. Cossairt, Report No. CR3159,
TRECOM Technical Report 63-27,
July 1963, pp. Incl. illus. and
tables (Contract DA 44-177-AMC-9(T)
Task 1D021701A04804.

Unclassified Report

Analytical studies and experimental
investigations were conducted to
(over)

Martin Company, Orlando Division, 1. Aerodynamics
Orlando, Fla., RECIRCULATION PRINCIPLE FOR GROUND EFFECT MACHINES:
INVESTIGATION OF IMPROVEMENTS BY
MAJOR MODIFICATIONS TO MCTV,
K. Cossairt, Report No. CR3159,
TRECOM Technical Report 63-27,
July 1963, pp. Incl. illus. and
tables (Contract DA 44-177-AMC-9(T)
Task 1D021701A04804.

Unclassified Report

Analytical studies and experimental
investigations were conducted to
(over)

Martin Company, Orlando Division, 1. Aerodynamics
Orlando, Fla., RECIRCULATION PRINCIPLE FOR GROUND EFFECT MACHINES:
INVESTIGATION OF IMPROVEMENTS BY
MAJOR MODIFICATIONS TO MCTV,
K. Cossairt, Report No. CR3159,
TRECOM Technical Report 63-27,
July 1963, pp. Incl. illus. and
tables (Contract DA 44-177-AMC-9(T)
Task 1D021701A04804.

Unclassified Report

Analytical studies and experimental
investigations were conducted to
(over)

determine the best overall MCTV performance obtainable with essentially major modifications. Testing was done in the existing two-dimensional test facility with various configurations of old (existing) and new two-dimensional recirculating ejector models. Based on these experimental data, estimates are made as to the lifting capability, static stability and control of the proposed modified MCTV. In addition, experimental data is presented for the use of skirts and trunks for several configurations. The effect of ground surface roughness is also considered.

determine the best overall MCTV performance obtainable with essentially major modifications. Testing was done in the existing two-dimensional test facility with various configurations of old (existing) and new two-dimensional recirculating ejector models. Based on these experimental data, estimates are made as to the lifting capability, static stability and control of the proposed modified MCTV. In addition, experimental data is presented for the use of skirts and trunks for several configurations. The effect of ground surface roughness is also considered.

determine the best overall MCTV performance obtainable with essentially major modifications. Testing was done in the existing two-dimensional test facility with various configurations of old (existing) and new two-dimensional recirculating ejector models. Based on these experimental data, estimates are made as to the lifting capability, static stability and control of the proposed modified MCTV. In addition, experimental data is presented for the use of skirts and trunks for several configurations. The effect of ground surface roughness is also considered.

determine the best overall MCTV performance obtainable with essentially major modifications. Testing was done in the existing two-dimensional test facility with various configurations of old (existing) and new two-dimensional recirculating ejector models. Based on these experimental data, estimates are made as to the lifting capability, static stability and control of the proposed modified MCTV. In addition, experimental data is presented for the use of skirts and trunks for several configurations. The effect of ground surface roughness is also considered.

Martin Company, Orlando Division, 1. Aerodynamics
Orlando, Fla., RECIRCULATION PRINCIPLE FOR GROUND EFFECT MACHINES:
INVESTIGATION OF IMPROVEMENTS BY MAJOR MODIFICATIONS TO MCTV,
K. Cossairt, Report No. JR3159, TRECOM Technical Report 63-27,
July 1963, pp. Incl. illus. and tables (Contract DA 44-177-AMC-9(T)
Task 1D021701AO4804.

Unclassified Report

Analytical studies and experimental investigations were conducted to (over)

Martin Company, Orlando Division, 1. Aerodynamics
Orlando, Fla., RECIRCULATION PRINCIPLE FOR GROUND EFFECT MACHINES:
INVESTIGATION OF IMPROVEMENTS BY MAJOR MODIFICATIONS TO MCTV,
K. Cossairt, Report No. OR3159, TRECOM Technical Report 63-27,
July 1963, pp. Incl. illus. and tables (Contract DA 44-177-AMC-9(T)
Task 1D021701AO4804.

Unclassified Report

Analytical studies and experimental investigations were conducted to (over)

Martin Company, Orlando Division, 1. Aerodynamics
Orlando, Fla., RECIRCULATION PRINCIPLE FOR GROUND EFFECT MACHINES:
INVESTIGATION OF IMPROVEMENTS BY MAJOR MODIFICATIONS TO MCTV,
K. Cossairt, Report No. OR3159, TRECOM Technical Report 63-27,
July 1963, pp. Incl. illus. and tables (Contract DA 44-177-AMC-9(T)
Task 1D021701AO4804.

Unclassified Report

Analytical studies and experimental investigations were conducted to (over)

Martin Company, Orlando Division, 1. Aerodynamics
Orlando, Fla., RECIRCULATION PRINCIPLE FOR GROUND EFFECT MACHINES:
INVESTIGATION OF IMPROVEMENTS BY MAJOR MODIFICATIONS TO MCTV,
K. Cossairt, Report No. OR3159, TRECOM Technical Report 63-27,
July 1963, pp. Incl. illus. and tables (Contract DA 44-177-AMC-9(T)
Task 1D021701AO4804.

Unclassified Report

Analytical studies and experimental investigations were conducted to (over)

determine the best overall MCTV performance obtainable with essentially major modifications. Testing was done in the existing two-dimensional test facility with various configurations of old (existing) and new two-dimensional recirculating ejector models. Based on these experimental data, estimates are made as to the lifting capability, static stability and control of the proposed modified MCTV. In addition, experimental data is presented for the use of skirts and trunks for several configurations. The effect of ground surface roughness is also considered.

determine the best overall MCTV performance obtainable with essentially major modifications. Testing was done in the existing two-dimensional test facility with various configurations of old (existing) and new two-dimensional recirculating ejector models. Based on these experimental data, estimates are made as to the lifting capability, static stability and control of the proposed modified MCTV. In addition, experimental data is presented for the use of skirts and trunks for several configurations. The effect of ground surface roughness is also considered.

determine the best overall MCTV performance obtainable with essentially major modifications. Testing was done in the existing two-dimensional test facility with various configurations of old (existing) and new two-dimensional recirculating ejector models. Based on these experimental data, estimates are made as to the lifting capability, static stability and control of the proposed modified MCTV. In addition, experimental data is presented for the use of skirts and trunks for several configurations. The effect of ground surface roughness is also considered.

determine the best overall MCTV performance obtainable with essentially major modifications. Testing was done in the existing two-dimensional test facility with various configurations of old (existing) and new two-dimensional recirculating ejector models. Based on these experimental data, estimates are made as to the lifting capability, static stability and control of the proposed modified MCTV. In addition, experimental data is presented for the use of skirts and trunks for several configurations. The effect of ground surface roughness is also considered.

UNCLASSIFIED

UNCLASSIFIED